Electronic Supplementary Information

Photofunctional cyclometallated iridium(III) polypyridine methylsulfone complexes as sulfhydryl-specific reagents for bioconjugation, bioimaging and photocytotoxic applications

Lili Huang,[a] Peter Kam-Keung Leung,[ab] Lawrence Cho-Cheung Lee,[ac] Guang-Xi Xu,[a] Yun-Wah Lam*[a] and Kenneth Kam-Wing Lo*[ab] Email: bhkenlo@cityu.edu.hk

[a] Department of Chemistry, City University of Hong Kong, Tat Chee Avenue, Hong Kong, P. R. China

[b] State Key Laboratory of Terahertz and Millimetre Waves, City University of Hong Kong, Tat Chee Avenue, Kowloon, Hong Kong, P. R. China

[c] Laboratory for Synthetic Chemistry and Chemical Biology Limited, Units 1503 – 1511, 15/F, Building 17W, Hong Kong Science Park, New Territories, Hong Kong, P. R. China

Table of Contents

Experimental and Results

Materials

All solvents were of analytical reagent grade and purified according to standard procedures.[1] Na_2CO_3, $NaHCO_3$, Mg_2SO_4, $NaBH_4$, K_2CO_3, KPF_6, tris(2-carboxyethyl)phosphine (TCEP), trifluoroacetic acid (TFA) and 1,3-diphenylisobenzofuran (DPBF) were purchased from Acros. 4,4'-Dimethyl-2,2'-bipyridine, SeO_2, $Na_2S_2O_5$, phenol, iridium(III) chloride trihydrate ($IrCl_3 \cdot 3H_2O$) and 3-(4,5-dimethylthiazol-2-yl)-2,5-diphenyltetrazolium bromide (MTT) were purchased from Aldrich. The peptides CYHWYGYTPQNVI (GE11), CKDEL (ER) and CPKKKRKV (NLS) were purchased from GL Biochem. Bovine serum albumin (BSA) and human serum albumin (HSA) were purchased from Calbiochem. All these chemicals were used without further purification. 4-Bromomethyl-4'-methyl-2,2'-bipyridine (bpy-Br),[2] 6-hydroxy-2-(methylsulfonyl)benzo[*d*]thiazole,[3] 5-(methylsulfonyl)-1-(4-hydroxyphenyl)-1*H*-tetrazole,[4] 2-(methylsulfonyl)-5-(4-hydroxyphenyl)-1,3,4-oxadiazole[4] and benzo[*a*]phenazine (Hbpz)[5] were prepared according to literature procedures. All buffer components were of biological grade and used as received. Autoclaved Milli-Q H_2O was used for the preparation of the aqueous solutions. MDA-MB-231, A431 and HEK-293T cells were obtained from American Type Culture Collection. Dulbecco's Modified Eagle Medium (DMEM), Minimum Essential Medium (MEM), fetal bovine serum (FBS), penicillin/streptomycin, sodium pyruvate, phosphate-buffered saline (PBS), trypsin-EDTA, LysoTracker Green, MitoTracker Green, CellMask Deep Red, lactate dehydrogenase (LDH) cytotoxicity assay kit, Alexa Fluor 647 annexin V conjugate, annexin V binding buffer and propidium iodide (PI) were purchased from Invitrogen.

Physical Measurements and Instrumentation

^{1}H NMR spectra were recorded on a Bruker AVANCE III 400 or 600 MHz spectrometer at 298 K using deuterated solvents. Chemical shifts (δ, ppm) were reported relative to tetramethylsilane (TMS). Positive-ion electrospray ionisation (ESI) mass spectra were recorded on a SCIEX API-3200 Triple-Q MS/MS mass spectrometer at 298 K. High-resolution electrospray ionisation (HR-ESI) mass spectra were recorded on a Bruker micrOTOF-QII. MALDI-TOF mass spectra of the samples were recorded on an Applied Biosystems 4800 Plus MALDI TOF/TOF^{TM} Analyser. IR spectra of the samples in KBr pellets were recorded in the range of 4000 – 400 cm^{-1} using a Perkin Elmer Spectrum 100 FTIR spectrometer. Elemental analyses were carried out on an Elementar Analysensysteme GmbH Vario MICRO elemental analyser. Electronic absorption spectra were recorded on an Agilent 8453 diode array spectrophotometer. Steady-state emission spectra were recorded on a HORIBA FluoroMax-4 spectrofluorometer. Unless specified otherwise, all solutions for photophysical studies were degassed with no fewer than four successive freeze-pump-thaw cycles and stored in a 10-cm^3 round bottomed flask equipped with a side-arm 1-cm fluorescence cuvette and sealed from the atmosphere by a Rotaflo HP6/6 quick-release Teflon stopper. Luminescence quantum yields (Φ_{em}) were measured by optically dilute method[6] using an aerated aqueous solution of the $[Ru(bpy)_3]Cl_2$ (Φ_{em} = 0.04, excitation wavelength at 455 nm) as the standard solution.[7] The concentrations of the standard and sample solutions were adjusted until the absorbance at 455 nm was 0.1. Emission lifetimes were measured on an Edinburgh Instruments LP920 laser flash photolysis spectrometer using the third harmonic output (355 nm; 6 – 8 ns fwhm pulse width) of a Spectra-Physics Quanta-Ray Q-switched LAB-150 pulsed

Nd:YAG laser (10 Hz) as the excitation source. High-performance liquid chromatography (HPLC) was performed on an Agilent 1260 Infinity II system coupled with a diode array detector WR. The dynamical light scattering (DLS) methodology followed recommendations outlined in the NIST-protocol.[8] The measurements were performed on Malvem Zetasizer Nano ZS at 298 K. The results were presented as number-based distributions.

Synthesis

4-(4-(2-(Methylsulfonyl)-benzo[*d*]thiazol-6-yl)oxymethyl)-4'-methyl-2,2'-bipyridine (bpy-btz)

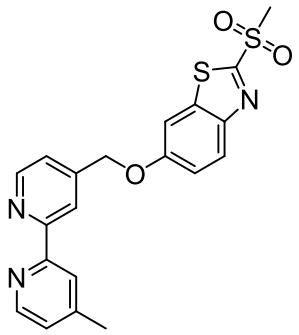

A mixture of bpy-Br (100 mg, 0.38 mmol), 6-hydroxy-2-(methylsulfonyl)benzo[*d*]thiazole (87 mg, 0.38 mmol) and K_2CO_3 (79 mg, 0.57 mmol) in DMF (1 mL) was stirred at 298 K for 18 h. The solvent was removed under reduced pressure and the brown residual solid was purified by column chromatography on silica gel using CH_2Cl_2/MeOH (200:1, *v*/*v*) as the eluent. The solution containing the product was collected and the solvent was removed under reduced pressure to afford the product as a white solid. Yield: 112 mg (72%). ^{1}H NMR (400 MHz, chloroform-*d*, 298 K, TMS): δ8.74 (d, *J* = 5.0 Hz, 1H, H6 of bpy), 8.59 (d, *J* = 5.0 Hz, 1H, H6' of bpy), 8.57 (s, 1H, H3 of bpy), 8.32 (s, 1H, H3' of bpy), 8.13 (d, *J* = 9.1 Hz, 1H, H4 of benzothiazole ring), 7.49 (d, *J* = 2.4 Hz, 1H, H7 of benzothiazole ring), 7.46 (d, *J* = 4.9 Hz, 1H, H5 of bpy), 7.38 (dd, *J* = 9.1 and 2.5 Hz, 1H, H5 of benzothiazole ring), 7.24 (d, *J* = 4.7 Hz, 1H, H5' of bpy), 5.31 (s, 2H, CH_2 of bpy), 3.40 (s, 3H, CH_3 of sulfone), 2.50 (s, 3H, CH_3 of bpy). ^{13}C NMR (150 MHz, chloroform-*d*, 298 K, TMS): δ163.7, 158.3, 155.2, 149.7, 148.7, 147.4, 146.2, 138.6, 126.3, 125.1, 122.3, 121.5, 119.1, 118.6, 105.1, 69.1, 42.6, 21.3. HR-ESI-MS (positive-ion mode, *m*/*z*): $[M + H^+]^+$ calcd for $C_{20}H_{18}N_3O_3S_2$ 412.0790, found 412.1021; $[M + Na^+]^+$ calcd for $C_{20}H_{17}N_3O_3S_2Na$ 434.0609, found 434.0815.

4-(4-(5-(Methylsulfonyl)-1*H*-tetrazol-1-yl)phenoxymethyl)-4'-methyl-2,2'-bipyridine (bpy-mstp)

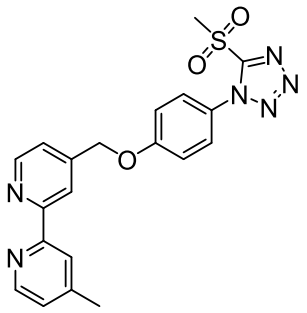

The synthetic procedure was similar to that for bpy-btz except that 5-(methylsulfonyl)-1-(4-hydroxyphenyl)-1*H*-tetrazole (91 mg, 0.38 mmol) was used instead of 6-hydroxy-2-(methylsulfonyl)benzo[*d*]thiazole. Yield: 80 mg (50%). ^{1}H NMR (400 MHz, acetone-d_6, 298 K, TMS): δ 8.72 (d, *J* = 4.6 Hz, 1H, H6 of bpy), 8.62 (s, 1H, H3 of bpy), 8.55 (d, *J* = 4.6 Hz, 1H, H6' of bpy), 8.35 (s, 1H, H3' of bpy), 7.75 (d, *J* = 8.6 Hz, 2H, H3 and H5 of phenyl ring), 7.57 (d, *J* = 4.1 Hz, 1H, H5 of bpy), 7.37 (d, *J* = 8.6 Hz, 2H, H2 and H6 of phenyl ring), 7.27 (d, *J* = 4.1 Hz, 1H, H5' of bpy), 5.47 (s, 2H, CH_2 of bpy), 3.65 (s, 3H, CH_3 of sulfone), 2.47 (s, 3H, CH_3 of bpy). ^{13}C NMR (150 MHz, chloroform-*d*, 298 K, TMS): δ 160.4, 156.5, 155.3, 154.0, 149.7, 148.8, 148.6, 146.2, 126.6, 126.2, 125.1, 122.2, 121.5, 119.0, 105.8, 68.9, 43.8, 21.3, 14.2. HR-ESI-MS (positive-ion mode, *m*/*z*): $[M + H^+]^+$ calcd for $C_{20}H_{19}N_6O_3S$ 423.1239, found 423.1457; $[M + Na^+]^+$ calcd for $C_{20}H_{18}N_6O_3SNa$ 445.1059, found 445.1306.

4-(4-(2-(Methylsulfonyl)-1,3,4-oxadiazol-5-yl)phenoxymethyl)-4'-methyl-2,2'-bipyridine (bpy-odz)

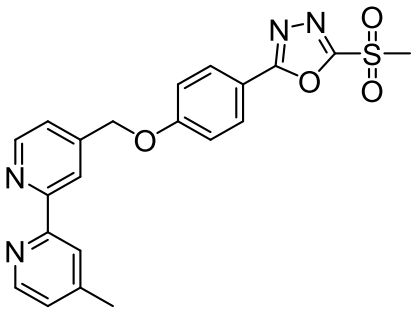

The synthetic procedure was similar to that for bpy-btz except that 2-(methylsulfonyl)-5-(4-hydroxyphenyl)-1,3,4-oxadiazole (91 mg, 0.38 mmol) was used instead of 6-hydroxy-2-(methylsulfonyl)benzo[*d*]thiazole. Yield: 56 mg (35%). ^{1}H NMR (400 MHz, DMSO-d_6, 298 K, TMS): δ 8.71 (d, *J* = 5.0 Hz, 1H, H6 of bpy), 8.56 (d, *J* = 4.9 Hz, 1H, H6' of bpy), 8.49 (s, 1H, H3 of bpy), 8.27 (s, 1H, H3' of bpy), 8.08 (d, *J* = 8.8 Hz, 2H, H3 and H5 of phenyl ring), 7.53 (d, *J* = 4.2 Hz, 1H, H5 of bpy), 7.34 – 7.30 (m, 3H, H5' of bpy and H2 and H6 of phenyl ring), 5.45 (s, 2H, CH_2 of bpy), 3.71 (s, 3H, CH_3 of sulfone), 2.43 (s, 3H, CH_3 of bpy). ^{13}C NMR (150 MHz, chloroform-*d*, 298 K, TMS): δ 166.5, 162.1, 161.7, 155.1, 149.6, 148.7, 146.2, 129.8, 125.1, 122.3, 121.5, 119.1, 115.7, 115.1, 68.6, 43.0, 21.3. HR-ESI-MS (positive-ion mode, *m*/*z*): $[M + H^+]^+$ calcd for $C_{21}H_{19}N_4O_4S$ 423.1127, found 423.1381; $[M + Na^+]^+$ calcd for $C_{21}H_{18}N_4O_4SNa$ 445.0946, found 445.1172.

4-Phenoxymethyl-4’-methyl-2,2’-bipyridine (bpy-ph)

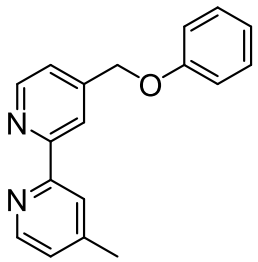

The synthetic procedure was similar to that for bpy-btz except that phenol (36 mg, 0.38 mmol) was used instead of 6-hydroxy-2-(methylsulfonyl)benzo[*d*]thiazole. Yield: 79 mg (75%). ^{1}H NMR (400 MHz, DMSO-d_6, 298 K, TMS): δ 8.68 (d, *J* = 4.9 Hz, 1H, H6 of bpy), 8.55 (d, *J* = 4.9 Hz, 1H, H6’ of bpy), 8.47 (s, 1H, H3 of bpy), 8.26 (s, 1H, H3’ of bpy), 7.50 (d, *J* = 4.3 Hz, 1H, H5 of bpy), 7.34 – 7.29 (m, 3H, H5’ of bpy and H3 and H5 of phenyl ring), 7.05 (d, *J* = 8.1 Hz, 2H, H2 and H6 of phenyl ring), 6.97 (t, *J* = 7.3 Hz, 1H, H4 of phenyl ring), 5.29 (s, 2H, CH_2 of bpy), 2.42 (s, 3H, CH_3 of bpy). ^{13}C NMR (150 MHz, DMSO-d_6, 298 K, TMS): δ 158.4, 156.0, 155.3, 149.9, 149.5, 148.5, 148.1, 130.1, 125.6, 122.4, 121.8, 121.6, 118.8, 115.3, 68.1, 21.2. HR-ESI-MS (positive-ion mode, *m*/*z*): $[M + H^+]^+$ calcd for $C_{18}H_{17}N_2O$ 277.1341, found 277.1512; $[M + Na^+]^+$ calcd for $C_{18}H_{16}N_2ONa$ 299.1160, found 299.1342.

$[Ir_2(bpz)_4Cl_2]$

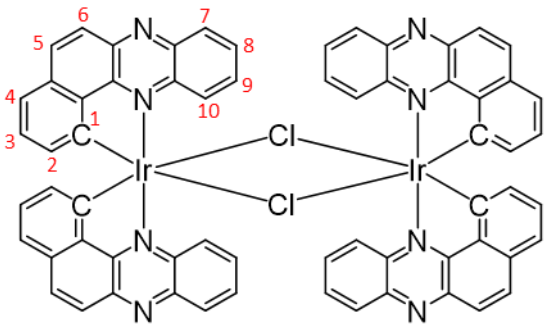

The synthetic procedure is modified from a literature method.[9] A mixture of $IrCl_3 \cdot 3H_2O$ (400 mg, 1.14 mmol) and Hbpz (575 mg, 2.50 mmol) in 2-ethoxyethanol/H_2O (40 mL; 3:1, *v*/*v*) was heated to reflux under an inert atmosphere of nitrogen in the dark for 24 h. The dark green solution was filtered and the solvent was removed under reduced pressure to give a dark green solid. The green solid was dissolved in CH_2Cl_2 and purified by column chromatography on silica gel using CH_2Cl_2 as the eluent. The solvent was removed under reduced pressure to afford $[Ir_2(bpz)_4Cl_2]$ as a dark green solid. Yield: 313 mg (40%). ^{1}H NMR (400 MHz, chloroform-*d*, 298 K, TMS): δ8.65 (d, *J* = 8.8 Hz, 4H, H7 of bpz), 8.09 (d, *J* = 7.6 Hz, 4H, H4 of bpz), 7.88 (d, *J* = 9.2 Hz, 4H, H6 of bpz), 7.85 (d, *J* = 9.2 Hz, 4H, H5 of bpz), 7.73 (t, *J* = 8.0 Hz, 4H, H8 of bpz), 7.27 (d, *J* = 7.6 Hz, 4H, H10 of bpz), 6.73 – 6.68 (m, 8H, H3 and H9 of bpz), 6.10 (d, *J* = 7.6 Hz, 4H, H2 of bpz).

[Ir(bpz)$_2$(bpy-btz)](PF$_6$) (1)

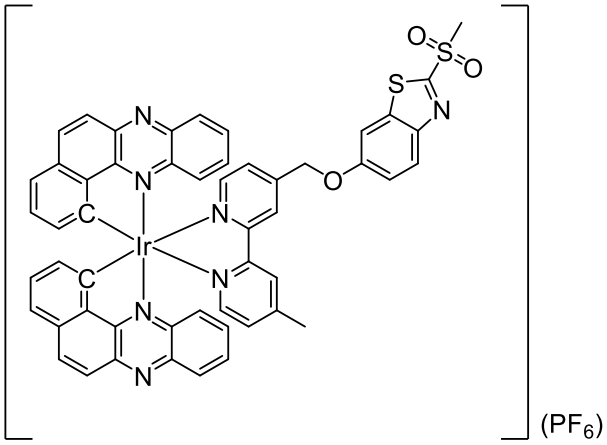

A mixture of [Ir$_2$(bpz)$_4$Cl$_2$] (41 mg, 0.03 mmol) and bpy-btz (24 mg, 0.06 mmol) in CH$_2$Cl$_2$/MeOH (20 mL) (1:1, *v*/*v*) was stirred under an inert atmosphere of nitrogen in the dark for 18 h. After addition of solid KPF$_6$ (55 mg, 0.3 mmol), the black mixture was stirred for 2 h. The solvent was removed under reduced pressure and the black residue was purified by column chromatography on silica gel using CH$_2$Cl$_2$/MeOH (100:1, *v*/*v*) as the eluent. The solvent was removed under reduced pressure to give a black solid. Subsequent recrystallisation of the black solid from CH$_2$Cl$_2$/Et$_2$O afforded complex **1** as black crystals. Yield: 38 mg (52%). ^{1}H NMR (600 MHz, DMSO-d_6, 298 K, TMS): δ8.76 (s, 1H, H3 of bpy), 8.64 (s, 1H, H3’ of bpy), 8.40 – 8.37 (m, 2H, H7 of bpz), 8.31 (dd, *J* = 9.3 and 3.5 Hz, 2H, H6 of bpz), 8.19 (d, *J* = 9.1 Hz, 1H, H4 of benzothiazole ring), 8.02 (dd, *J* = 9.2 and 2.3 Hz, 2H, H5 of bpz), 7.92 (d, *J* = 2.6 Hz, 1H, H7 of benzothiazole ring), 7.89 (t, *J* = 8.2 Hz, 1H, H8 of bpz), 7.85 (t, *J* = 8.2 Hz, 1H, H8 of bpz), 7.76 (d, *J* = 7.7 Hz, 2H, H4 of bpz), 7.65 – 7.62 (m, 2H, H6 and H6’ of bpy), 7.50 (t, *J* = 7.9 Hz, 1H, H9 of bpz), 7.46 (d, *J* = 5.8 Hz, 1H, H5 of bpy), 7.42 – 7.39 (m, 2H, H5’ of bpy and H5 of benzothiazole ring), 7.34 (t, *J* = 8.0 Hz, 1H, H9 of bpz), 7.28 (d, *J* = 8.7 Hz, 1H, H10 of bpz), 7.20 – 7.18 (m, 3H, H3 and H10 of bpz), 6.49 (d, *J* = 7.5 Hz, 1H, H2 of bpz), 6.47 (d, *J* = 7.4 Hz, 1H, H2 of bpz), 5.42 (s, 2H, CH$_2$ of bpy), 3.58 (s, 3H, CH$_3$ of sulfone), 2.45

(s, 3H, CH_3 of bpy). ^{13}C NMR (150 MHz, DMSO-d_6, 298 K, TMS): δ 207.0, 165.2, 157.7, 156.1, 155.2, 155.0, 154.9, 153.2, 151.1, 150.9, 149.2, 148.3, 147.4, 145.6, 145.5, 143.6, 141.4, 141.3, 141.1, 141.0, 138.3, 135.9, 135.8, 135.1, 133.2, 133.0, 132.2, 131.9, 131.8, 131.7, 131.6, 130.7, 130.6, 130.4, 127.4, 126.7, 126.2, 123.0, 122.7, 122.6, 122.1, 119.1, 107.0, 68.1, 42.7, 31.2, 21.3. IR (KBr) $\tilde{\nu}$/cm^{-1}: 1342 (S=O), 840 (PF_6^-). HR-ESI-MS (positive-ion mode, *m*/*z*): $[M - PF_6^-]^+$ calcd for $IrC_{52}H_{35}N_7O_3S_2$ 1062.1872, found 1062.1537. Elemental analysis calcd for $IrC_{52}H_{35}N_7O_3S_2PF_6$: C 51.76, H 3.52, N 7.40, found: C 51.85, H 3.45, N 7.56%.

[Ir(bpz)$_2$(bpy-mstp)](PF$_6$) (2)

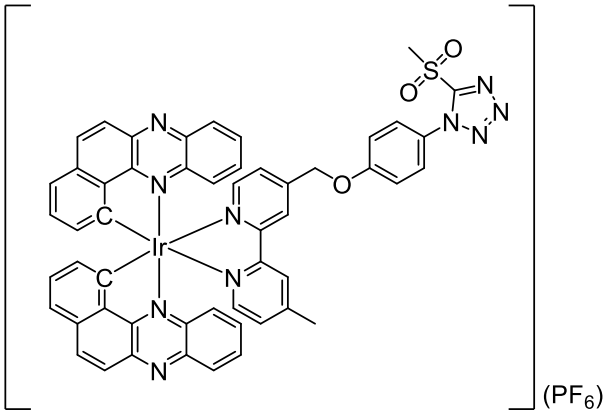

The synthetic procedure was similar to that for complex **1**, except that bpy-mstp (25 mg, 0.06 mmol) was used instead of bpy-btz. Subsequent recrystallisation of the black solid from CH_2Cl_2/Et_2O afforded complex **2** as black crystals. Yield: 39 mg (54%). ^{1}H NMR (600 MHz, DMSO-d_6, 298 K, TMS): δ 8.78 (s, 1H, H3 of bpy), 8.63 (s, 1H, H3' of bpy), 8.41 – 8.38 (m, 2H, H7 of bpz), 8.32 (dd, *J* = 9.4 and 5.6 Hz, 2H, H6 of bpz), 8.03 (dd, *J* = 9.2 and 7.7 Hz, 2H, H5 of bpz), 7.96 – 7.90 (m, 2H, H8 of bpz), 7.76 (dd, *J* = 7.6 and 2.7 Hz, 2H, H4 of bpz), 7.70 (d, *J* = 9.0 Hz, 2H, H3 and H5 of phenyl ring), 7.66 – 7.64 (m, 2H, H6 and H6' of bpy), 7.51 (t, *J* = 8.5 Hz, 1H, H9 of bpz), 7.45 (d, *J* = 5.8 Hz, 1H, H5 of bpy), 7.40 (d, *J* = 5.8 Hz, 1H, H5' of bpy), 7.36

(t, *J* = 8.5 Hz, 1H, H9 of bpz), 7.29 (d, *J* = 8.9 Hz, 1H, H10 of bpz), 7.24 (d, *J* = 9.0 Hz, 2H, H2 and H4 of phenyl ring), 7.21 – 7.18 (m, 3H, H3 and H10 of bpz), 6.50 (d, *J* = 7.5 Hz, 1H, H2 of bpz), 6.47 (d, *J* = 7.5 Hz, 1H, H2 of bpz), 5.40 (s, 2H, CH_2 of bpy), 3.67 (s, 3H, CH_3 of sulfone), 2.45 (s, 3H, CH_3 of bpy). ^{13}C NMR (150 MHz, DMSO-d_6, 298 K, TMS): δ 159.9, 156.1, 155.2, 155.1, 155.0, 154.7, 153.2, 151.2, 150.9, 150.8, 149.3, 148.3, 145.6, 145.5, 143.7, 143.6, 141.4, 141.1, 141.0, 135.9, 135.8, 135.2, 133.2, 133.1, 132.2, 131.9, 131.8, 131.6, 130.8, 130.4, 128.4, 127.4, 126.7, 126.6, 126.2, 123.1, 122.7, 122.5, 122.1, 115.9, 67.9, 65.4, 44.3, 31.2, 21.3, 15.6. IR (KBr) $\tilde{\nu}$/cm^{-1}: 1337 (S=O), 840 (PF_6^-). HR-ESI-MS (positive-ion mode, *m*/*z*): $[M - PF_6^-]^+$ calcd for $IrC_{52}H_{36}N_{10}O_3S$ 1073.2322, found 1073.2005. Elemental analysis calcd for $IrC_{52}H_{36}N_{10}O_3SPF_6$: C 50.36, H 3.11, N 11.15, found: C 50.52, H 2.94, N 11.33%.

[Ir(bpz)$_2$(bpy-odz)](PF$_6$) (3)

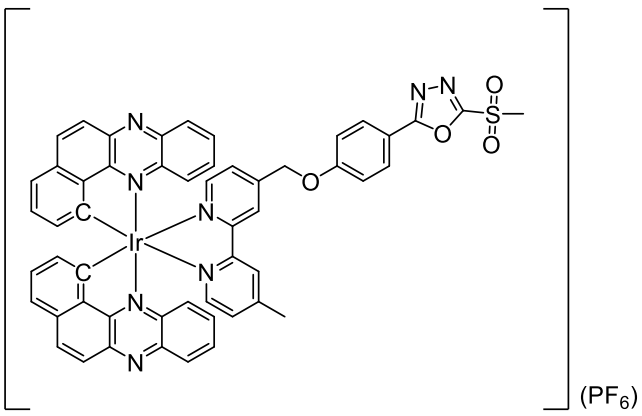

The synthetic procedure was similar to that for complex **1**, except that bpy-odz (25 mg, 0.06 mmol) was used instead of bpy-btz. Subsequent recrystallisation of the black solid from CH_2Cl_2/Et_2O afforded complex **3** as black crystals. Yield: 39 mg (53%). ^{1}H NMR (600 MHz, DMSO-d_6, 298 K, TMS): δ 8.76 (s, 1H, H3 of bpy), 8.63 (s, 1H, H3’ of bpy), 8.40 (d, *J* = 8.4 Hz, 2H, H7 of bpz), 8.32 (d, *J* = 9.3 Hz, 2H, H6 of bpz), 8.06 (d, *J* = 8.6 Hz, 2H, H3 and H5 of phenyl

ring), 8.03 (d, *J* = 9.2 Hz, 2H, H5 of bpz), 7.87 – 7.82 (m, 2H, H8 of bpz), 7.76 (d, *J* = 7.5 Hz, 2H, H4 of bpz), 7.68 – 7.67 (m, 2H, H6 and H6' of bpy), 7.50 (t, *J* = 7.6 Hz, 1H, H9 of bpz), 7.46 (d, *J* = 5.6 Hz, 1H, H5 of bpy), 7.42 – 7.40 (m, 2H, H9 of bpz and H5' of bpy), 7.29 – 7.20 (m, 6H, H3 and H10 of bpz and H2 and H4 of phenyl ring), 6.49 (d, *J* = 7.8 Hz, 1H, H2 of bpz), 6.48 (d, *J* = 7.9 Hz, 1H, H2 of bpz), 5.42 (s, 2H, CH_2 of bpy), 3.72 (s, 3H, CH_3 of sulfone), 2.45 (s, 3H, CH_3 of bpy). ^{13}C NMR (150 MHz, DMSO-d_6, 298 K, TMS): δ 166.1, 162.3, 161.6, 156.1, 155.2, 155.0, 154.9, 153.2, 151.1, 150.9, 149.2, 148.3, 145.6, 145.5, 143.6, 141.4, 141.3, 141.1, 141.0, 135.9, 135.8, 135.2, 133.2, 133.1, 132.2, 131.9, 131.8, 131.7, 131.6, 130.8, 130.7, 130.4, 130.0, 127.2, 126.6, 126.2, 123.0, 122.7, 122.6, 122.1, 116.5, 115.6, 67.7, 65.4, 43.4, 21.3, 15.6. IR (KBr) $\tilde{\nu}$/cm^{-1}: 1345 (S=O), 841 (PF_6^-). HR-ESI-MS (positive-ion mode, *m*/*z*): [M – PF_6^-]$^+$ calcd for $IrC_{53}H_{36}N_8O_4S$ 1073.2209, found 1073.1883. Elemental analysis calcd for $IrC_{53}H_{36}N_8O_4SPF_6$: C 51.76, H 3.52, N 7.40, found: C 51.52, H 3.50, N 7.56%.

[Ir(bpz)$_2$(bpy-ph)](PF$_6$) (4)

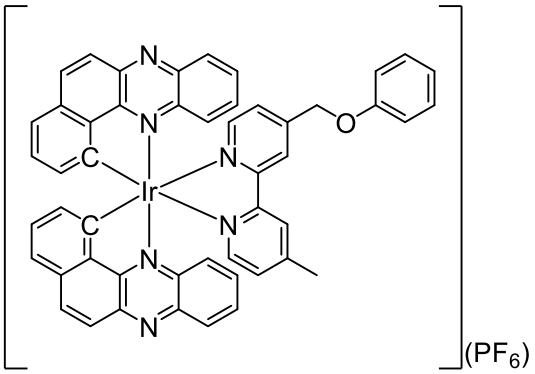

The synthetic procedure was similar to that for complex **1**, except that bpy-ph (17 mg, 0.06 mmol) was used instead of bpy-btz. Subsequent recrystallisation of the black solid from CH_2Cl_2/Et_2O afforded complex **4** as black crystals. Yield: 38 mg (59%). ^{1}H NMR (600 MHz,

DMSO-d_6, 298 K, TMS): δ 8.72 (s, 1H, H3 of bpy), 8.61 (s, 1H, H3' of bpy), 8.42 – 8.38 (m, 2H, H7 of bpz), 8.31 (dd, *J* = 9.3 and 2.4 Hz, 2H, H6 of bpz), 8.03 (dd, *J* = 9.2 and 4.6 Hz, 2H, H5 of bpz), 7.92 – 7.89 (m, 2H, H8 of bpz), 7.76 (d, *J* = 7.6 Hz, 2H, H4 of bpz), 7.62 (d, *J* = 5.6 Hz, 1H, H6 of bpy'), 7.59 (d, *J* = 6.1 Hz, 1H, H6' of bpy), 7.50 (t, *J* = 7.8 Hz, 1H, H9 of bpz), 7.45 (d, *J* = 5.9 Hz, 1H, H5 of bpy), 7.39 (d, *J* = 5.7 Hz, 1H, H5' of bpy), 7.32 – 7.27 (m, 4H, H9 and H10 of bpz and H3 and H5 of phenyl ring), 7.20 – 7.17 (m, 3H, H3 and H10 of bpz), 7.00 (t, *J* = 7.2 Hz, 1H, H4 of phenyl ring), 6.97 (d, *J* = 8.2 Hz, 2H, H2 and H6 of phenyl ring), 6.49 (d, *J* = 7.6 Hz, 1H, H2 of bpz), 6.46 (d, *J* = 7.4 Hz, 1H, H2 of bpz), 5.28 (s, 2H, CH_2 of bpy), 2.44 (s, 3H, CH_3 of bpy). ^{13}C NMR (150 MHz, DMSO-d_6, 298 K, TMS): δ 157.9, 156.0, 155.3, 155.0, 153.2, 151.9, 145.5, 143.6, 141.3, 141.1, 140.9, 135.8, 135.2, 133.2, 133.0, 132.2, 131.8, 131.6, 130.8, 130.3, 130.1, 127.2, 126.6, 123.0, 122.7, 122.5, 122.1, 112.0, 115.4, 67.4, 55.5, 31.2, 21.3. IR (KBr) $\tilde{\nu}$/cm^{-1}: 840 (PF_6^-). HR-ESI-MS (positive-ion mode, *m*/*z*): $[M - PF_6^-]^+$ calcd for $IrC_{50}H_{34}N_6O$ 927.2423, found 927.2269. Elemental analysis calcd for $IrC_{50}H_{34}N_6OPF_6$: C 54.24, H 3.36, N 7.53, found: C 54.22, H 3.09, N 7.59%.

Preparation of the Cysteine and Peptide Conjugates of Complex 2

A mixture of complex **2** (2.0 μmol) and L-cysteine or the cysteine-containing peptide (3.0 μmol) in potassium phosphate buffer (100 mM, pH 8.0)/DMF (1:1, *v*/*v*, 1 mL) containing TCEP (30 μmol) was stirred at 37°C in the dark for 30 min. The solution was diluted with a mixture of H_2O and CH_3CN (9 mL, *v*/*v*, 1:1) and purified, in batches, by semi-preparative reversed-phase HPLC (RP-HPLC). The HPLC purifications were performed on an Agilent semi-preparative column (ZORBAX Eclipse XDB-C18 column: 9.4 × 250 mm, 5 μm) using H_2O containing 0.1% (*v*/*v*) TFA (solvent A) and CH_3CN containing 0.1% (*v*/*v*) TFA (solvent B) as the solvents with a linear gradient of 50 – 100% B over 20 min and a flow rate of 4 mL min^{-1}. The detector was set at 210 or 350 nm and fractions containing the product were combined and lyophilised. The purified product was characterised by analytical RP-HPLC and ESI-MS (Fig. S12 and S13). The HPLC analyses were carried out using an Agilent analytical column (ZORBAX Eclipse Plus C18: 4.6 × 150 mm, 5 μm) with a linear gradient of 10 – 100% B over 20 min and a flow rate of 1 mL min^{-1}. **2-Cys**. Yield: 2.1 mg (85%). t_R = 14.10 min. Positive-ion ESI-MS ion cluster at *m*/*z* 1115.0 $[M - CF_3CO_2^-]^+$. **2-GE11**. Yield: 4.5 mg (81%). t_R = 16.18 min. Positive-ion ESI-MS ion clusters at *m*/*z* 879.9 $[M + 2 \times H^+ - CF_3CO_2^-]^{3+}$, 1318.8 $[M + H^+ - CF_3CO_2^-]^{2+}$. **2-ER**. Yield: 2.9 mg (84%). t_R = 17.02 min. Positive-ion ESI-MS ion cluster at *m*/*z* 822.0 $[M + H^+ - CF_3CO_2^-]^{2+}$. **2-NLS**. Yield: 3.5 mg (83%). t_R =14.05 min. Positive-ion ESI-MS ion clusters at *m*/*z* 661.0 $[M + 2 \times H^+ - CF_3CO_2^-]^{3+}$, 990.7 $[M + H^+ - CF_3CO_2^-]^{2+}$.

Preparation of the Protein Conjugates of Complex 2

A mixture of complex **2** (0.82 μmol) and BSA or HSA (0.164 μmol) in potassium phosphate

buffer (100 mM, pH 8.0)/DMSO (9:1, *v*/*v*, 200 μL) was incubated at 37°C in the dark for 12 h. The reaction mixture was centrifuged to remove any solid residue and the deep red supernatant was diluted to 1 mL with potassium phosphate buffer (50 mM, pH 7.4). The solution was loaded onto a PD-10 column (Cytiva) that had been equilibrated with the same buffer. The first red band that came out of the column was collected and the solution was concentrated with a YM-30 centricon (Amicon) to 100 μL. The labelled protein was further purified by HPLC equipped with a size-exclusion column (Agilent Bio SEC-3, 100 Å, 4.6 × 150 mm). The mobile phase was potassium phosphate buffer (50 mM, pH 7.4) at a flow rate of 0.4 mL min^{-1}. The retention time of the labelled protein was *ca*. 2.53 min. Iridium-to-protein ratios were estimated based on the absorption spectral data according to the following equation:

$$\frac{[\mathrm{Ir}]}{[\mathrm{Protein}]} = \frac{A_{380}\varepsilon_{280p}}{A_{280}\varepsilon_{380Ir} - A_{380}\varepsilon_{280Ir}}$$

where A_{280} and A_{380} are the absorbance values of the conjugates at 280 and 380 nm, respectively; ε_{280p} is the extinction coefficient of the protein at 280 nm; ε_{280Ir} and ε_{380Ir} are those of **2-Cys** at 280 and 380 nm, respectively. The iridium-to-protein ratios of **2-BSA** and **2-HSA** were determined to be *ca*. 0.98 and 0.75, respectively.

Kinetics Studies

All reactions were performed on a 100-μL scale. The reaction kinetics of bpy-btz, bpy-mstp, complexes **1** and **2** (25 μM) with L-cysteine (250 μM) and that of bpy-odz and complex **3** (25

μM) with L-cysteine (125 μM) in potassium phosphate buffer (100 mM, pH 8.0)/DMF (4:1, *v*/*v*) containing TCEP (750 μM) at 298 K was measured by RP-HPLC. The reactions at different time points were quenched by the addition of 900 μL of H_2O/MeOH (1:1, *v*/*v*) containing 0.1% TFA and then analysed by RP-HPLC. The second-order rate constants (k_2) were determined by fitting the data to the following equation:

$$y = \frac{ln\frac{[A]_o[B]_t}{[A]_t[B]_o}}{([B]_o - [A]_o)} = k_2 t$$

where $[A]_o$ and $[A]_t$ are the concentrations of the heteroaromatic methylsulfone-containing compound (ligand or complex) at time = 0 and t s, respectively; and $[B]_o$ and $[B]_t$ are the concentrations of cysteine at time = 0 and t s, respectively. All kinetic curves generated using OriginPro 8.0 software package are summarised in Fig. S5 and S6.

Determination of Singlet Oxygen ($^1O_2$) Generation Quantum Yields (Φ_Δ)

The $^1O_2$ generation quantum yields were determined via detecting the oxidation of DPBF using absorbance measurements.[10] The irreversible 1,4-cycloaddition reaction of DPBF with $^1O_2$ leads to a decrease in the absorbance of DPBF at *ca.* 418 nm. Freshly prepared, air-equilibrated solutions containing the samples or the standard $[Ru(bpy)_3]Cl_2$ (Φ_Δ = 0.73 in air-equilibrated MeOH and Φ_Δ = 0.22 in air-equilibrated H_2O)[11] with absorbance at 450 nm adjusted to 0.15 and DPBF (100 μM) were excited at 450 nm using a Xenon lamp (Ushio) (150 W) with a bandwidth of 20 nm. The decrease of the absorbance at 418 nm caused by photobleaching of DPBF was measured and corrected in all experiments. The following

equation was used for the calculation of Φ_Δ:

$$\Phi_\Delta^{unknown} = \Phi_\Delta^{reference} \times \frac{m^{unknown} \times F^{reference}}{m^{reference} \times F^{unknown}}$$

where *m* is the slope of a linear fit of the change of absorbance at 418 nm against the irradiation time and *F* is the absorption correction factor, which is given as $F = 1 - 10^{-AL}$ (*A* = absorbance at 450 nm and *L* = path length of the cuvette).

Stability of the Cysteine and Peptide Conjugates in Biological Media

After the cysteine and peptide conjugates of complex **2** (10 μM) were incubated in DMEM/DMSO (99:1, *v*/*v,* 200 μL) at 37°C for 0 or 4 h, 1 mL of MeOH was added to the mixture. The proteins and other precipitates from the plasma were separated solely by centrifugation. The supernatant was filtered and analysed by analytical RP-HPLC and ESI-MS.

Cell Cultures

MDA-MB-231 and HEK-293T cells were cultured in DMEM containing 10% FBS and 1% penicillin/streptomycin in an incubator at 37°C under a 5% CO_2 atmosphere. A431 cells were cultured in MEM with 10% FBS, 1% penicillin/streptomycin and 1% sodium pyruvate at 37°C under a 5% CO_2 atmosphere. They were subcultured every 2 – 3 days.

Determination of Cellular Uptake by Inductively Coupled Plasma-Mass Spectrometry (ICP-MS)

MDA-MB-231, A431 and HEK-293T cells were grown in a 50-mm tissue culture dish and incubated at 37°C under a 5% CO_2 atmosphere for 48 h. The culture medium was removed and replaced with a fresh medium containing the conjugates of complex **2** (10 μM) or the methylsulfone-free complex **4** (10 μM). After incubation at 37°C under a 5% CO_2 atmosphere for 4 h (for the conjugates of complex **2**) or 1 h (for complex **4**), the medium was removed and the cell layer was washed gently with PBS (1 mL × 3). The cell layer was then trypsinised and 1 mL of the mixture was put in a 1.5-mL Eppendorf centrifuge tube. The cell number was counted with a Logos Biosystems LUNA-II automated cell counter. The harvested cells were digested with 65% HNO_3 (1 mL) at 60°C for 2 h and the iridium contents were analysed with a PerkinElmer NexION 2000 ICP-MS.

Live-Cell Confocal Imaging

MDA-MB-231, A431 and HEK-293T cells in growth medium were seeded on a sterilised coverslip in a 35-mm tissue culture dish and grown at 37°C under a 5% CO_2 atmosphere for 48 h. The growth medium was removed and replaced with the conjugates of complex **2** (10 μM, 4 h) or complex **4** (1 μM, 30 min) in growth medium/DMSO (99:1, *v*/*v*) at 37°C under a 5% CO_2 atmosphere. The medium was removed and the cell layer was gently washed with PBS (1 mL × 3). The coverslip was mounted onto a sterilised glass slide and then imaging was performed using a Leica TCS SPE confocal microscope with an oil immersion 63× objective and an excitation wavelength at 488 nm. In costaining experiments, after treatment with the

conjugates of complex **2** (10 μM, 4 h) or complex **4** (1 μM, 30 min), the medium was removed and the cell layer was gently washed with PBS (1 mL × 3). The cells were then incubated with LysoTracker Green (100 nM, 20 min), MitoTracker Green (100 nM, 20 min) or CellMask Deep Red (5 μg mL^{-1}, 10 min) in growth medium at 37°C under a 5% CO_2 atmosphere. The medium was then removed and the cell layer was gently washed with PBS (1 mL × 3). The excitation wavelength of LysoTracker Green and MitoTracker Green was 488 nm and that of CellMask Deep Red was 635 nm. The Pearson's correlation coefficients were determined using the programme ImageJ (Version 1.4.3.67).

MTT Assays

MDA-MB-231 cells were seeded in a 96-well flat-bottomed microplate (*ca.* 10,000 cells per well) in growth medium (100 μL) and incubated at 37°C under a 5% CO_2 atmosphere for 48 h. The growth medium was removed and replaced with the conjugates of complex **2** or complex **4** in growth medium/DMSO (99:1, *v*/*v*) at 37°C under a 5% CO_2 atmosphere for 24 or 48 h. The medium was removed and MTT in PBS (10 μL, 5 mg mL^{-1}) was added to each well. The microplates were incubated at 37°C under a 5% CO_2 atmosphere for 4 h. The growth medium was removed and DMSO (100 μL) was added to each well. The microplates were further incubated at 37°C under a 5% CO_2 atmosphere for 15 min. The absorbance of the solutions at 570 nm was measured with a SPECTRAmax 340 microplate reader (Molecular Devices Corp., Sunnyvale, CA).

LDH Assays

MDA-MB-231 cells were seeded in two 96-well flat-bottomed microplates (*ca.* 10,000 cells per well) in growth medium (100 μL) and incubated at 37°C under a 5% CO_2 atmosphere for 48 h. The culture medium was removed and replaced with the conjugates of complex **2** or complex **4** in growth medium/DMSO (99:1, *v*/*v*). After incubation for 24 or 48 h, medium of each sample well (50 μL) was transferred to a new 96-well flat bottom plate, followed by the addition of LDH reaction mixture (50 μL). The mixed solution was incubated in the dark at 25°C for 30 min, then stop solution (50 μL) was added to each sample well. The absorbance of the solutions at 490 nm was measured with a SPECTRAmax 340 microplate reader (Molecular Devices Corp., Sunnyvale, CA). Culture medium and complete lysate of cells without treatment were used for the detection of LDH background and maximal value, respectively. All LDH values were calculated by subtraction of the background value and normalised to the mean maximal value.

Annexin V/PI Assays

MDA-MB-231 cells in growth medium were grown in a 35-mm tissue culture dish at 37°C under a 5% CO_2 atmosphere for 48 h. After incubation with the cysteine and peptide conjugates (5 μM) and protein conjugates (10 μM) of complex **2** and complex **4** (0.5 μM) for 24 or 48 h, the medium was removed and the cell layer was washed gently with PBS (1 mL × 3). The cell layer was then trypsinised and centrifuged at 1,500 rpm for 1 min. The cell pellet was washed with PBS (1 mL) and subjected to centrifugation. The cells were resuspended in an annexin V binding buffer (100 μL) in the flow cytometer tubes, followed by the addition

of Alexa Fluor 647 annexin V conjugate (5 μL) and PI (2 μL, 100 μg mL^{-1}). The cell suspension was kept in the dark for 15 min. The annexin V binding buffer (400 μL) was added to the suspension before analysis by flow cytometer (Beckman CytoFLEX). The untreated cultured cells were used as a control group for background correction. The experiments were performed in triplicates and analysed using the FlowJo V10 software.

Photocytotoxicity MTT Assays

MDA-MB-231, A431 and HEK-293T cells were seeded in two 96-well flat-bottomed microplates (*ca.* 10,000 cells per well) in growth medium (100 μL) and incubated at 37°C under a 5% CO_2 atmosphere for 24 h. The growth medium was removed and replaced with the conjugates of complex **2** or complex **4** in growth medium/DMSO (99:1, *v*/*v*) at 37°C under a 5% CO_2 atmosphere for 4 h. After treatment, the medium was removed, the cells were washed with PBS (100 μL) and phenol red-free growth medium (100 μL) was added to each well. One of the microplates was irradiated at λ_{ex} = 450 nm (10 mW cm^{-2}) with an LED cellular photocytotoxicity irradiator (PURI Materials, Shenzhen, China) for 20 min, whereas the other one was kept in the dark. The cells were then replenished with fresh growth medium (100 μL) and further incubated at 37°C under a 5% CO_2 atmosphere for 24 h. Then, MTT in PBS (10 μL, 5 mg mL^{-1}) was added to each well. The microplates were incubated at 37°C under a 5% CO_2 atmosphere for 4 h. The growth medium was removed and DMSO (100 μL) was added to each well. The microplates were further incubated at 37°C under a 5% CO_2 atmosphere for 15 min. The absorbance of the solutions at 570 nm was measured with a SPECTRAmax 340 microplate reader (Molecular Devices Corp., Sunnyvale, CA).

Results of MTT Assays, LDH Assays and Annexin V/PI Assays

MDA-MB-231 cells were treated with the conjugates of complex **2** (**2-Cys**, **2-ER**, **2-GE11**, **2-NLS**, **2-BSA** and **2-HSA**) and the methylsulfone-free complex **4** at different incubation times (24 and 48 h) prior to analyses by the MTT, LDH and Annexin V/PI assays. MTT assays indicated that all the conjugates of complex **2** displayed moderate cytotoxicity upon incubation for 24 h ($IC_{50} > 14.29$ μM) and 48 h ($IC_{50} > 6.76$ μM), while complex **4** exhibited much higher cytotoxicity (IC_{50} = 0.66 and 0.74 μM for 24 and 48 h, respectively) (Table S3 and Fig. S21). Upon increasing the incubation time from 24 to 48 h, the cysteine and peptide conjugates of complex **2** showed increased cytotoxic activity, while there were no obvious changes for the protein conjugates of complex **2** and complex **4**. Comparing to other transition metal-based serum albumin nanoparticles, the protein conjugates displayed relatively low cytotoxicity (9 – 70 μM),[12] which is an attractive feature for photodynamic therapy.[13] The determination of the IC_{90} values of the conjugates of complex **2** and complex **4** was attempted. Unfortunately, the IC_{90} values of the conjugates of complex **2** cannot be determined as the highest concentrations of the peptide and protein conjugates tested were limited to *ca.* 20 and 200 μM, respectively, due to solubility reasons, and at these concentrations, the cell viability was > 10%. The IC_{90} values of complex **4** were determined to be 3.52 and 4.30 μM for an incubation period of 24 and 48 h, respectively. According to LDH leakage results, incubation of the cells with the conjugates caused less than 40% of the total LDH released to the medium at all the concentrations or incubation times studied (Fig. S22). However, the total LDH release was up to 66% for complex **4** at 5 μM, suggesting that this complex induced necrotic cell death, which is characterised by significant plasma membrane

damage.[14] The cell death mechanisms of the conjugates of complex **2** and complex **4** were further investigated by annexin V/PI assays using flow cytometry. High populations of apoptotic cells (annexin V^+/PI^-) were found in the cells incubated with the conjugates of complex **2** for 24 and 48 h, suggesting that apoptosis is the major cell death mechanism for these conjugates.[15] For complex **4**, high populations of necrotic cells (annexin V^-/PI^+) were observed, indicating that necrosis is the main mode of cell death for this complex.[16]

Table S1. Electronic absorption spectral data of complexes **1** – **4** in CH_2Cl_2 and CH_3CN at 298 K.

Complex	Solvent	λ_{abs}/nm (ε/dm^3 mol^{-1} cm^{-1})
1	CH_2Cl_2	276 (85,795), 299 sh (61,795), 342 (16,315), 373 (13,940), 426 (14,810), 550 (8,140)
	CH_3CN	274 (64,480), 297 sh (45,820), 341 (13,200), 374 (10,585), 425 (11,425), 544 (5,790)
2	CH_2Cl_2	275 (85,510), 299 sh (48,325), 342 (15,380), 374 (13,180), 427 (14,320), 550 (7,630)
	CH_3CN	273 (71,480), 298 sh (39,390), 342 (14,065), 373 (13,375), 423 (13,170), 545 (6,545)
3	CH_2Cl_2	275 (85,700), 299 sh (52,590), 343 (12,675), 372 (10,765), 427 (11,450), 550 (5,660)
	CH_3CN	274 (65,075), 297 sh (40,300), 341 (12,980), 372 (8,765), 425 (9,650), 549 (4,770)
4	CH_2Cl_2	275 (81,640), 299 sh (47,660), 343 (15,555), 372 (13,260), 426 (14,395), 548 (6,690)
	CH_3CN	274 (58,780), 299 sh (32,595), 340 (12,160), 372 (9,730), 424 (11,195), 544 (5,815)

Table S2. Photophysical data and $^1O_2$ generation quantum yields of the conjugates of complex **2** at 298 K. $[Ru(bpy)_3]Cl_2$ was used as the reference (Φ_{em} = 0.04 in aerated H_2O,[7] Φ_Δ = 0.73 and 0.22 in aerated MeOH and H_2O,[11] respectively).

Conjugate	Solvent	λ_{em}/nm	τ_o/μs	Φ_{em}	Φ_Δ
2-Cys	Buffer[a]	710	0.18	0.0016	0.86[c]
2-GE11	Buffer[a]	710	0.15	0.0013	0.61[c]
2-ER	Buffer[a]	710	0.17	0.0018	0.74[c]
2-NLS	Buffer[a]	710	0.17	0.0018	0.79[c]
2-BSA	H_2O[b]	685	1.35 (82%), 0.26 (18%)	0.0094	0.17[d]
2-HSA	H_2O[b]	693	1.02 (86%), 0.18 (14%)	0.0048	0.11[d]

[a] Degassed potassium phosphate buffer (50 mM, pH 7.4)/MeOH (1:1, *v*/*v*).

[b] Degassed H_2O.

[c] In aerated MeOH.

[d] In aerated H_2O.

Table S3. Cytotoxicity (IC_{50}) of the conjugates of complex **2** and the methylsulfone-free complex **4** toward MDA-MB-231 cells determined by MTT assays.

Compound	IC_{50}/μM	
	24 h	48 h
2-Cys	15.54 ± 0.26	9.12 ± 0.93
2-ER	16.91 ± 0.02	11.57 ± 0.53
2-GE11	> 20	> 20
2-NLS	14.29 ± 0.12	6.76 ± 0.51
2-BSA	29.33 ± 0.72	32.55 ± 4.17
2-HSA	37.20 ± 0.85	38.62 ± 2.95
4	0.66 ± 0.01	0.74 ± 0.07

Table S4. Cellular uptake of the conjugates of complex **2** and the methylsulfone-free complex **4** toward MDA-MB-231, A431 and HEK-293T cells.

Compound	Amount of iridium per cell[a]/fmol		
	MDA-MB-231	A431	HEK-293T
2-Cys[b]	1.57 ± 0.03	1.82 ± 0.03	0.24 ± 0.03
2-GE11[b]	2.62 ± 0.04	1.95 ± 0.04	0.13 ± 0.01
2-ER[b]	1.17 ± 0.01	1.25 ± 0.02	0.15 ± 0.02
2-NLS[b]	1.40 ± 0.02	1.58 ± 0.01	0.32 ± 0.01
2-BSA[b]	0.77 ± 0.01	0.82 ± 0.01	0.06 ± 0.001
2-HSA[b]	0.95 ± 0.01	1.52 ± 0.01	0.15 ± 0.002
4[c]	1.76 ± 0.04	1.87 ± 0.05	1.66 ± 0.04

[a] Amount of iridium associated with an average cell upon incubation with the conjugates of complex **2** and the methylsulfone-free complex **4** (10 μM) at 37°C, as determined by ICP-MS.

[b] Incubation time = 4 h.

[c] Incubation time = 1 h due to the high cytotoxicity of complex **4**.

Table S5. Normalised (photo)cytotoxicity (IC_{50}) of the conjugates of complex **2** and complex **4** toward MDA-MB-231, A431 and HEK-293T cells determined by MTT assays. The cells were first incubated with the conjugates or complex **4** in the dark for 4 h, then washed thoroughly with PBS, incubated in the dark or irradiated at 450 nm (10 mW cm^{-2}) for 20 min, and subsequently incubated in the dark for 24 h. The values were estimated on the basis of the cellular uptake data (Table S4). Photocytotoxicity index (PI) = $IC_{50,dark}/IC_{50,light}$.

Compound	MDA-MB-231			A431			HEK-293T		
	$IC_{50,dark}/\mu M$	$IC_{50,light}/\mu M$	PI	$IC_{50,dark}/\mu M$	$IC_{50,light}/\mu M$	PI	$IC_{50,dark}/\mu M$	$IC_{50,light}/\mu M$	PI
2-Cys	> 2212	6.42	> 345	> 1726	13.25	> 130	> 292	6.39	> 46
2-GE11	> 2370	264.34	> 9	> 2878	58.44	> 49	> 159	80.01	> 2
2-ER	> 1520	33.38	> 46	> 1286	18.60	> 69	> 183	28.15	> 7
2-NLS	> 1920	8.21	> 234	> 1538	12.26	> 125	> 390	24.68	> 16
2-BSA	1412.33	11.67	121	1954.68	8.32	235	181.72	0.89	204
2-HSA	2299.19	23.02	100	2769.21	12.37	224	184.97	3.94	47
4	668.33	16.44	41	556.64	5.68	98	952.29	20.24	47

Fig. S1. Electronic absorption spectra of complexes **1** – **4** in CH_2Cl_2 (red) and CH_3CN (blue) at 298 K.

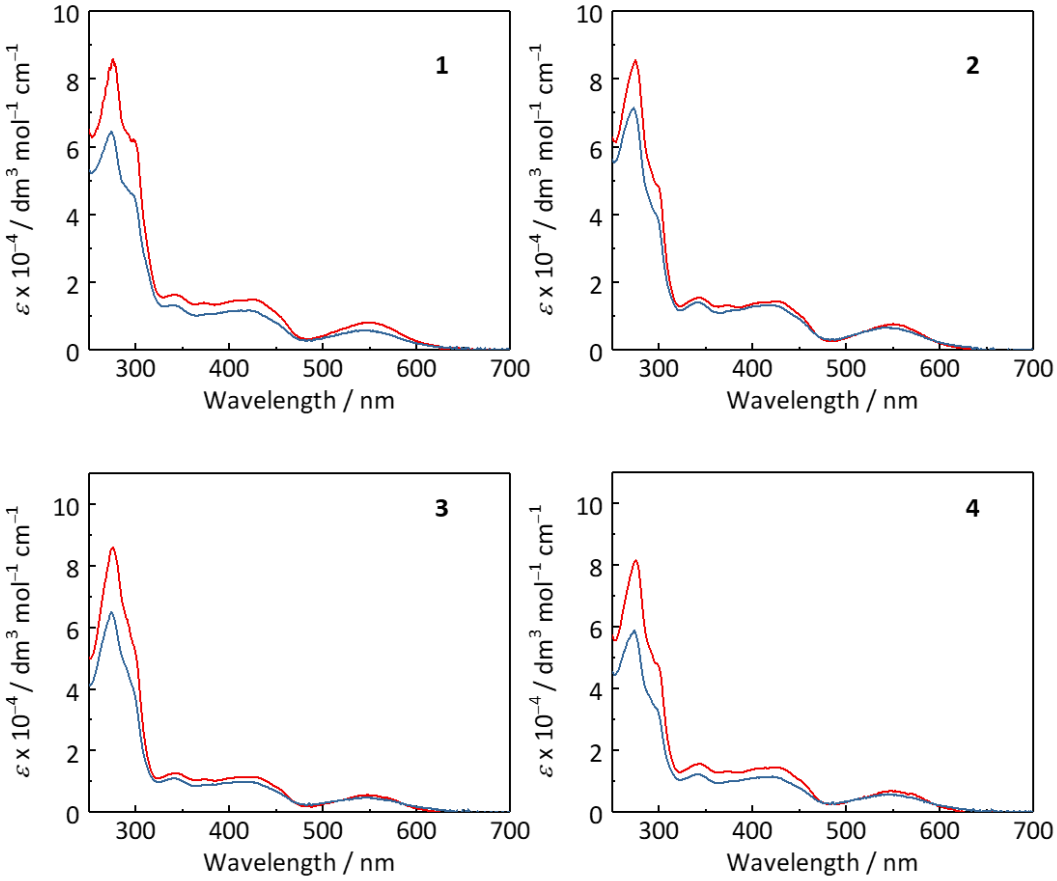

Fig. S2. Normalised emission spectra of complexes **1** – **4** in degassed CH_2Cl_2 (red) and CH_3CN (blue) at 298 K. Excitation wavelength = 350 nm.

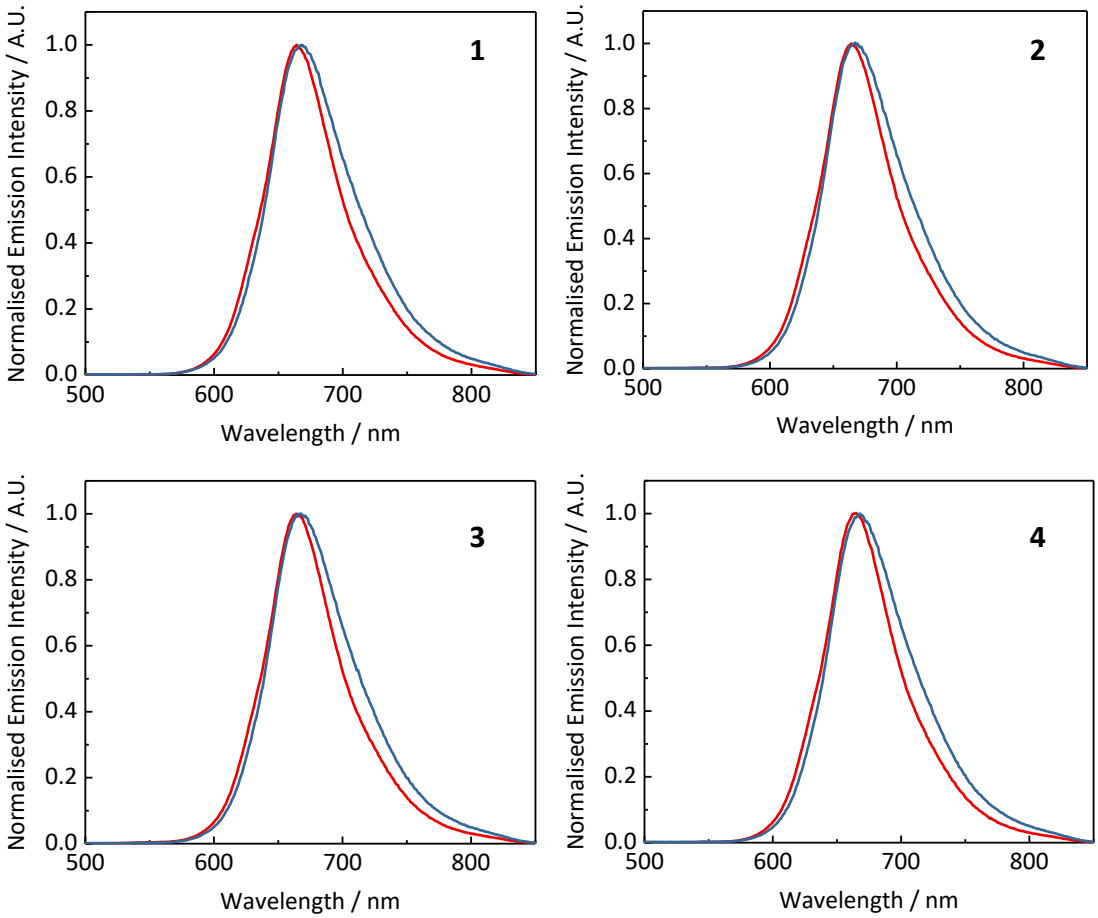

Fig. S3. HPLC chromatograms of complexes **1** – **3** (25 μM) (a, c and e) and the reaction mixtures of complexes **1** – **3** (25 μM) and L-cysteine (250 μM) (b, d and f) in potassium phosphate buffer (100 mM, pH 8.0)/DMF (4:1, *v*/*v*) containing TCEP (750 μM) after incubation at 37°C for 2 h (complex **1**) or 5 min (complexes **2** and **3**). The absorbance was monitored at 210 nm.

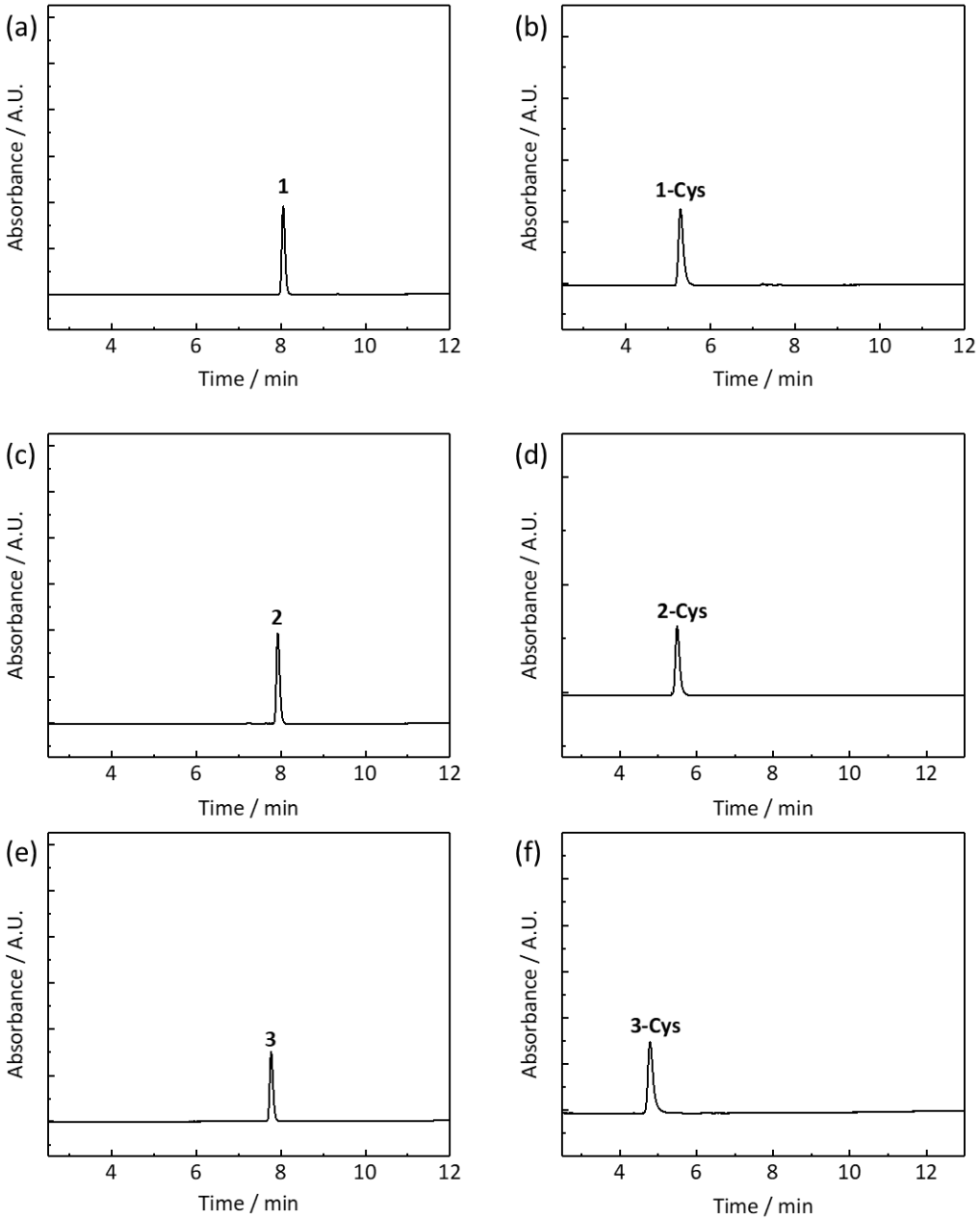

Fig. S4. ESI mass spectra of the reaction mixtures of (a) complex **1** (25 μM), (b) complex **2** (25 μM) and (c) complex **3** (25 μM) with L-cysteine (250 μM) in potassium phosphate buffer (100 mM, pH 8.0)/DMF (4:1, *v*/*v*) containing TCEP (750 μM) after incubation at 37°C for 2 h (complex **1**) or 5 min (complexes **2** and **3**).

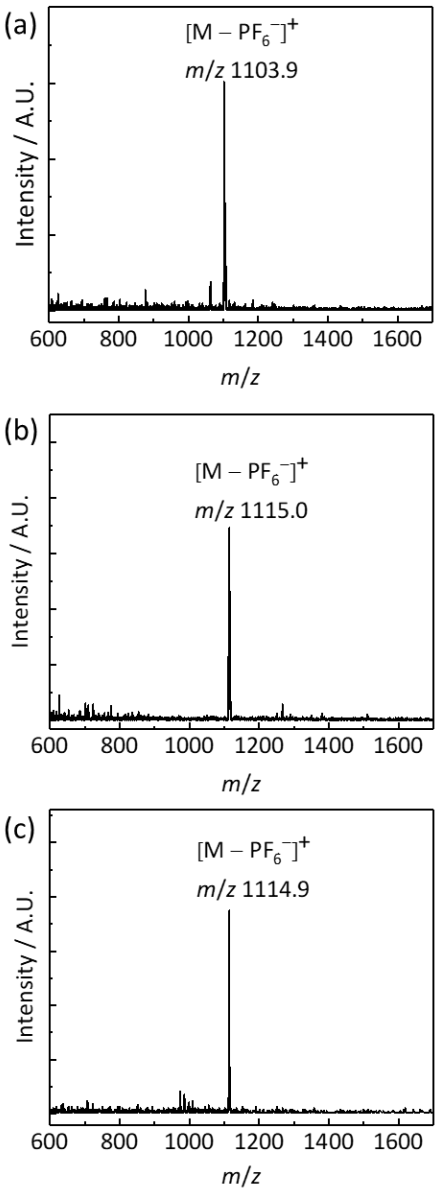

Fig. S5. Second-order kinetics for the reactions of (a) complex **1** (25 μM), (b) complex **2** (25 μM) and (c) complex **3** (25 μM) with L-cysteine (250 μM for complexes **1** and **2**; 125 μM for complex **3**) in potassium phosphate buffer (100 mM, pH 8.0)/DMF (4:1, *v*/*v*) containing TCEP (750 μM) after incubation at 37°C for different time periods. The slope of the linear fit corresponds to the k_2 of the reaction.

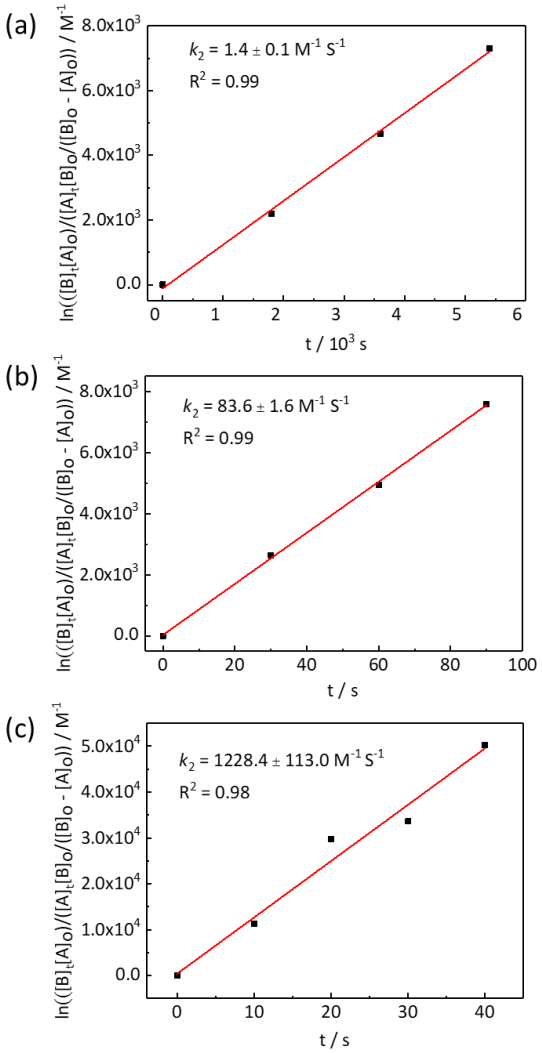

Fig. S6. Second-order kinetics for the reactions of (a) bpy-btz (25 μM), (b) bpy-mstp (25 μM) and (c) bpy-odz (25 μM) with L-cysteine (250 μM for ligands bpy-btz and bpy-mstp; 125 μM for bpy-odz) in potassium phosphate buffer (100 mM, pH 8.0)/DMF (4:1, *v*/*v*) containing TCEP (750 μM) after incubation at 37°C for different time periods. The slope of the linear fit corresponds to the k_2 of the reaction.

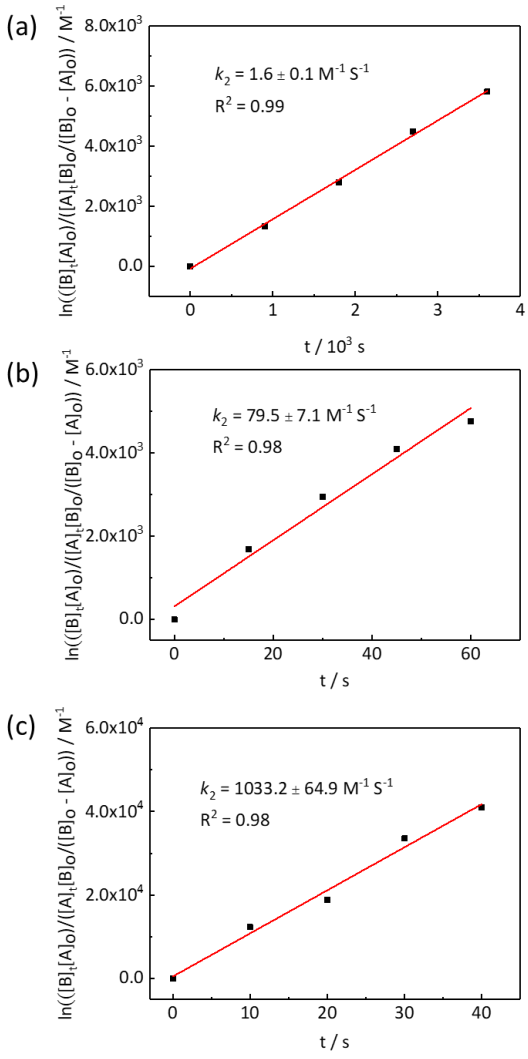

Fig. S7. HPLC chromatograms of (a) complex **1** (25 μM), (b) complex **2** (25 μM) and (c) complex **3** (25 μM) after incubation in potassium phosphate buffer (100 mM, pH 8.0)/DMF (4:1, *v*/*v*) at 37°C for 0 and 12 h. The absorbance was monitored at 350 nm.

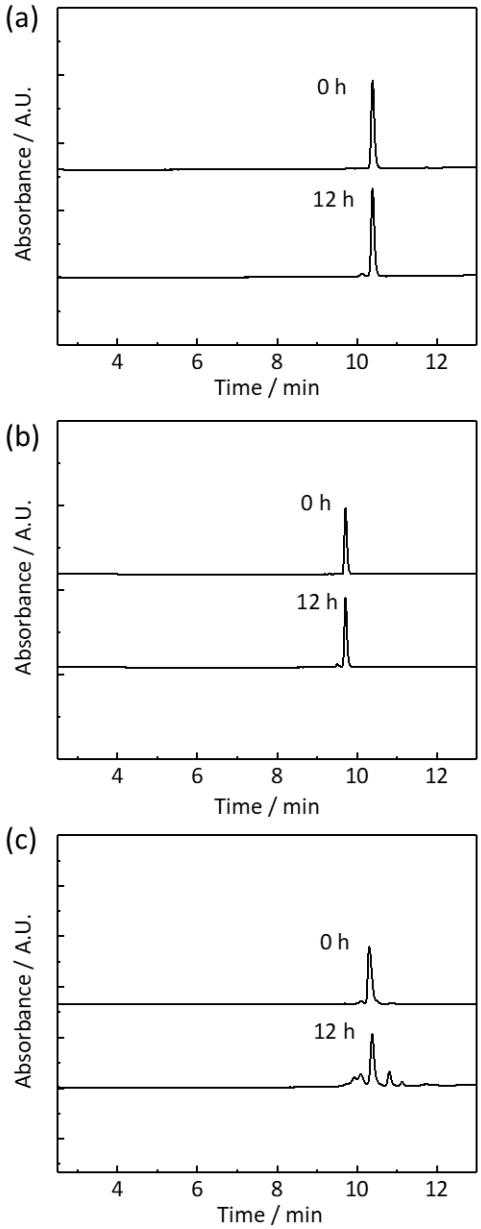

Fig. S8. ESI mass spectra of a mixture of complex **2** (25 μM) with (a) L-lysine (250 μM), (b) L-histidine (250 μM) and (c) L-serine (250 μM) in potassium phosphate buffer (100 mM, pH 8.0)/DMF (4:1, *v*/*v*) after incubation at 37°C for 0 and 12 h.

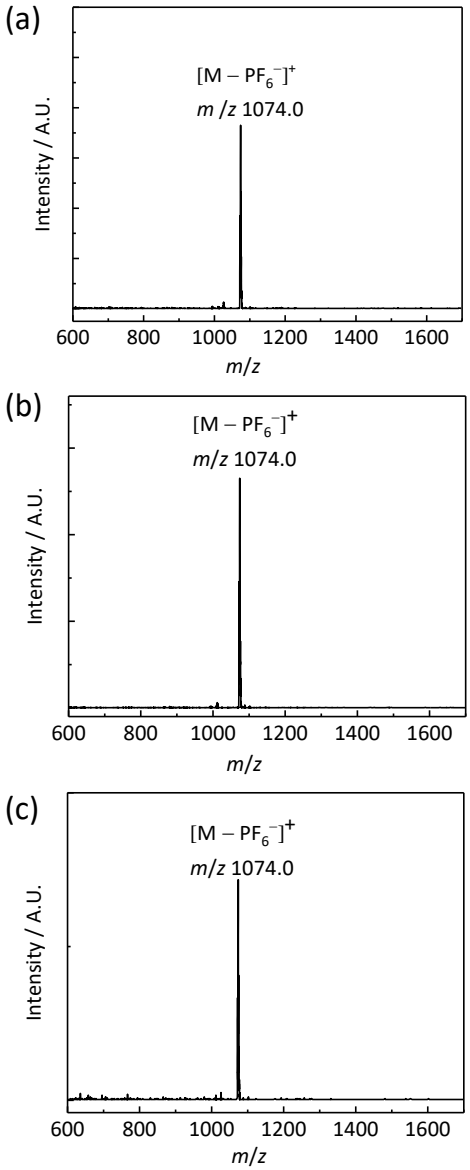

Fig. S9. HPLC chromatograms of (a) complex **2** (25 μM), (b) GE11 (250 μM) and (c) a reaction mixture of complex **2** (25 μM) and GE11 (250 μM) in potassium phosphate buffer (100 mM, pH 8.0)/DMF (4:1, *v*/*v*) containing TCEP (750 μM) after incubation at 37°C for 30 min. The absorbance was monitored at 210 nm.

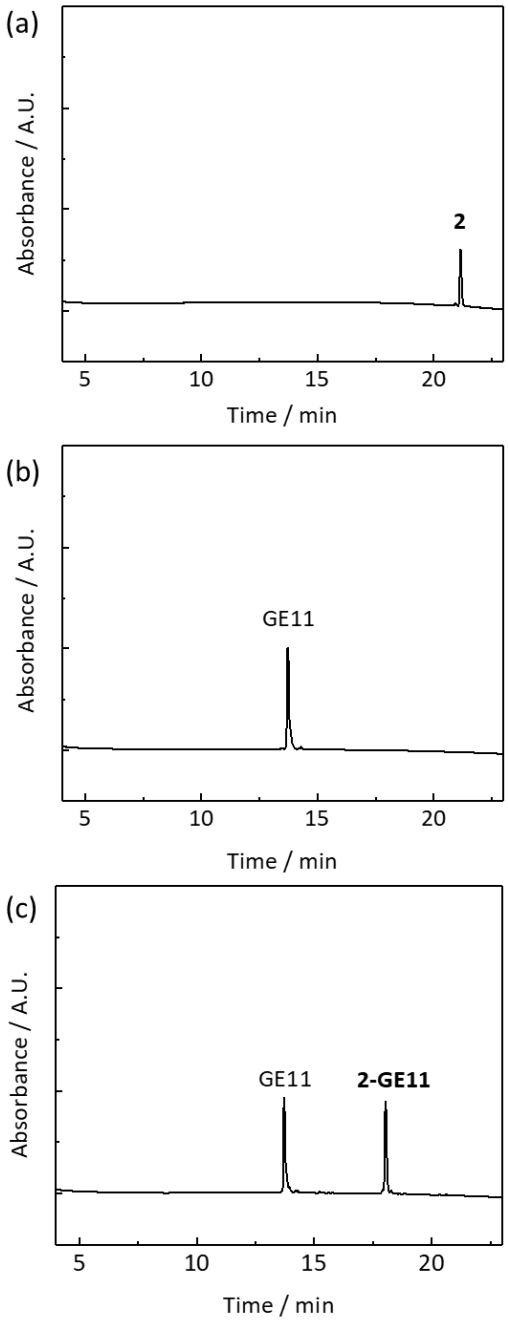

Fig. S10. HPLC chromatograms of (a) complex **2** (25 μM) and (b) a reaction mixture of complex **2** (25 μM) and ER (250 μM) in potassium phosphate buffer (100 mM, pH 8.0)/DMF (4:1, *v*/*v*) containing TCEP (750 μM) after incubation at 37°C for 30 min. The absorbance was monitored at 210 nm.

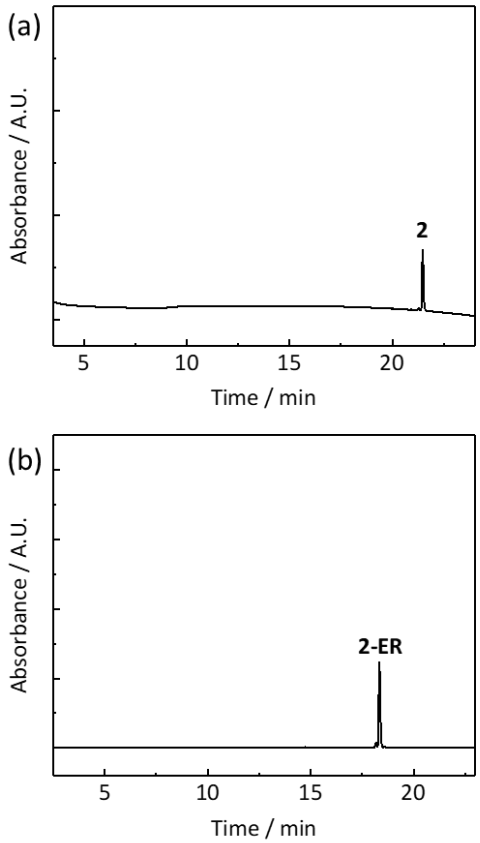

Fig. S11. HPLC chromatograms of (a) complex **2** (25 μM), (b) NLS (250 μM) and (c) a reaction mixture of complex **2** (25 μM) and NLS (250 μM) in potassium phosphate buffer (100 mM, pH 8.0)/DMF (4:1, *v*/*v*) containing TCEP (750 μM) after incubation at 37°C for 30 min. The absorbance was monitored at 210 nm.

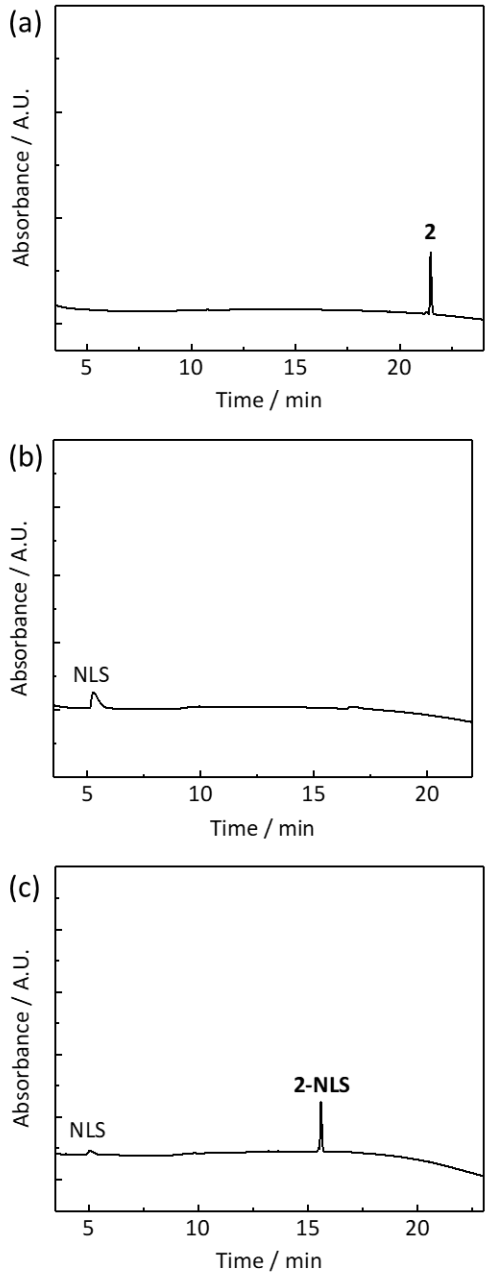

Fig. S12. HPLC chromatograms of purified **2-Cys**, **2-GE11**, **2-ER** and **2-NLS**. The absorbance was monitored at 350 nm.

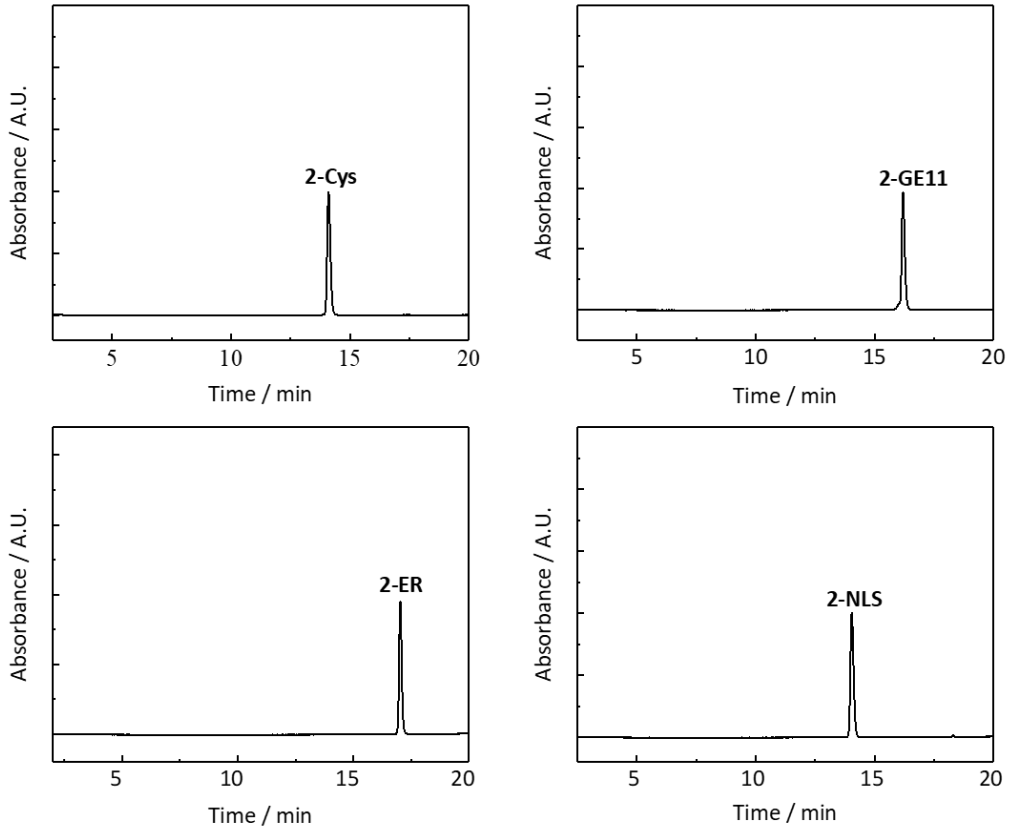

Fig. S13. ESI mass spectra of purified (a) **2-Cys**, (b) **2-GE11**, (c) **2-ER** and (d) **2-NLS**.

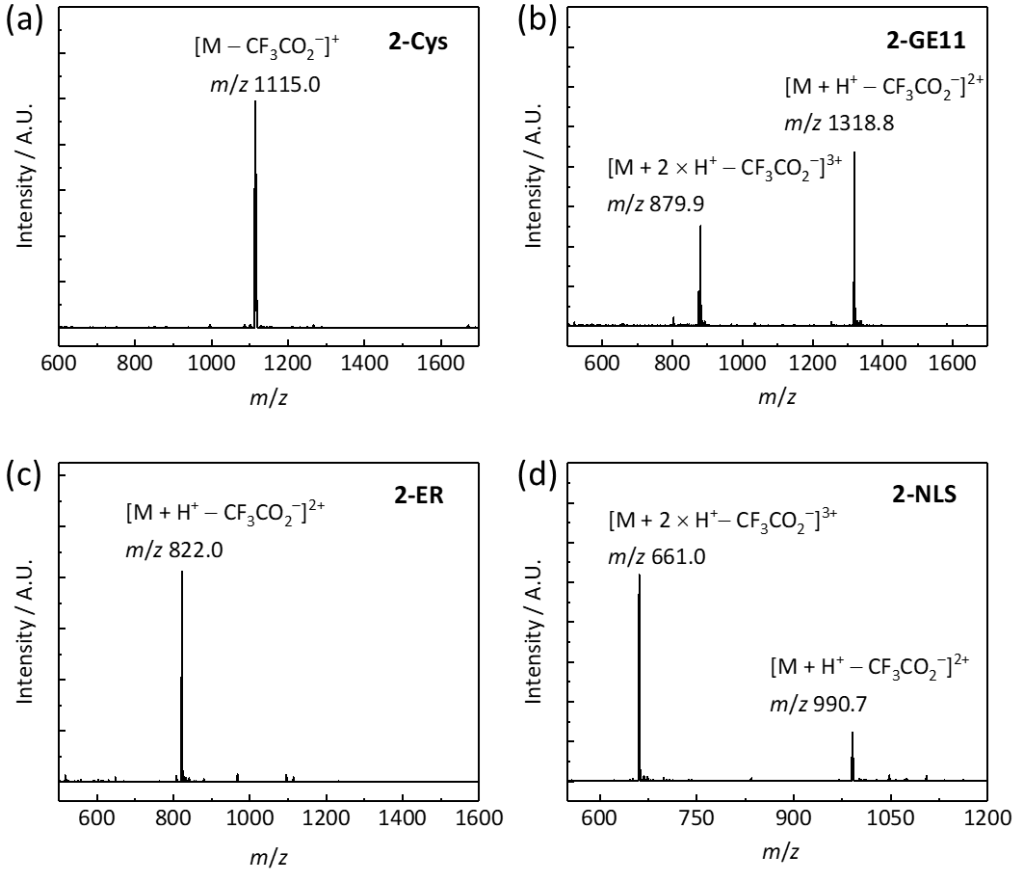

Fig. S14. MALDI-TOF mass spectra of BSA (red) and **2-BSA** (blue).

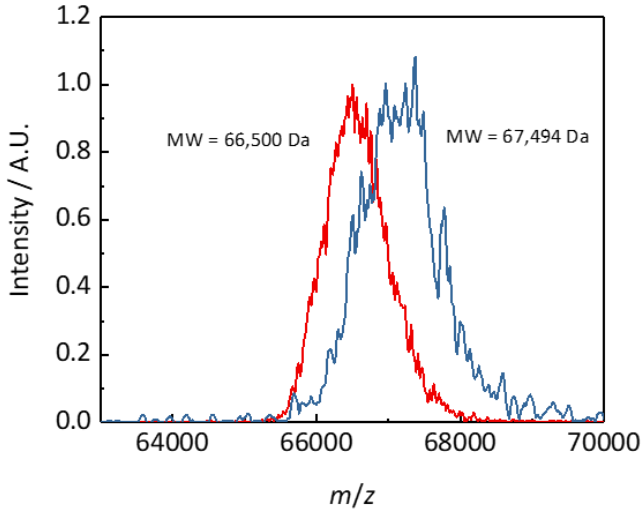

Fig. S15. MALDI-TOF mass spectra of HSA (red) and **2-HSA** (blue).

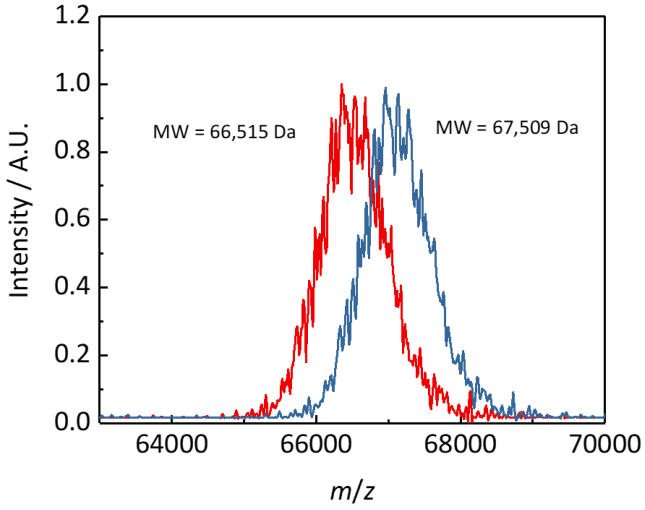

Fig. S16. HPLC chromatograms of (a) **2-Cys** (10 μM), (b) **2-GE11** (10 μM), (c) **2-ER** (10 μM) and (d) **2-NLS** (10 μM) after incubation in DMEM/DMSO (9:1, *v*/*v*) at 37°C for 0 or 4 h. The absorbance was monitored at 350 nm.

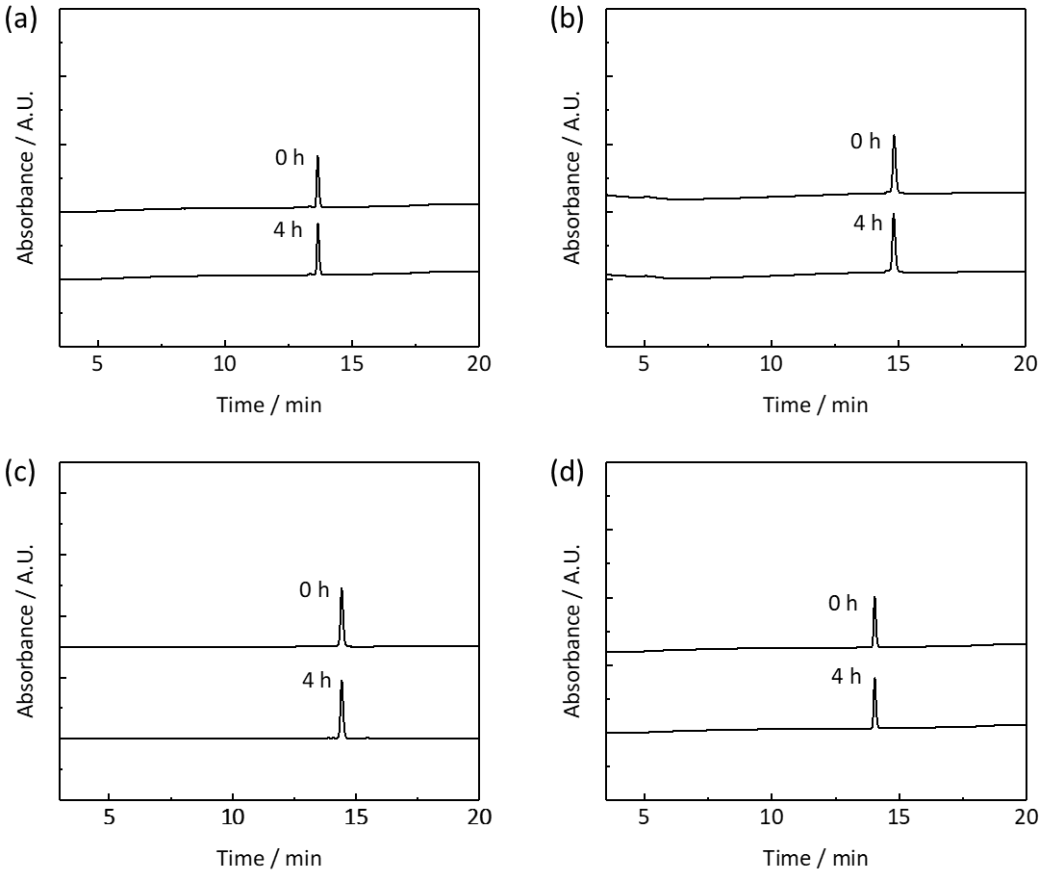

Fig. S17. ESI mass spectra of (a) **2-Cys** (10 μM), (b) **2-GE11** (10 μM), (c) **2-ER** (10 μM) and (d) **2-NLS** (10 μM) after incubation in DMEM/DMSO (9:1, *v*/*v*) at 37°C for 4 h.

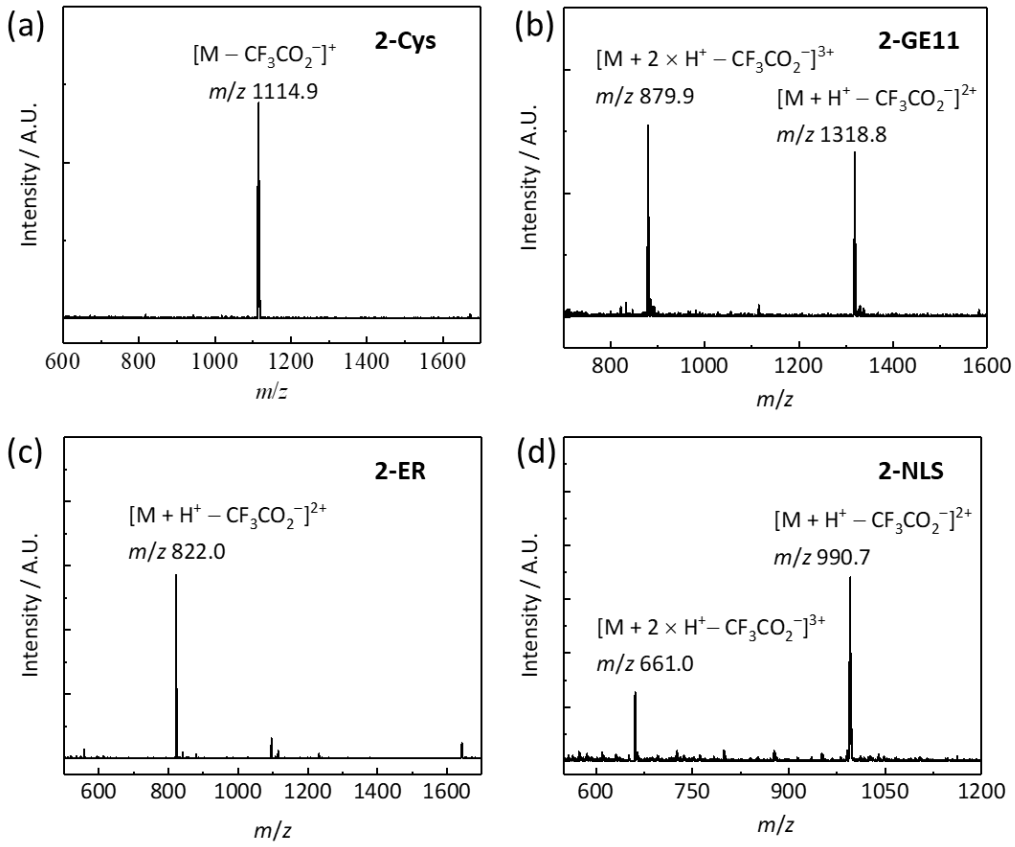

Fig. S18. DLS analysis of (a) **2-Cys** (5 μM), (b) **2-GE11** (5 μM), (c) **2-ER** (5 μM), (d) **2-NLS** (5 μM), (e) **2-BSA** (5 μM) and (f) **2-HSA** (5 μM) in DMEM/DMSO (99:1, *v*/*v*).

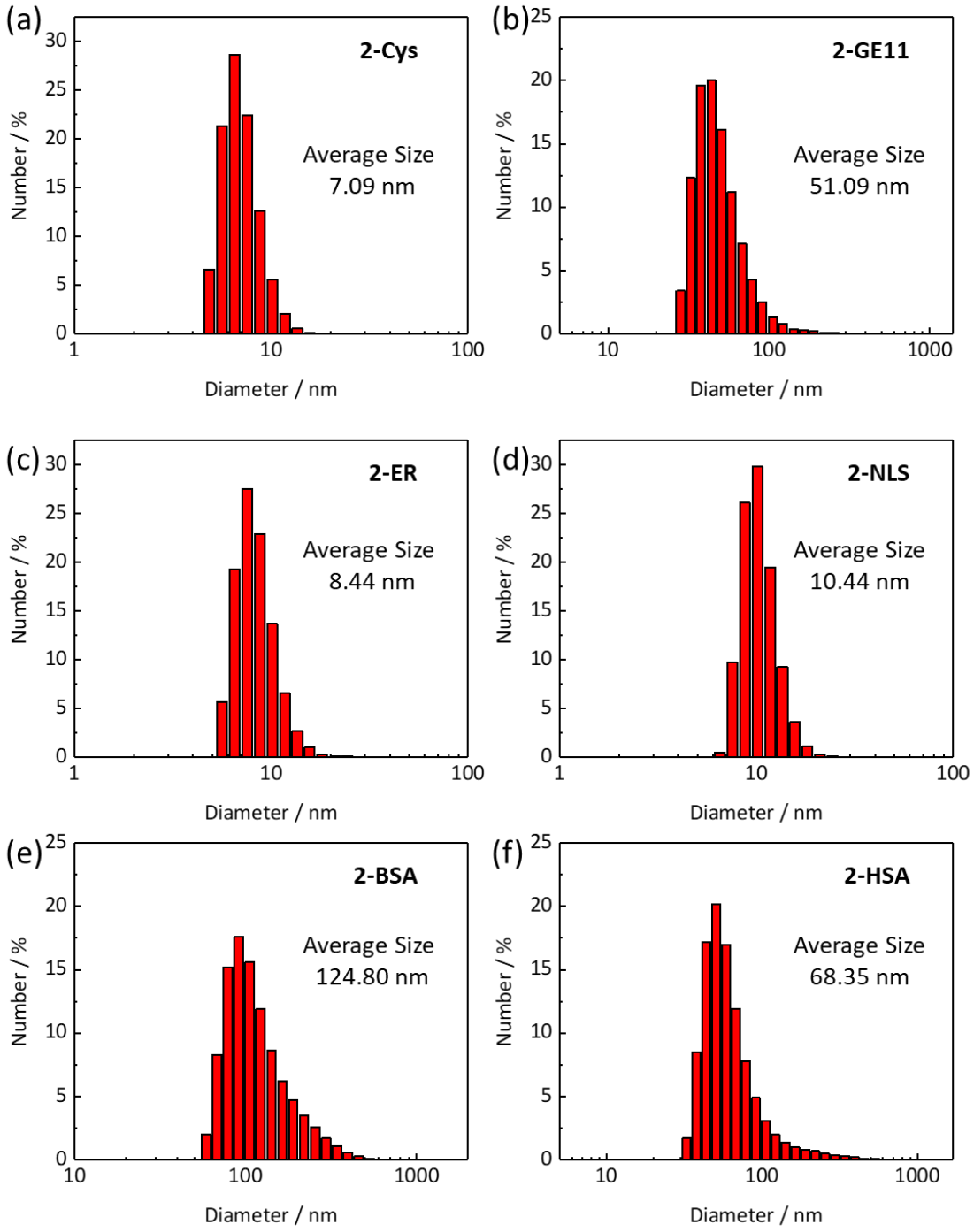

Fig. S19. LSCM images of MDA-MB-231, A431 and HEK-293T cells incubated with complex **4** (1 μM, 30 min, λ_{ex} = 488 nm, λ_{em} = 650 – 750 nm) at 37°C. Scale bar = 25 μm.

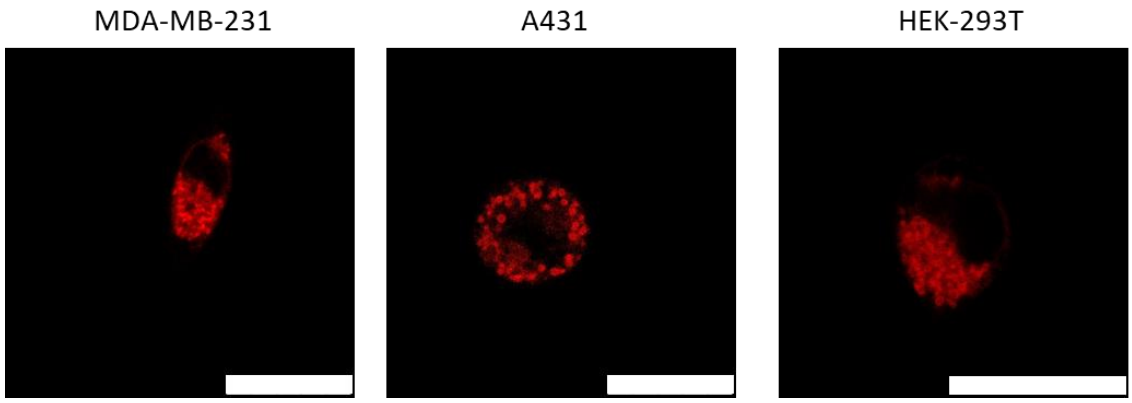

Fig. S20. LSCM images of MDA-MB-231 cells incubated with complex **4** (1 μM, 30 min, λ_{ex} = 488 nm, λ_{em} = 650 – 750 nm) and then with MitoTracker Green (100 nM, 20 min, λ_{ex} = 488 nm, λ_{em} = 506 – 526 nm) at 37°C. Scale bar = 25 μm. Pearson's correlation coefficient = 0.84.

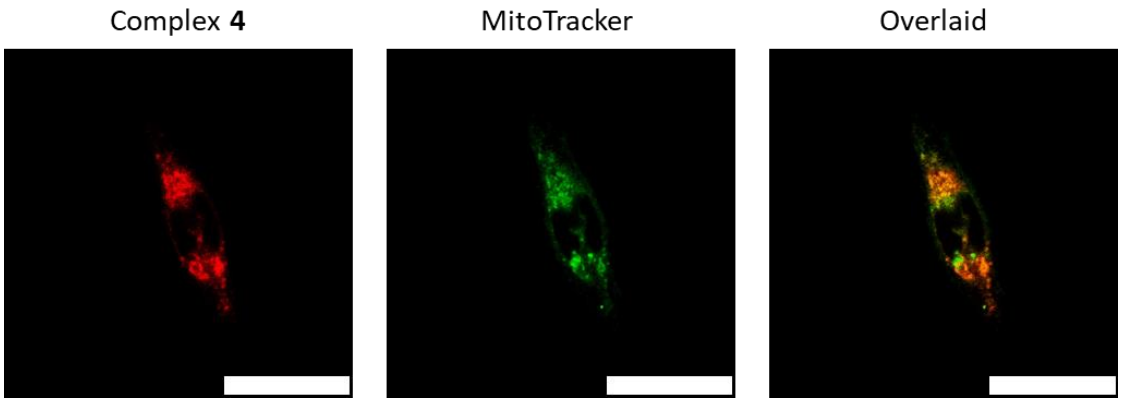

Fig. S21. Cell viability of MDA-MB-231 cells incubated with the conjugates of complex **2** and complex **4** at 37°C for 24 (red) and 48 h (blue) determined by MTT assays.

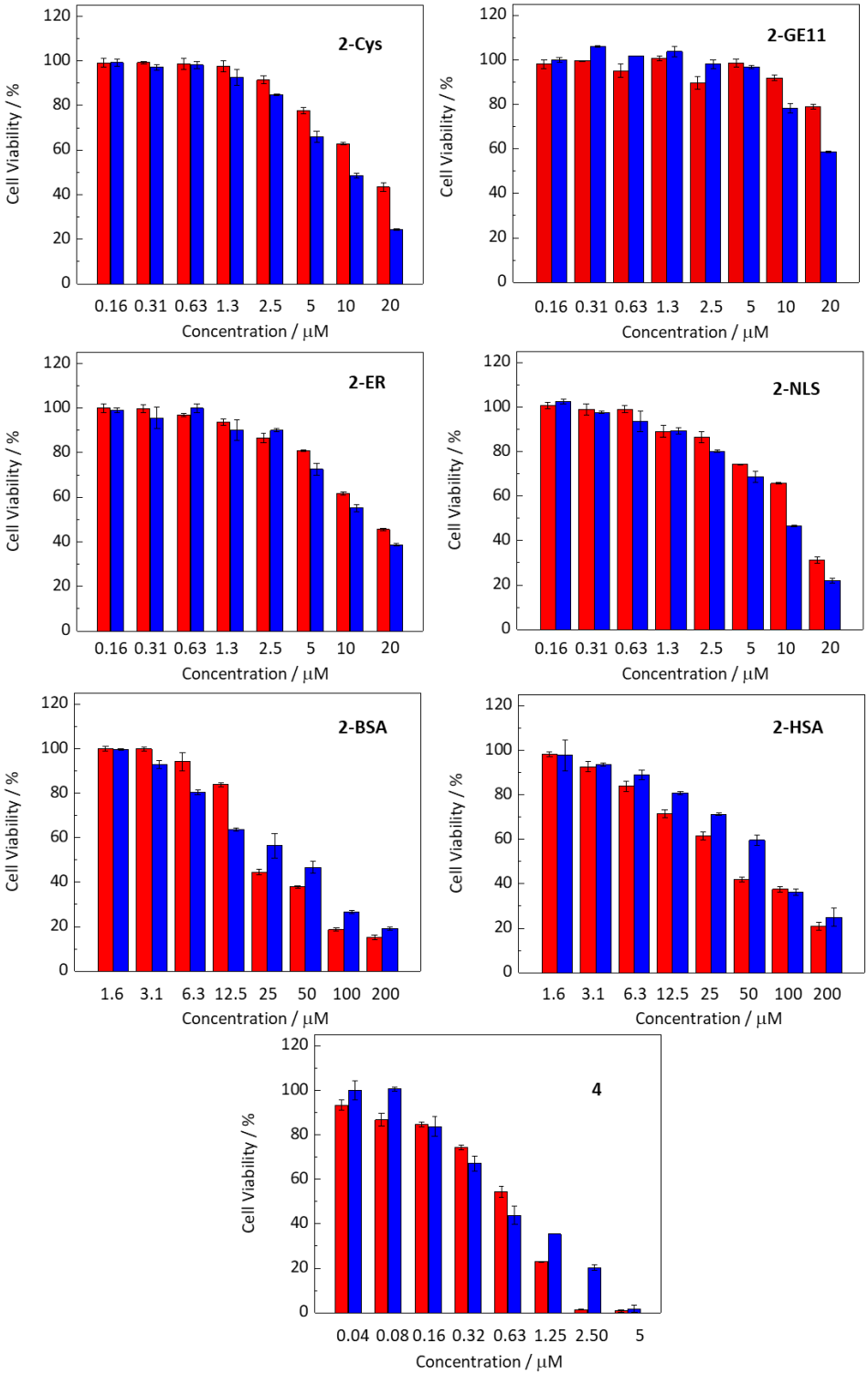

Fig. S22. LDH leakage analysis of MDA-MB-231 cells incubated with the conjugates of complex **2** and complex **4** at 37°C for 24 (red) and 48 h (blue).

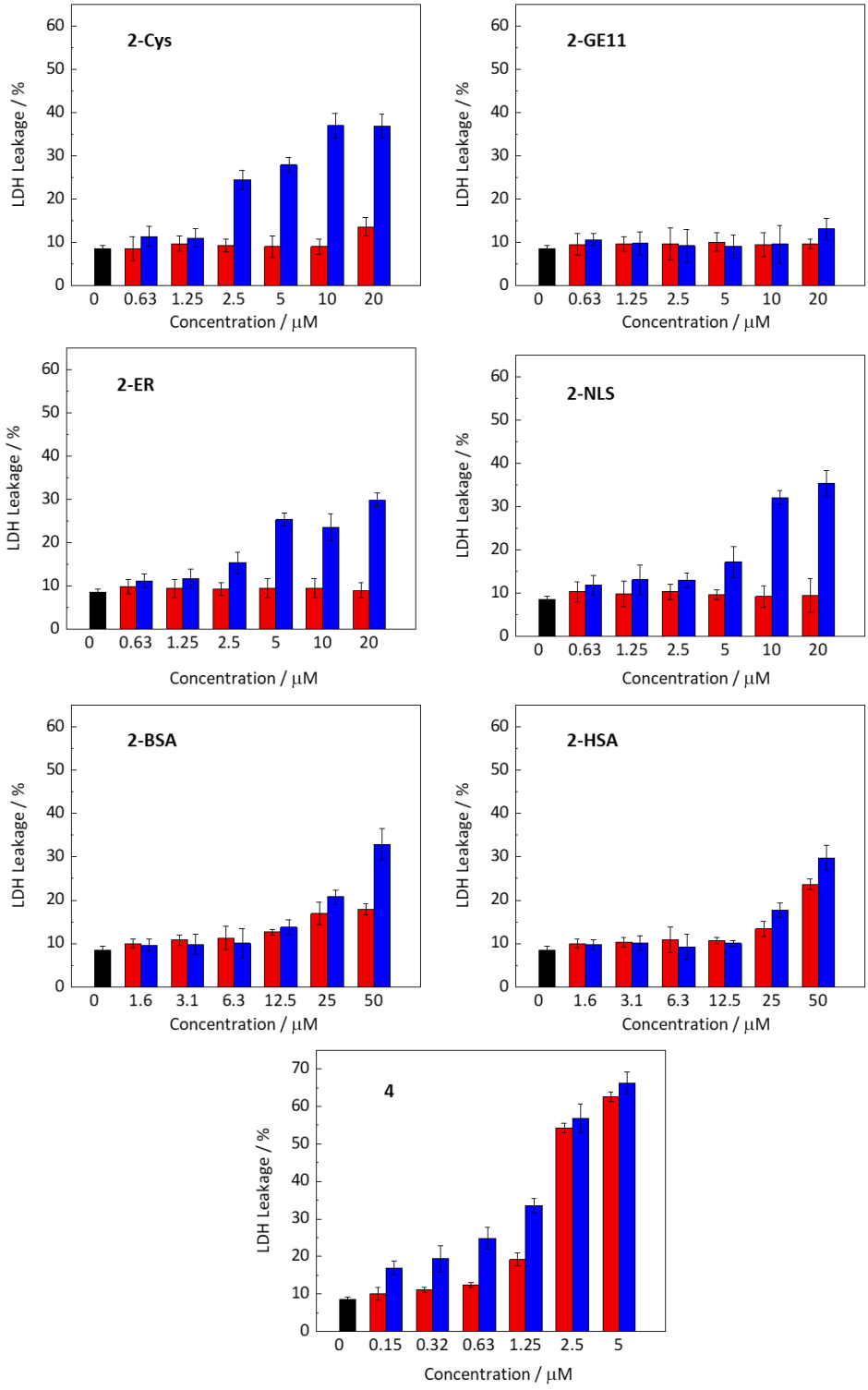

Fig. S23. Flow cytometric analysis of MDA-MB-231 cells treated with the cysteine and peptide conjugates (5 μM) and protein conjugates (10 μM) of complex **2** and complex **4** (0.5 μM) for 24 h in the dark. They were then stained with Alexa Fluor 647 annexin V conjugate (5 μL) and PI (2 μL, 100 μg mL^{-1}) and analysed by flow cytometry using 488 and 638 nm excitation.

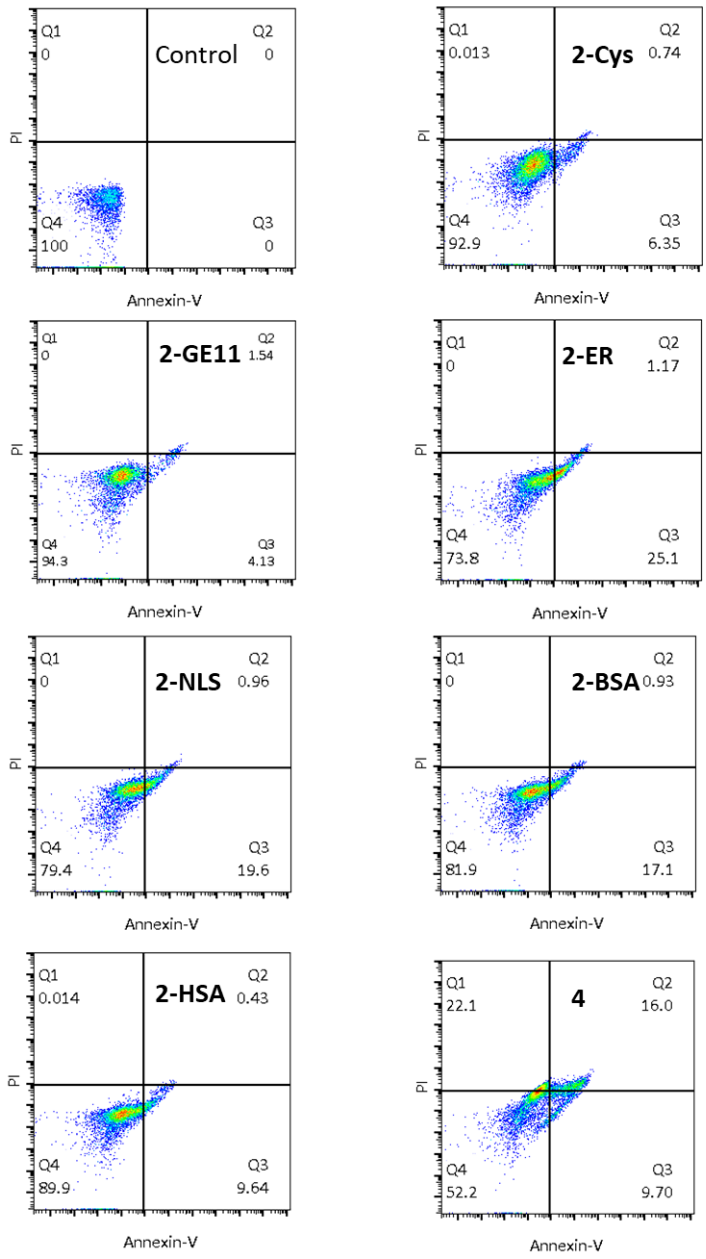

Fig. S24. Flow cytometric analysis of MDA-MB-231 cells treated with the cysteine and peptide conjugates (5 μM) and protein conjugates (10 μM) of complex **2** and complex **4** (0.5 μM) for 48 h in the dark. They were then stained with Alexa Fluor 647 annexin V conjugate (5 μL) and PI (2 μL, 100 μg mL^{-1}) and analysed by flow cytometry using 488 and 638 nm excitation.

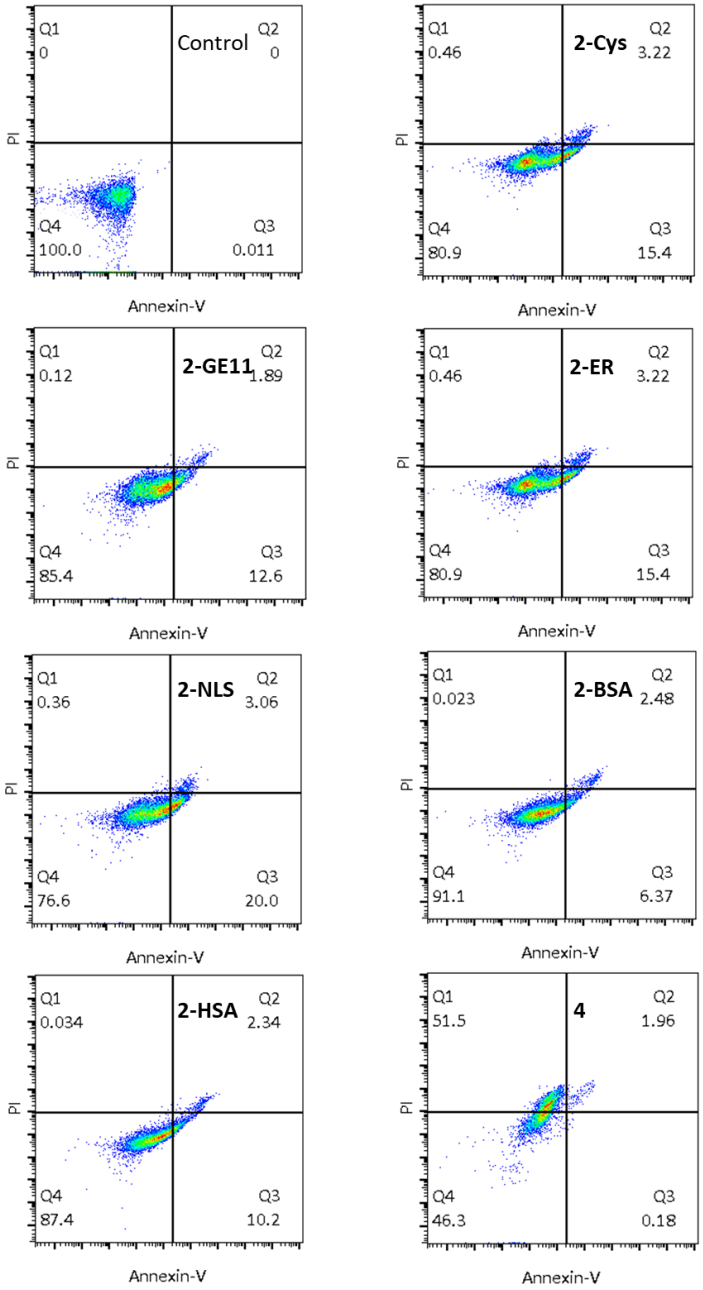

Fig. S25. ^{1}H NMR spectrum of bpy-btz in chloroform-*d* at 298 K.

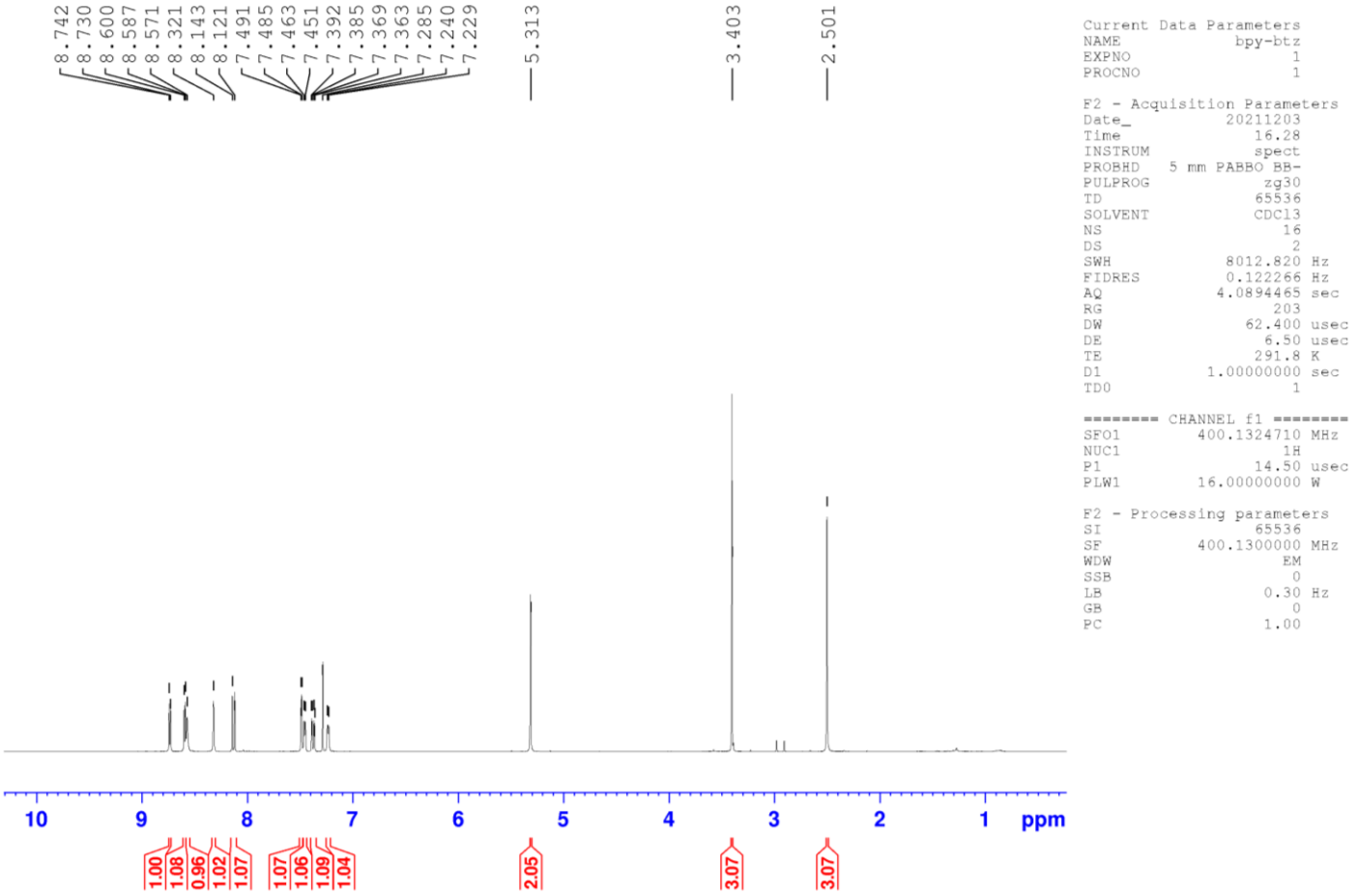

Fig. S26. ^{1}H NMR spectrum of bpy-mstp in acetone-d_6 at 298 K.

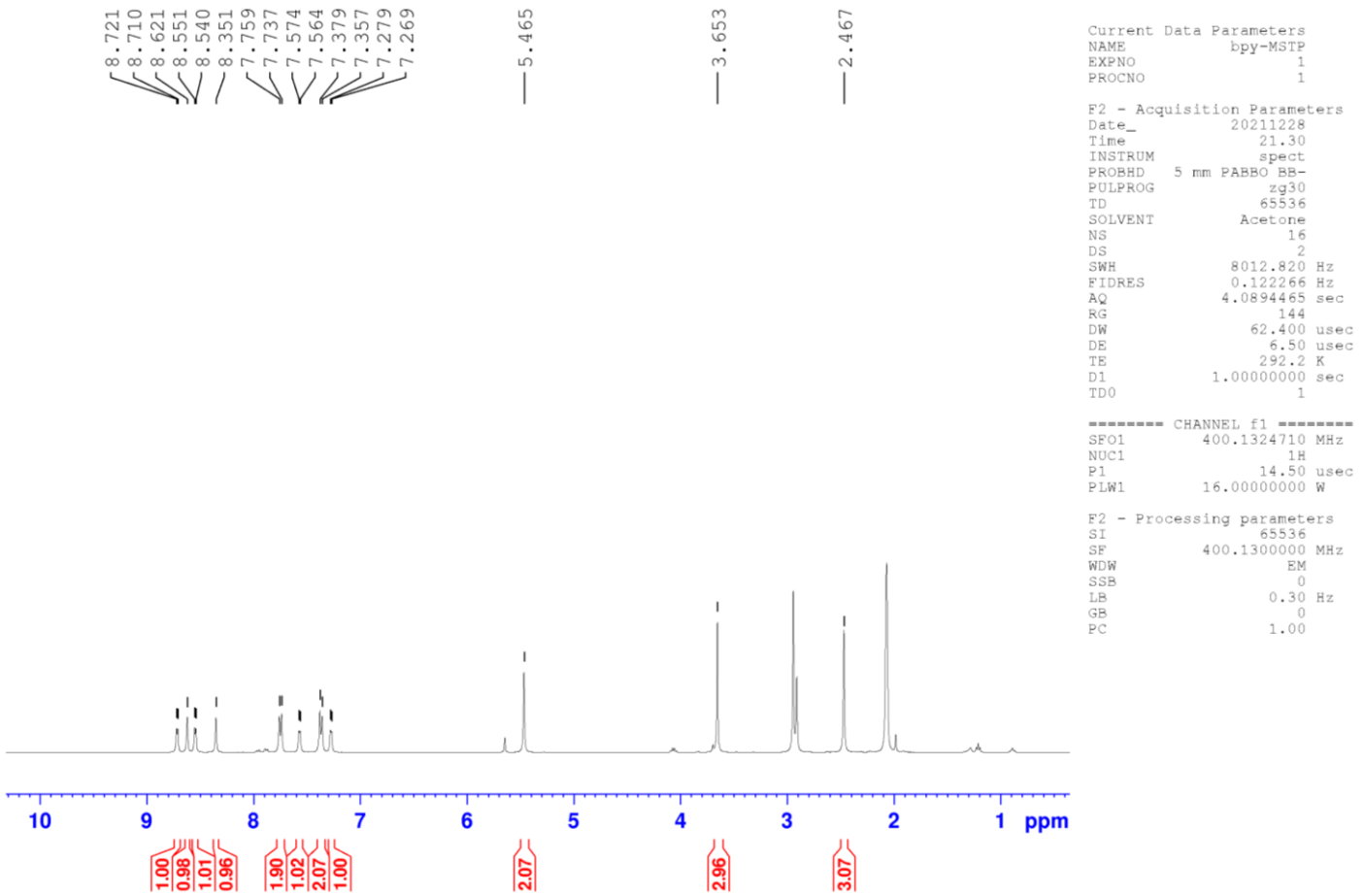


```
Current Data Parameters
NAME                  bpy-MSTP
EXPNO                        1
PROCNO                       1

F2 - Acquisition Parameters
Date_                 20211228
Time                     21.30
INSTRUM                  spect
PROBHD     5 mm PABBO BB-
PULPROG                  zg30
TD                      65536
SOLVENT                Acetone
NS                           16
DS                            2
SWH                   8012.820 Hz
FIDRES                0.122266 Hz
AQ                    4.0894465 sec
RG                          144
DW                       62.400 usec
DE                        6.50 usec
TE                       292.2 K
D1                    1.00000000 sec
TD0                          1

======== CHANNEL f1 ========
SFO1                400.1324710 MHz
NUC1                        1H
P1                       14.50 usec
PLW1               16.00000000 W

F2 - Processing parameters
SI                       65536
SF                  400.1300000 MHz
WDW                         EM
SSB                          0
LB                        0.30 Hz
GB                           0
PC                        1.00
```

Fig. S27. ^{1}H NMR spectrum of bpy-odz in DMSO-d_6 at 298 K.

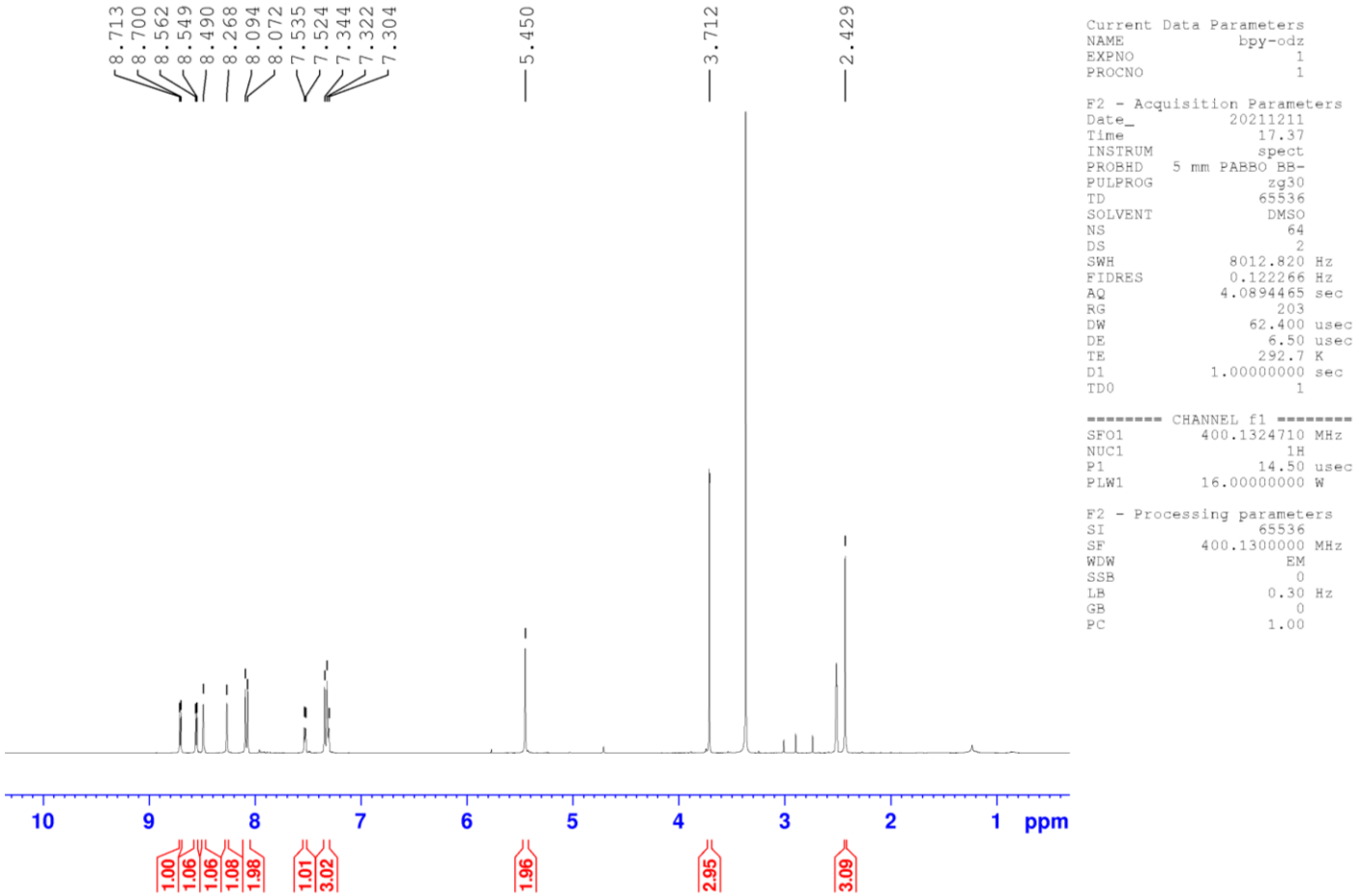

Fig. S28. ^{1}H NMR spectrum of bpy-ph in DMSO-d_6 at 298 K.

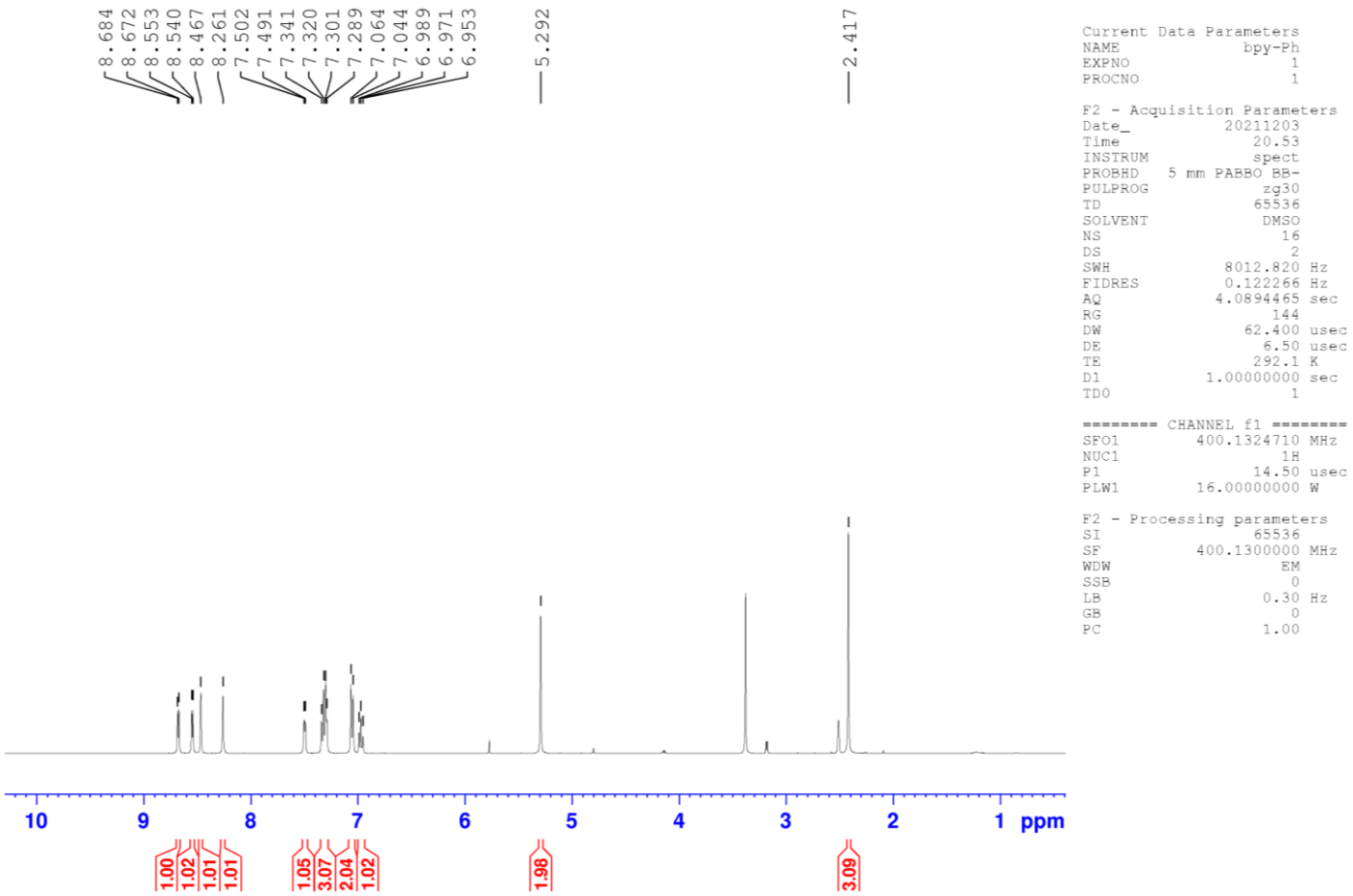

Fig. S29. ^{1}H NMR spectrum of $[Ir_2(bpz)_4Cl_2]$ in chloroform-*d* at 298 K.

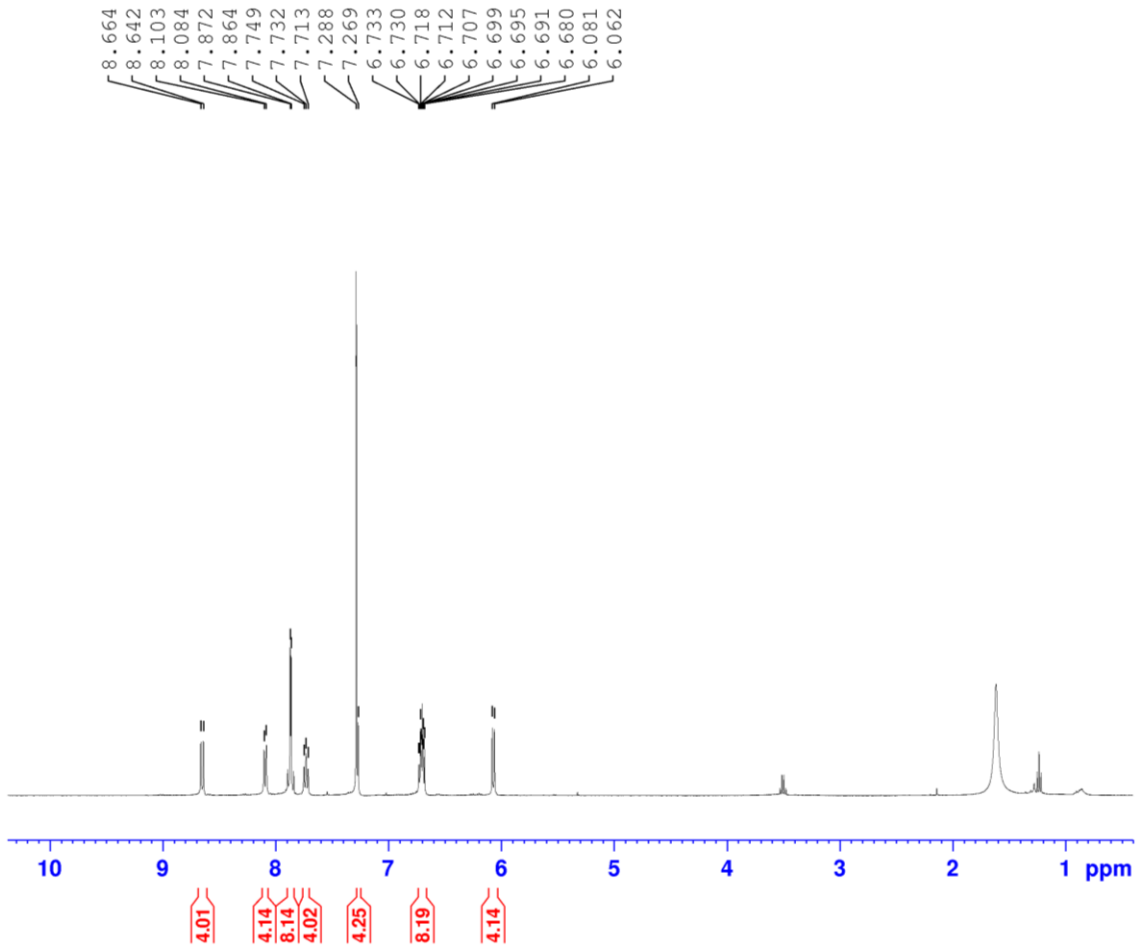


```
Current Data Parameters
NAME        Ir-bpz-dimer
EXPNO                  1
PROCNO                 1

F2 - Acquisition Parameters
Date_           20220413
Time              21.11
INSTRUM           spect
PROBHD   5 mm PABBO BB-
PULPROG             zg30
TD                65536
SOLVENT           CDCl3
NS                  128
DS                    2
SWH            8012.820 Hz
FIDRES         0.122266 Hz
AQ             4.0894465 sec
RG                  203
DW               62.400 usec
DE                6.50 usec
TE               292.5 K
D1          1.00000000 sec
TD0                   1

======== CHANNEL f1 ========
SFO1        400.1324710 MHz
NUC1                1H
P1                14.50 usec
PLW1        16.00000000 W

F2 - Processing parameters
SI                65536
SF          400.1300000 MHz
WDW                 EM
SSB                   0
LB                 0.30 Hz
GB                    0
PC                 1.00
```

Fig. S30. ^{1}H NMR spectrum of complex **1** in DMSO-d_6 at 298 K.

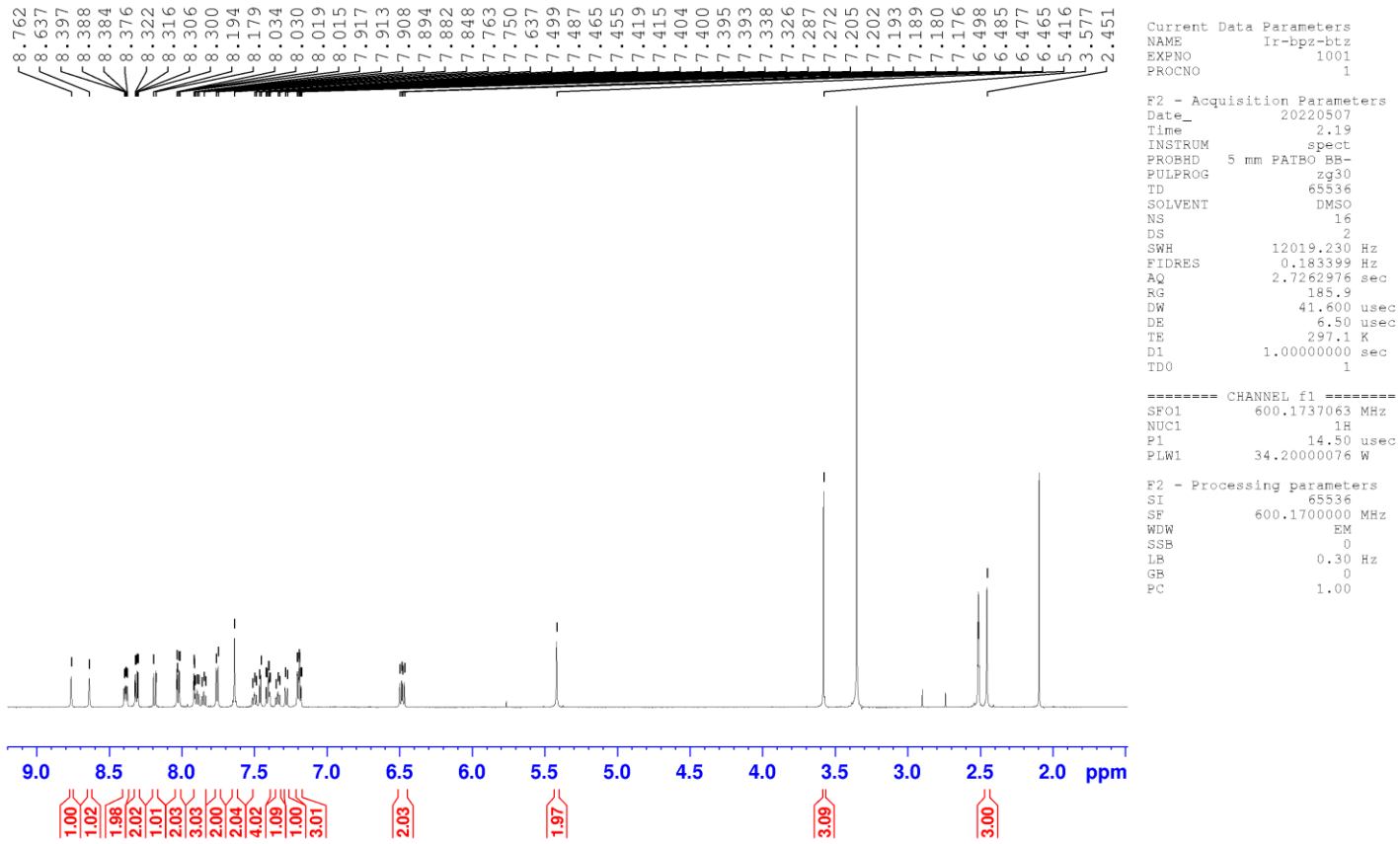


```
Current Data Parameters
NAME          Ir-bpz-btz
EXPNO               1001
PROCNO                 1

F2 - Acquisition Parameters
Date_           20220507
Time               2.19
INSTRUM           spect
PROBHD   5 mm PATBO BB-
PULPROG             zg30
TD                 65536
SOLVENT             DMSO
NS                    16
DS                     2
SWH           12019.230 Hz
FIDRES         0.183399 Hz
AQ             2.7262976 sec
RG                 185.9
DW                41.600 usec
DE                 6.50 usec
TE                297.1 K
D1            1.00000000 sec
TD0                    1

======== CHANNEL f1 ========
SFO1         600.1737063 MHz
NUC1                   1H
P1                 14.50 usec
PLW1         34.20000076 W

F2 - Processing parameters
SI                 65536
SF           600.1700000 MHz
WDW                   EM
SSB                    0
LB                  0.30 Hz
GB                     0
PC                  1.00
```

-

Fig. S31. ^{1}H NMR spectrum of complex **2** in DMSO-d_6 at 298 K.

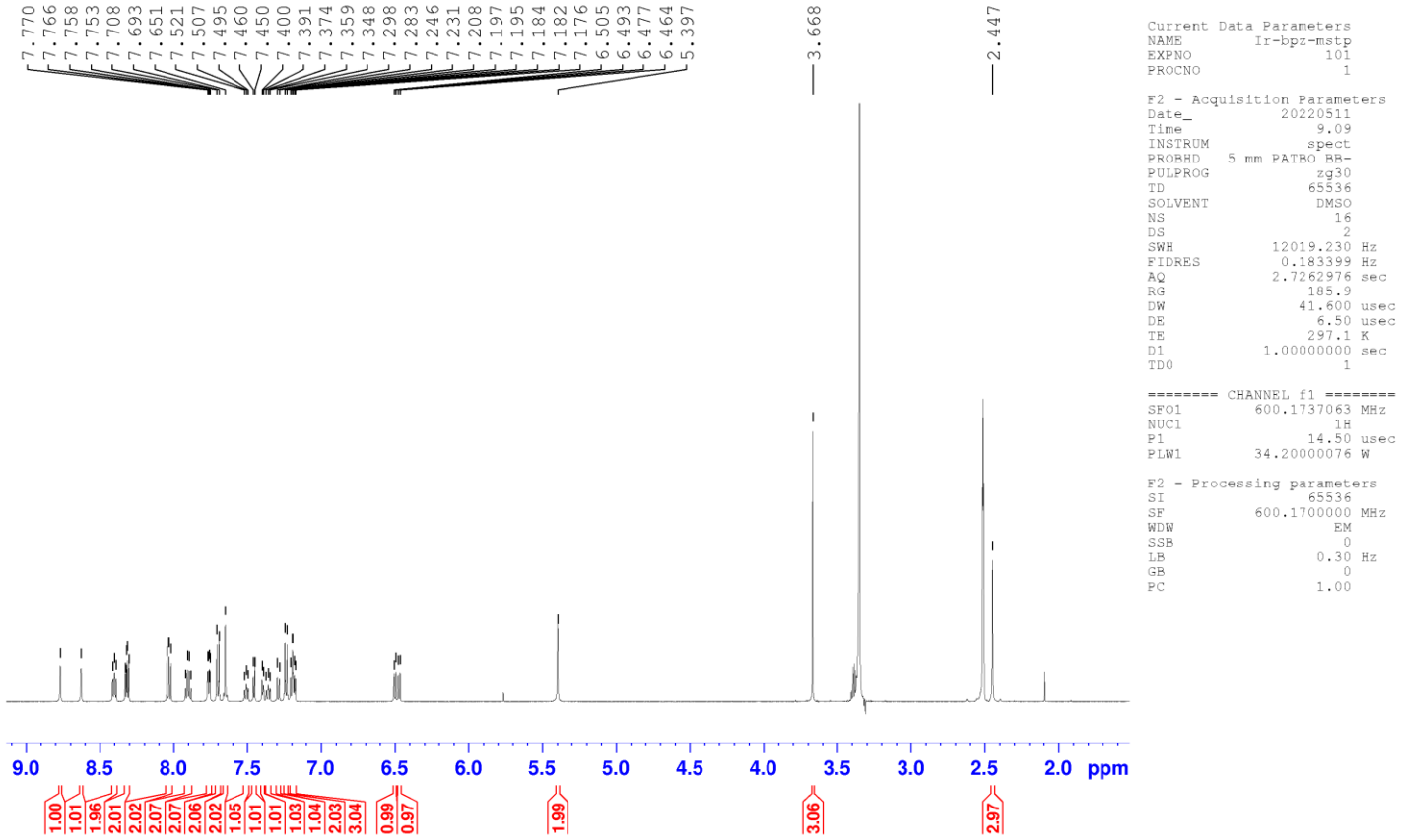


```
Current Data Parameters
NAME          Ir-bpz-mstp
EXPNO                 101
PROCNO                  1

F2 - Acquisition Parameters
Date_              20220511
Time                  9.09
INSTRUM              spect
PROBHD    5 mm PATBO BB-
PULPROG               zg30
TD                   65536
SOLVENT               DMSO
NS                      16
DS                       2
SWH             12019.230 Hz
FIDRES          0.183399 Hz
AQ              2.7262976 sec
RG                   185.9
DW                41.600 usec
DE                 6.50 usec
TE                297.1 K
D1             1.00000000 sec
TD0                     1

======== CHANNEL f1 ========
SFO1          600.1737063 MHz
NUC1                    1H
P1                  14.50 usec
PLW1          34.20000076 W

F2 - Processing parameters
SI                   65536
SF            600.1700000 MHz
WDW                     EM
SSB                      0
LB                  0.30 Hz
GB                       0
PC                    1.00
```

Fig. S32. ^{1}H NMR spectrum of complex **3** in DMSO-d_6 at 298 K.

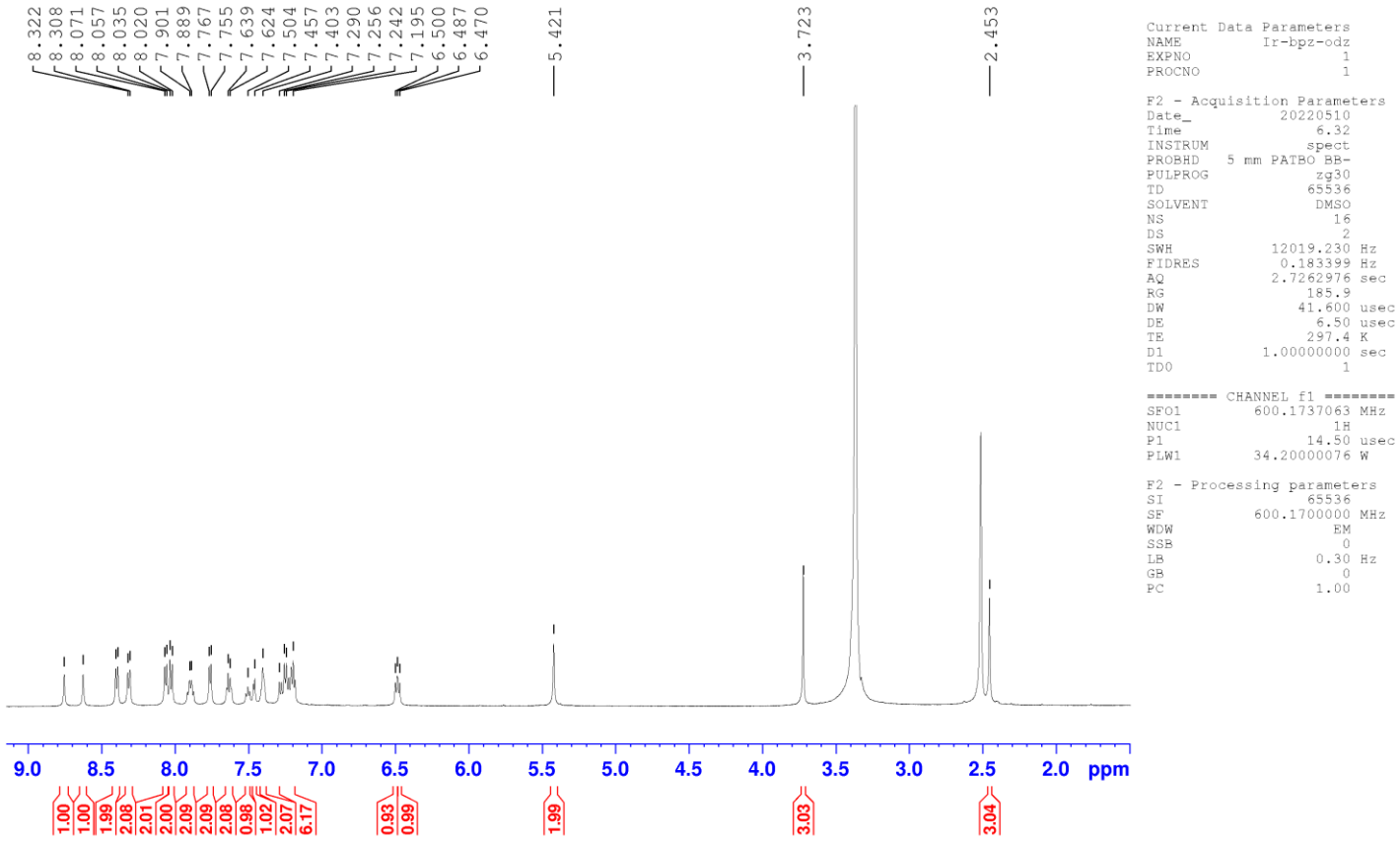

Fig. S33. ^{1}H NMR spectrum of complex **4** in DMSO-d_6 at 298 K.

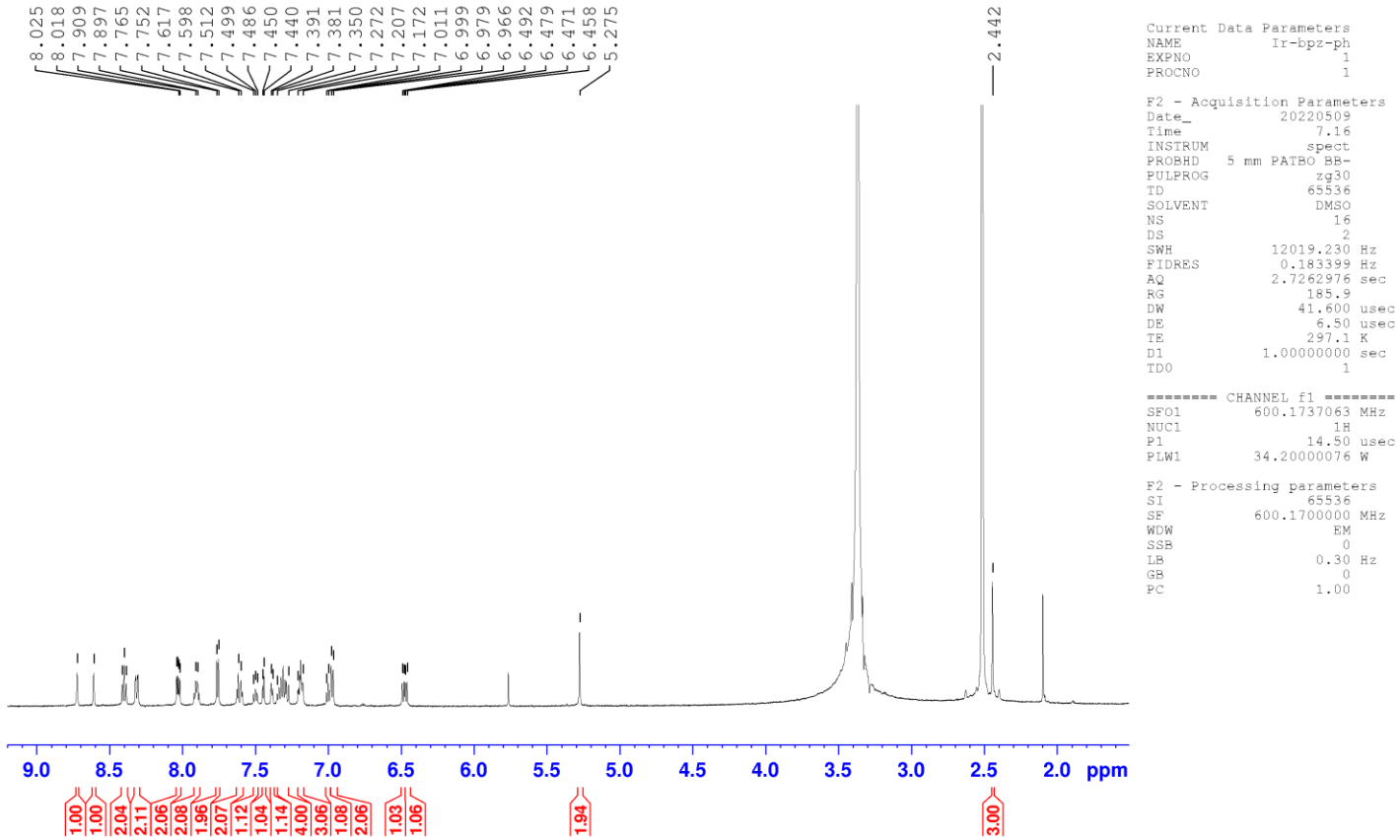

Fig. S34. ^{13}C NMR spectrum of bpy-btz in chloroform-*d* at 298 K.

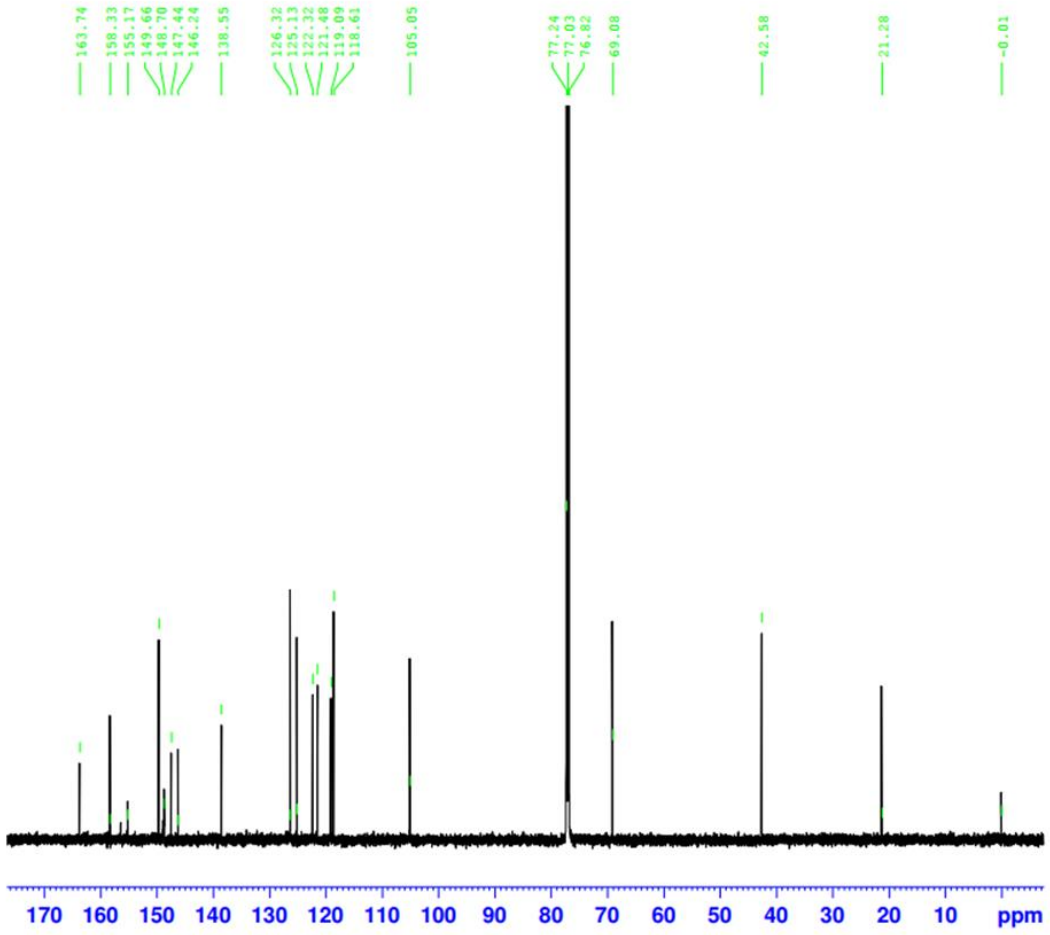

Current Data Parameters
NAME 06062022-KenLo-KLL-bpy-adz-CDCL3
EXPNO 102
PROCNO 1

F2 - Acquisition Parameters
Date_ 20220608
Time 5.26
INSTRUM spect
PROBHD 5 mm PATBO BB-
PULPROG zgpg30
TD 65536
SOLVENT CDCl3
NS 1471
DS 4
SWH 36057.691 Hz
FIDRES 0.550197 Hz
AQ 0.9087659 sec
RG 185.9
DW 13.867 usec
DE 6.50 usec
TE 299.1 K
D1 2.00000000 sec
D11 0.03000000 sec
TD0 1

======== CHANNEL f1 ========
SFO1 150.9279571 MHz
NUC1 13C
P1 11.50 usec
PLW1 40.79999924 W

======== CHANNEL f2 ========
SFO2 600.1724007 MHz
NUC2 1H
CPDPRG[2 waltz16
PCPD2 70.00 usec
PLW2 32.20000076 W
PLW12 1.57879996 W
PLW13 0.79412001 W

F2 - Processing parameters
SI 32768
SF 150.9128665 MHz
WDW EM
SSB 0
LB 1.00 Hz
GB 0
PC 1.40

Fig. S35. ^{13}C NMR spectrum of bpy-mstp in chloroform-*d* at 298 K.

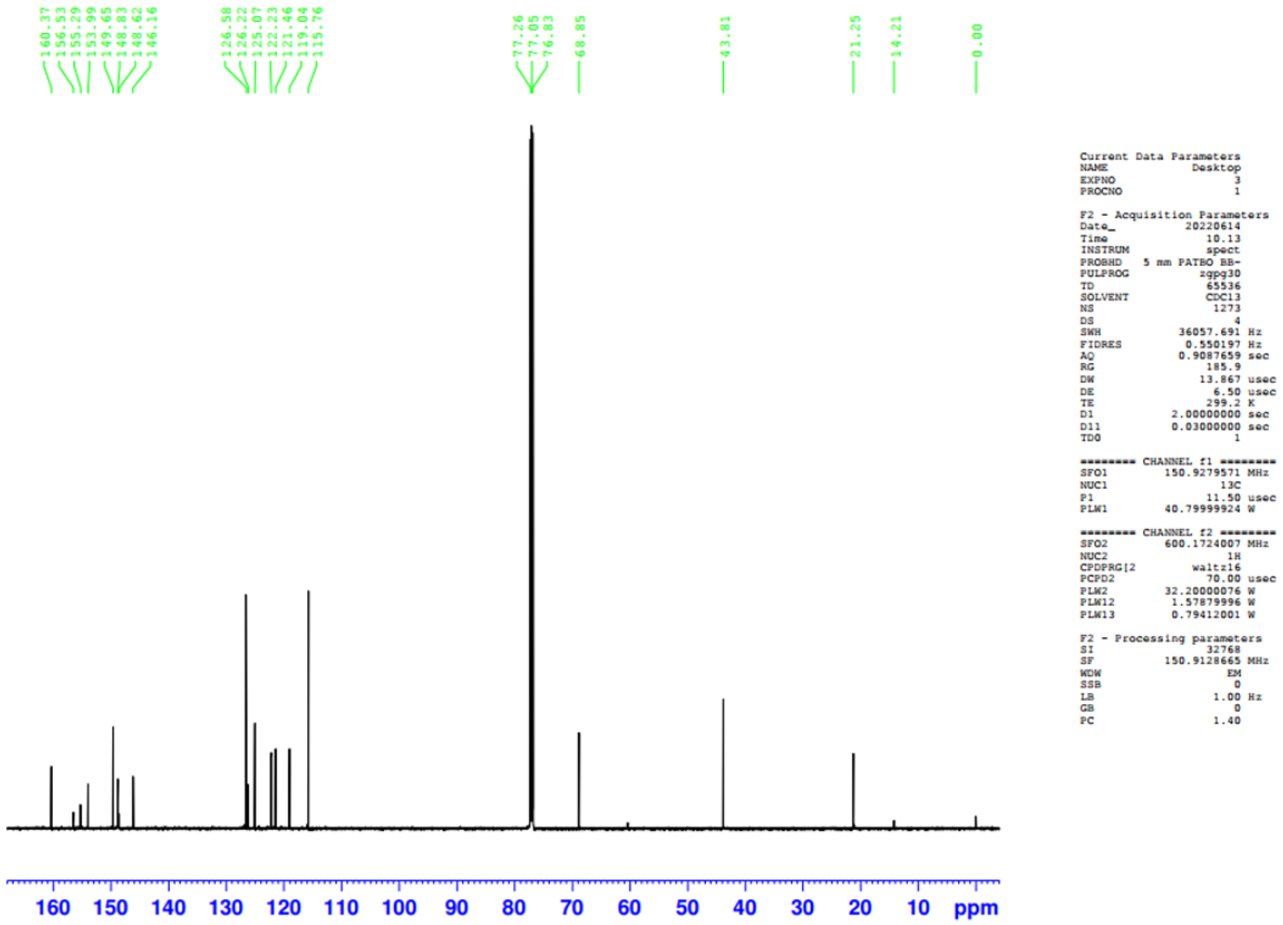


```
Current Data Parameters
NAME                  Desktop
EXPNO                       3
PROCNO                      1

F2 - Acquisition Parameters
Date_                20220614
Time                    10.13
INSTRUM                 spect
PROBHD   5 mm PATBO BB-
PULPROG                zgpg30
TD                      65536
SOLVENT                 CDCl3
NS                       1273
DS                          4
SWH                36057.691 Hz
FIDRES              0.550197 Hz
AQ                  0.9087659 sec
RG                      185.9
DW                     13.867 usec
DE                       6.50 usec
TE                      299.2 K
D1                 2.00000000 sec
D11                0.03000000 sec
TD0                         1

======== CHANNEL f1 ========
SFO1               150.9279571 MHz
NUC1                       13C
P1                       11.50 usec
PLW1               40.79999924 W

======== CHANNEL f2 ========
SFO2               600.1724007 MHz
NUC2                       1H
CPDPRG[2                waltz16
PCPD2                    70.00 usec
PLW2               32.20000076 W
PLW12               1.57879996 W
PLW13               0.79412001 W

F2 - Processing parameters
SI                         32768
SF                 150.9128665 MHz
WDW                           EM
SSB                            0
LB                          1.00 Hz
GB                             0
PC                          1.40
```

Fig. S36. ^{13}C NMR spectrum of bpy-odz in chloroform-*d* at 298 K.

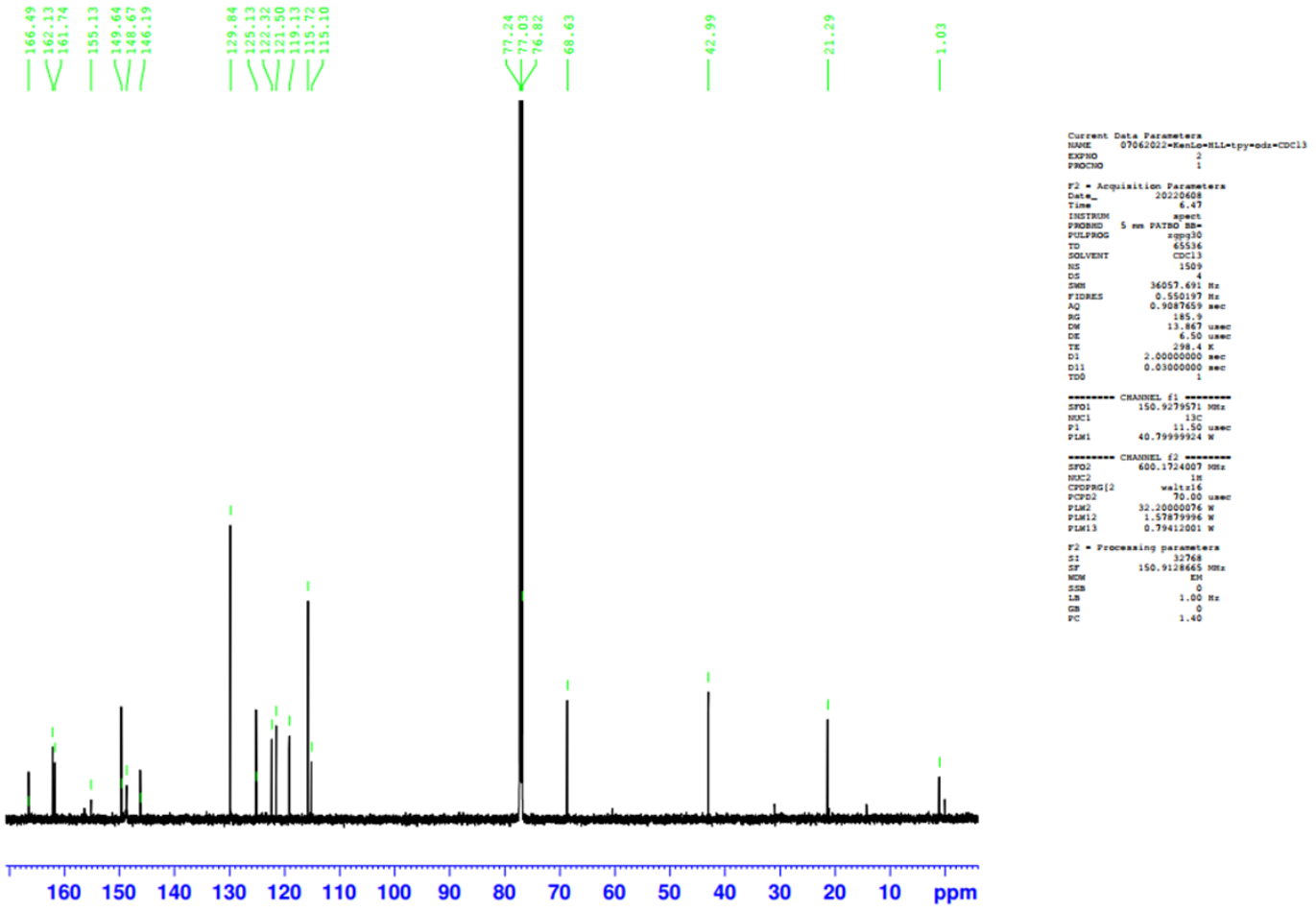

Fig. S37. ^{13}C NMR spectrum of bpy-ph in DMSO-d_6 at 298 K.

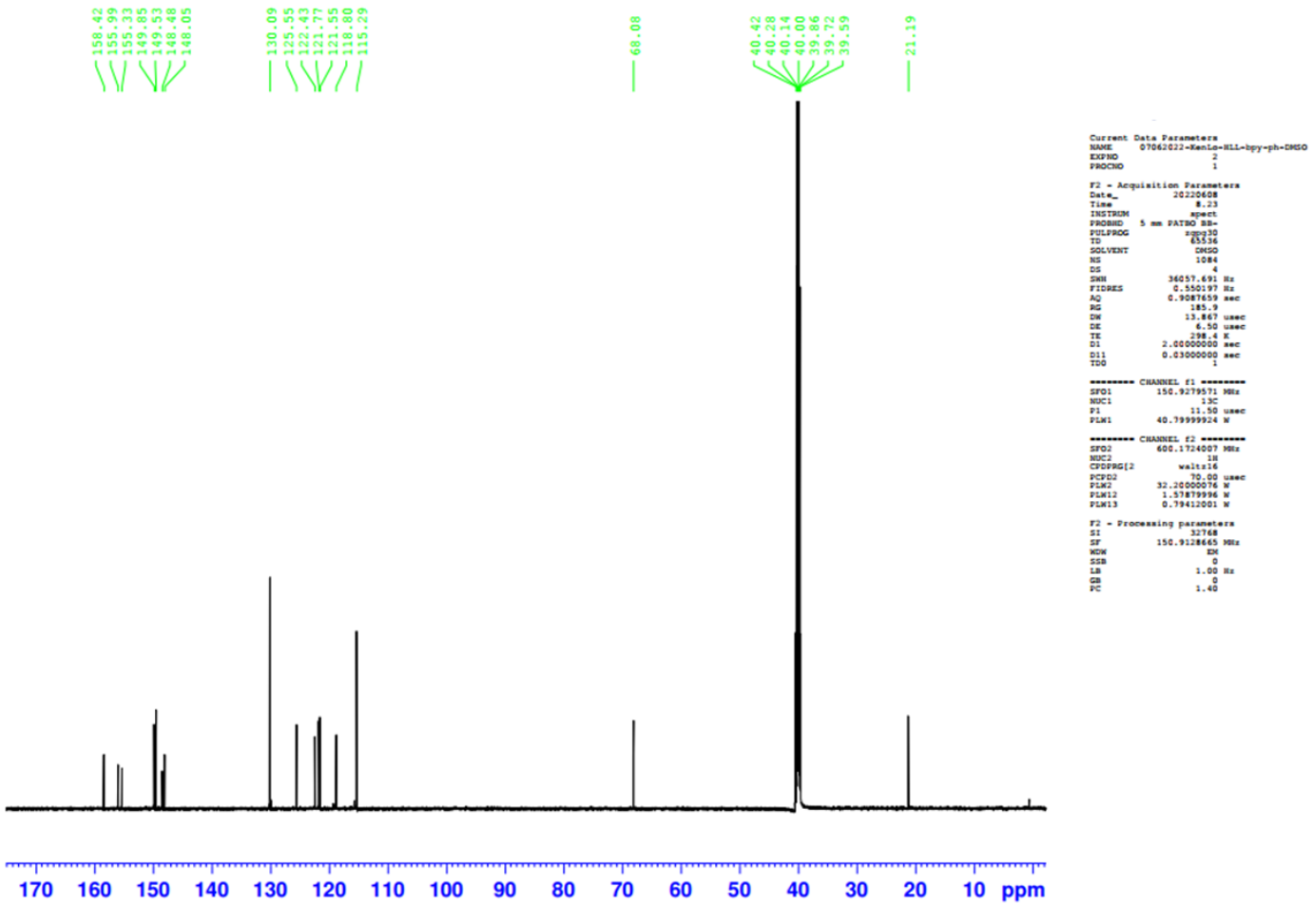

Fig. S38. ^{13}C NMR spectrum of complex **1** in DMSO-d_6 at 298 K.

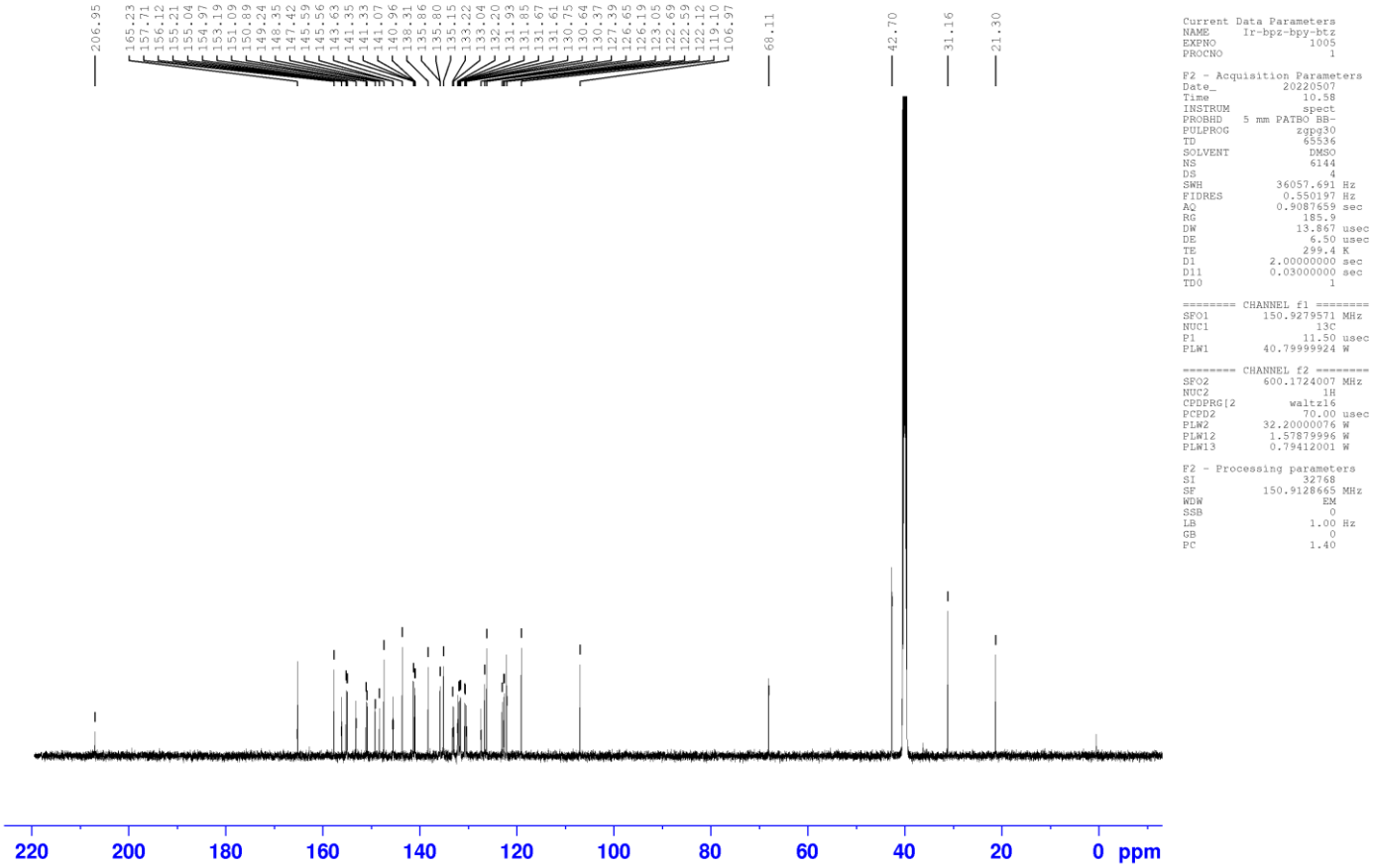


```
Current Data Parameters
NAME      Ir-bpz-bpy-btz
EXPNO              1005
PROCNO                1

F2 - Acquisition Parameters
Date_          20220507
Time             10.58
INSTRUM          spect
PROBHD   5 mm PATBO BB-
PULPROG         zgpg30
TD              65536
SOLVENT           DMSO
NS                6144
DS                   4
SWH          36057.691 Hz
FIDRES        0.550197 Hz
AQ           0.9087659 sec
RG               185.9
DW              13.867 usec
DE               6.50 usec
TE              299.4 K
D1           2.00000000 sec
D11          0.03000000 sec
TD0                  1

======== CHANNEL f1 ========
SFO1        150.9279571 MHz
NUC1               13C
P1               11.50 usec
PLW1        40.79999924 W

======== CHANNEL f2 ========
SFO2        600.1724007 MHz
NUC2               1H
CPDPRG[2        waltz16
PCPD2            70.00 usec
PLW2        32.20000076 W
PLW12        1.57879996 W
PLW13        0.79412001 W

F2 - Processing parameters
SI               32768
SF          150.9128665 MHz
WDW                EM
SSB                 0
LB               1.00 Hz
GB                  0
PC               1.40
```

Fig. S39. ^{13}C NMR spectrum of complex **2** in DMSO-d_6 at 298 K.

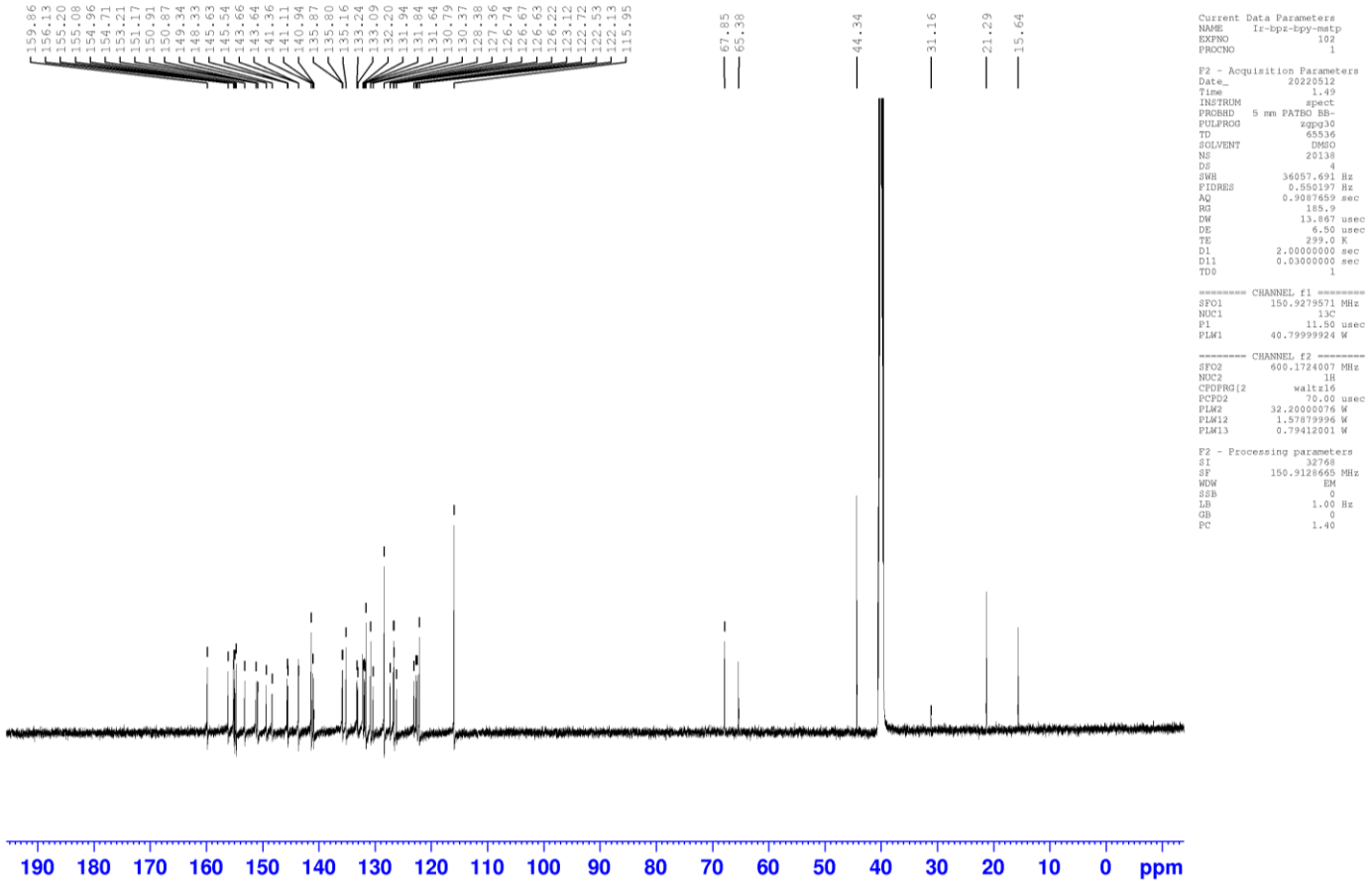

Fig. S40. ^{13}C NMR spectrum of complex **3** in DMSO-d_6 at 298 K.

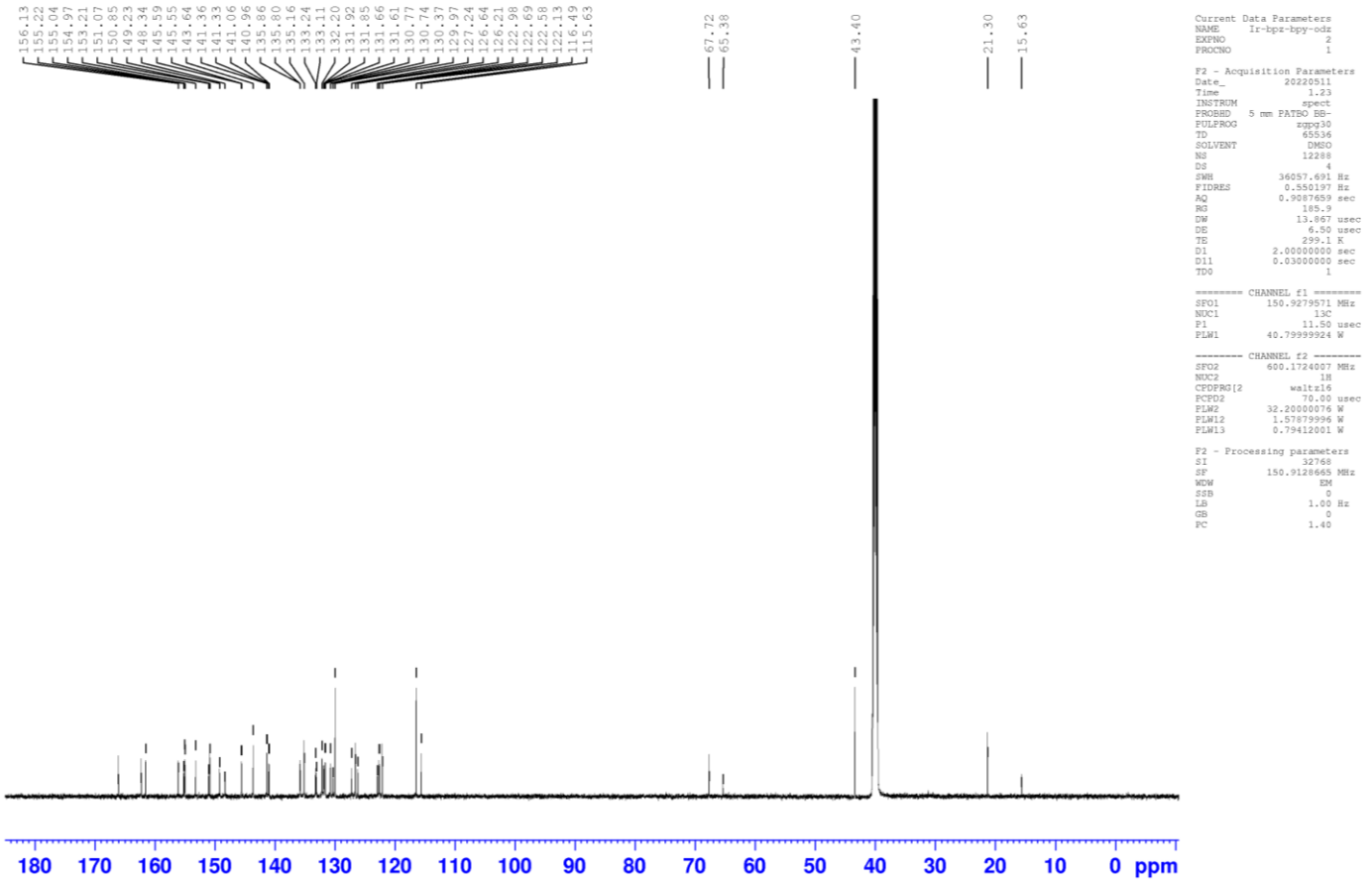

Fig. S41. ^{13}C NMR spectrum of complex **4** in DMSO-d_6 at 298 K.

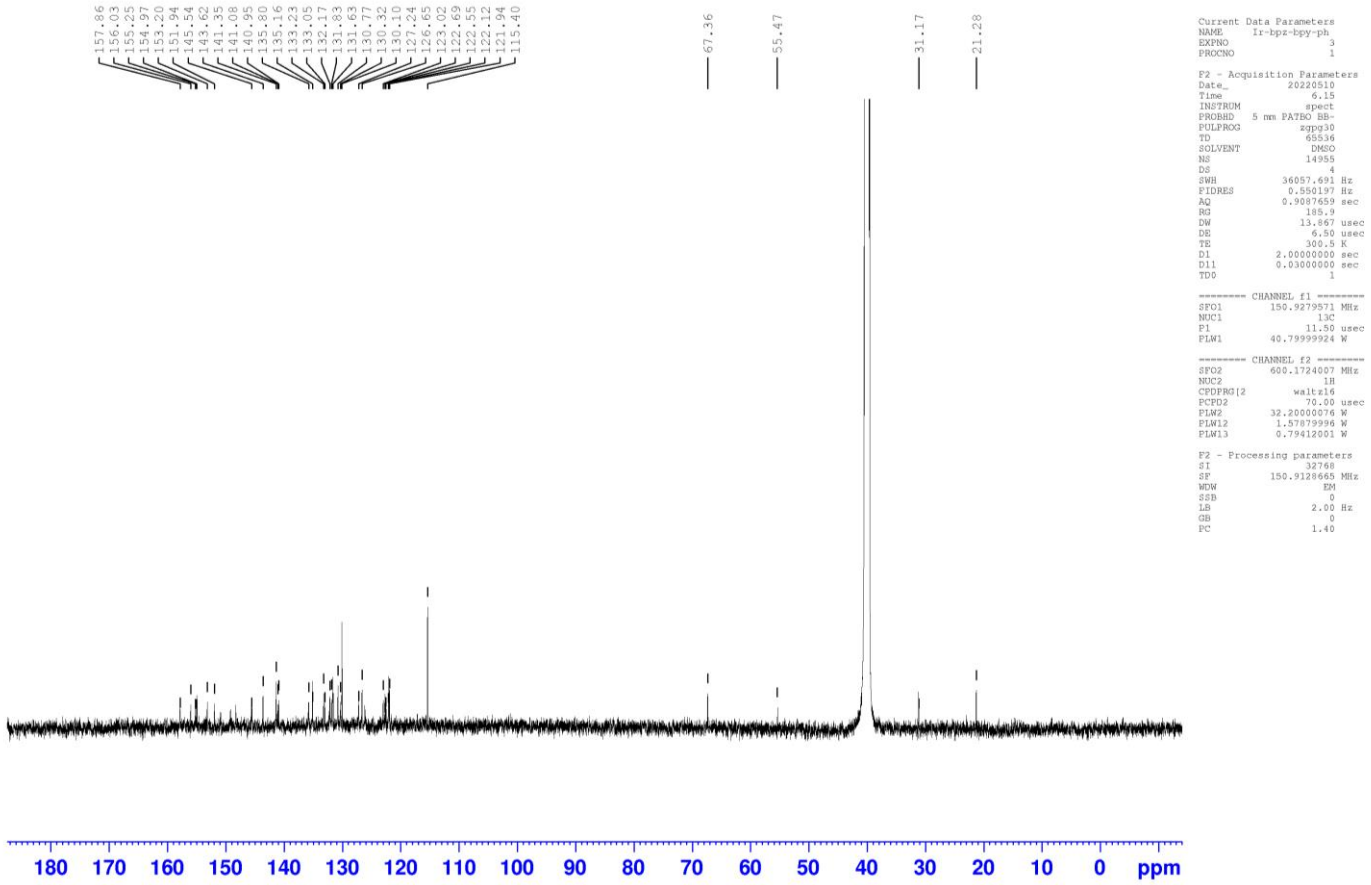

Fig. S42. HR-ESI mass spectra of bpy-btz ((a) – (c) experimental; (d) and (e) simulated).

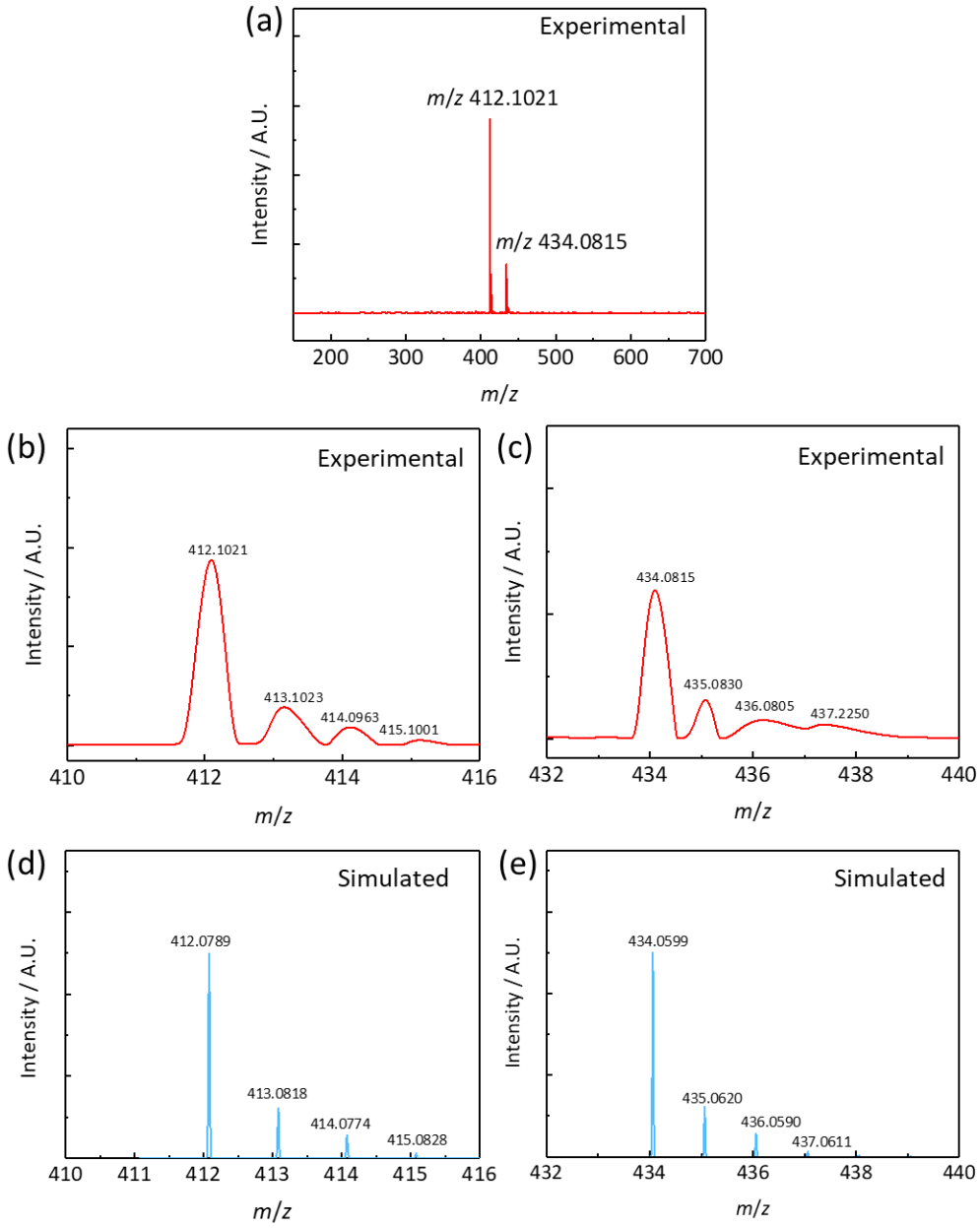

Fig. S43. HR-ESI mass spectra of bpy-mstp ((a) – (c) experimental; (d) and (e) simulated).

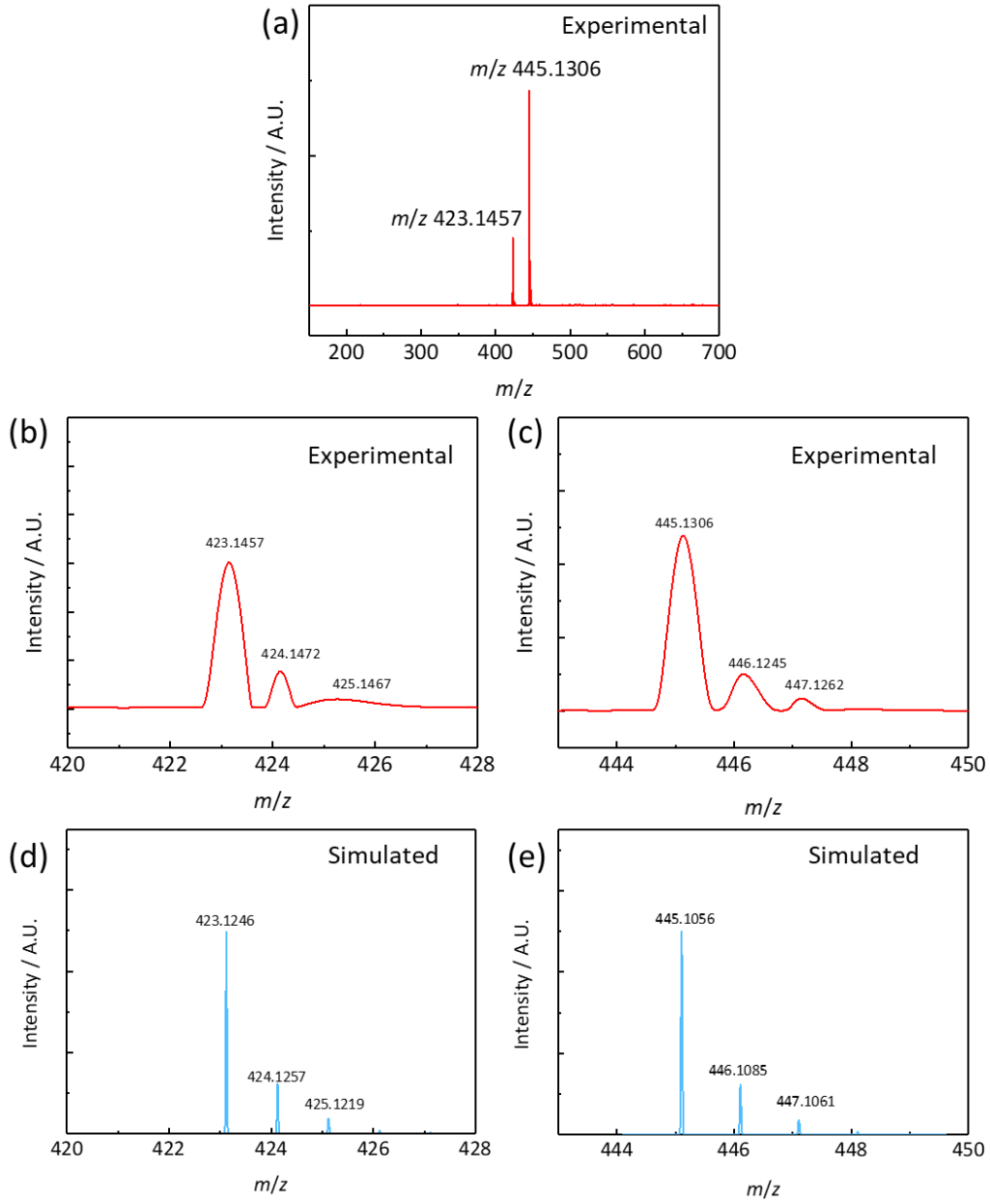

Fig. S44. HR-ESI mass spectra of bpy-odz ((a) – (c) experimental; (d) and (e) simulated).

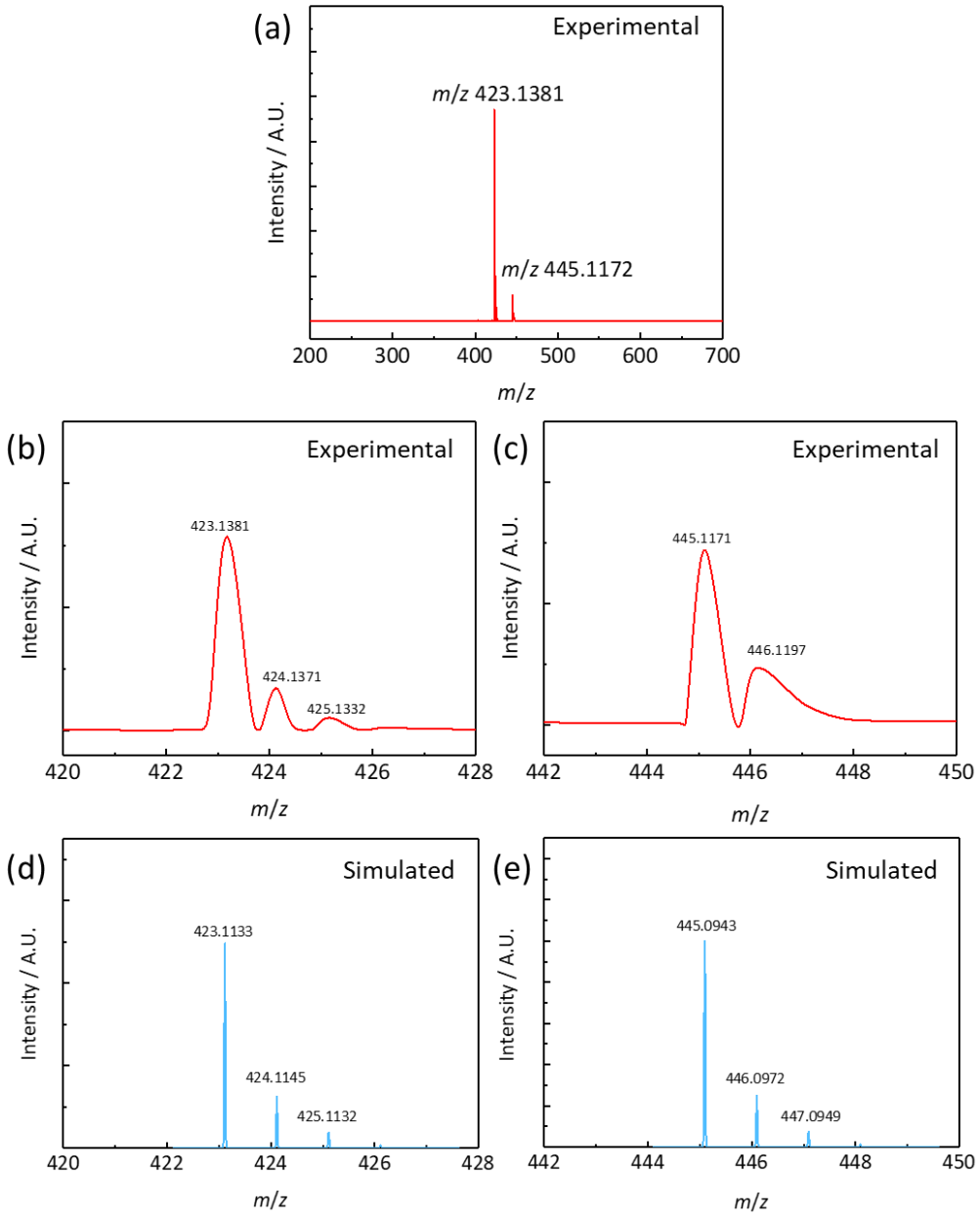

Fig. S45. HR-ESI mass spectra of bpy-ph ((a) – (c) experimental; (d) and (e) simulated).

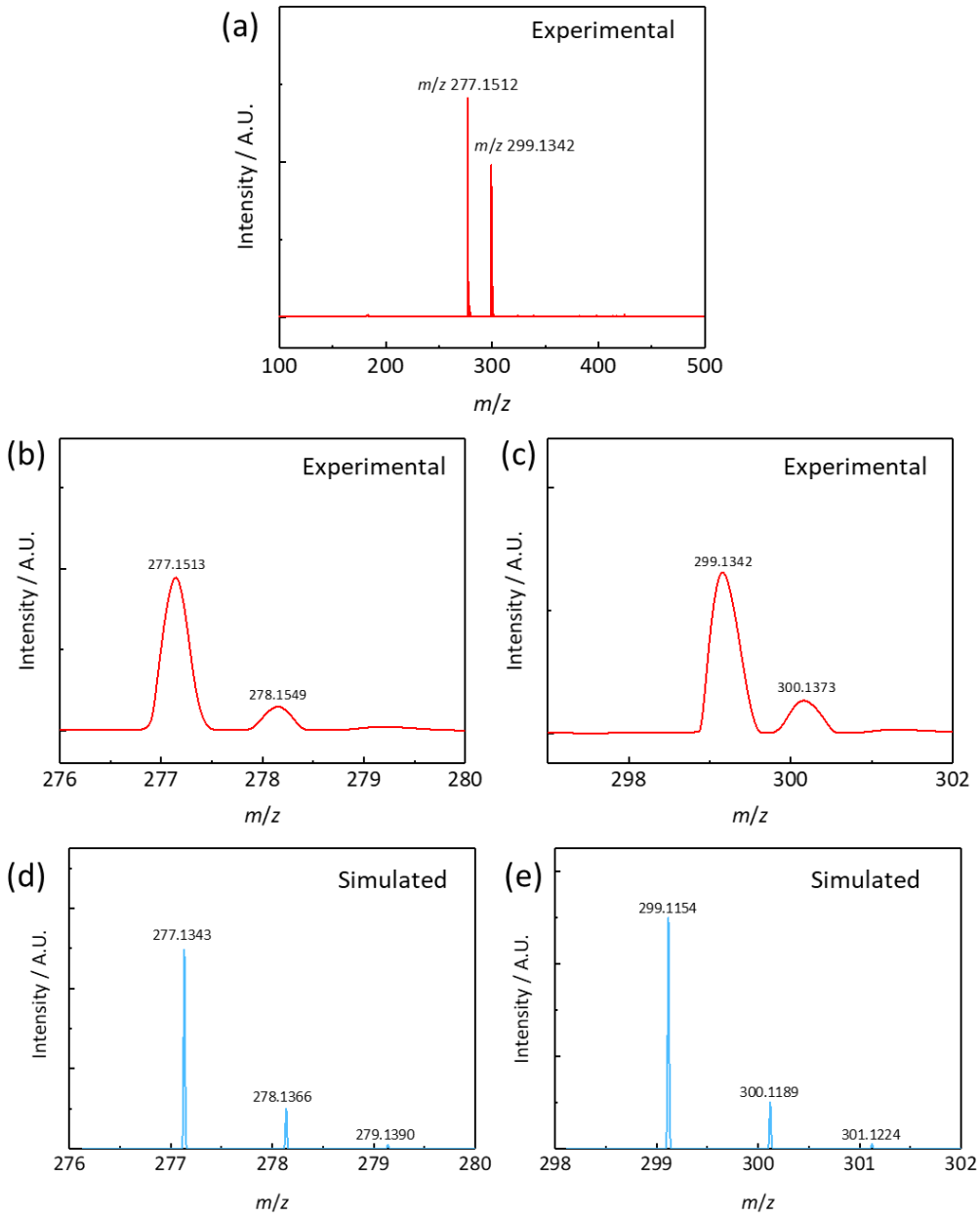

Fig. S46. HR-ESI mass spectra of complex **1** ((a) and (b) experimental; (c) simulated).

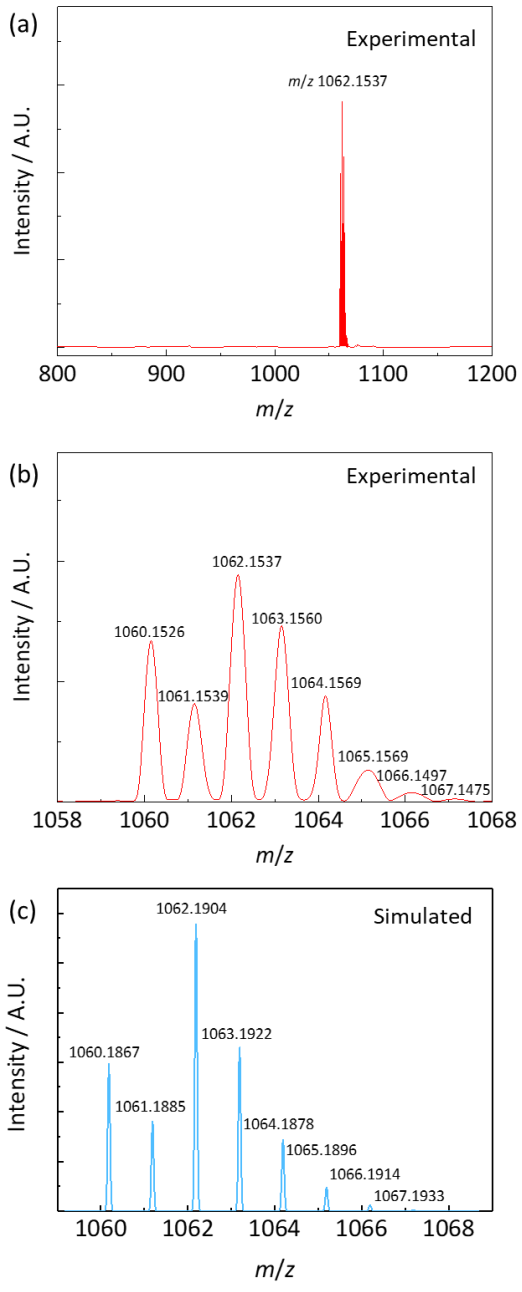

Fig. S47. HR-ESI mass spectra of complex **2** ((a) and (b) experimental; (c) simulated).

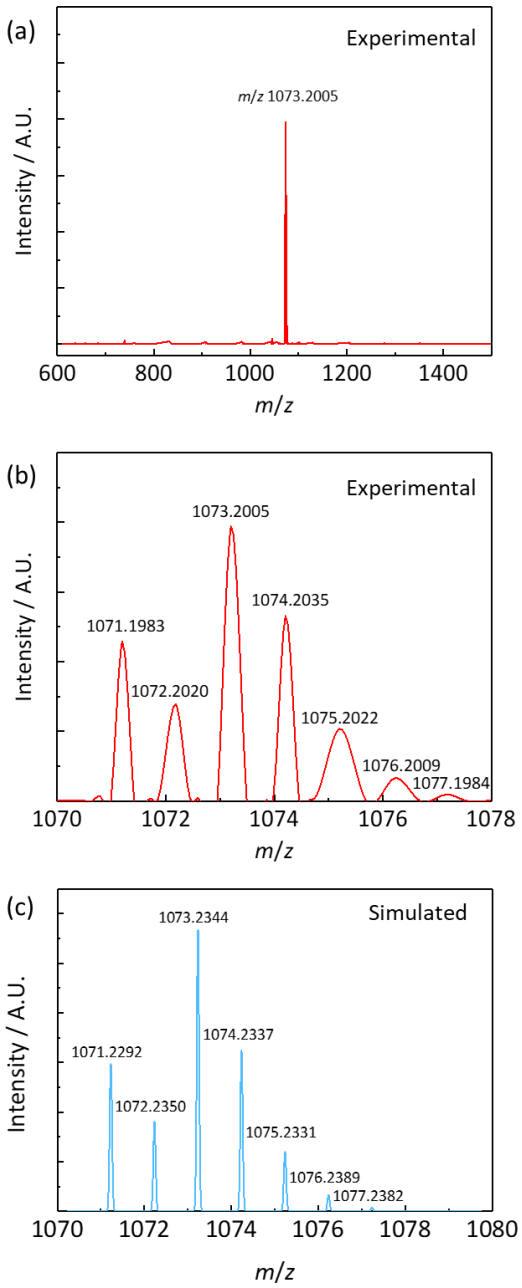

Fig. S48. HR-ESI mass spectra of complex **3** ((a) and (b) experimental; (c) simulated).

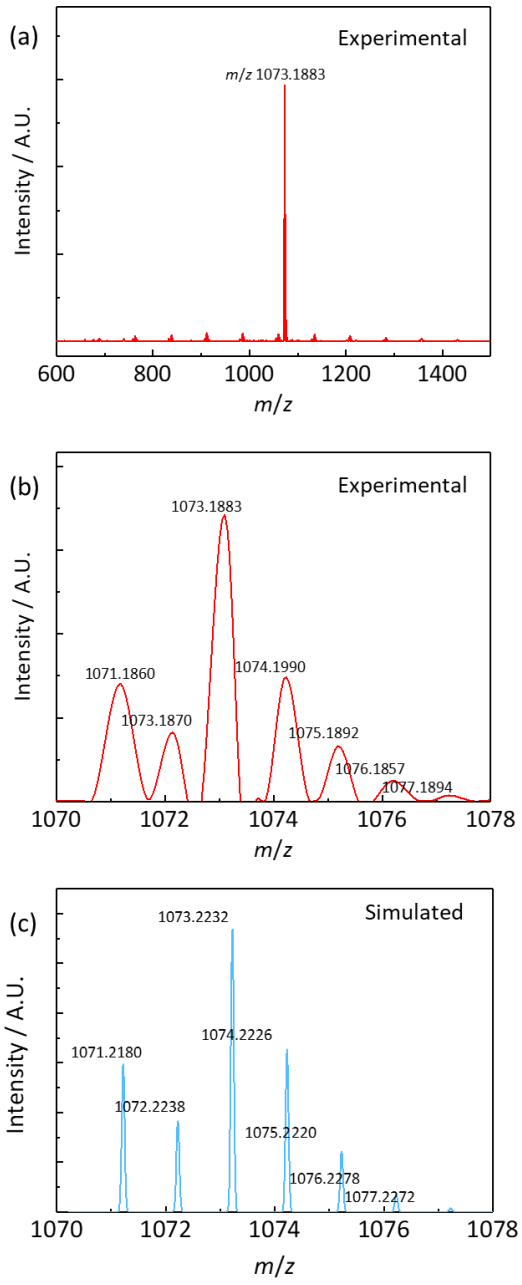

Fig. S49. HR-ESI mass spectra of complex **4** ((a) and (b) experimental; (c) simulated).

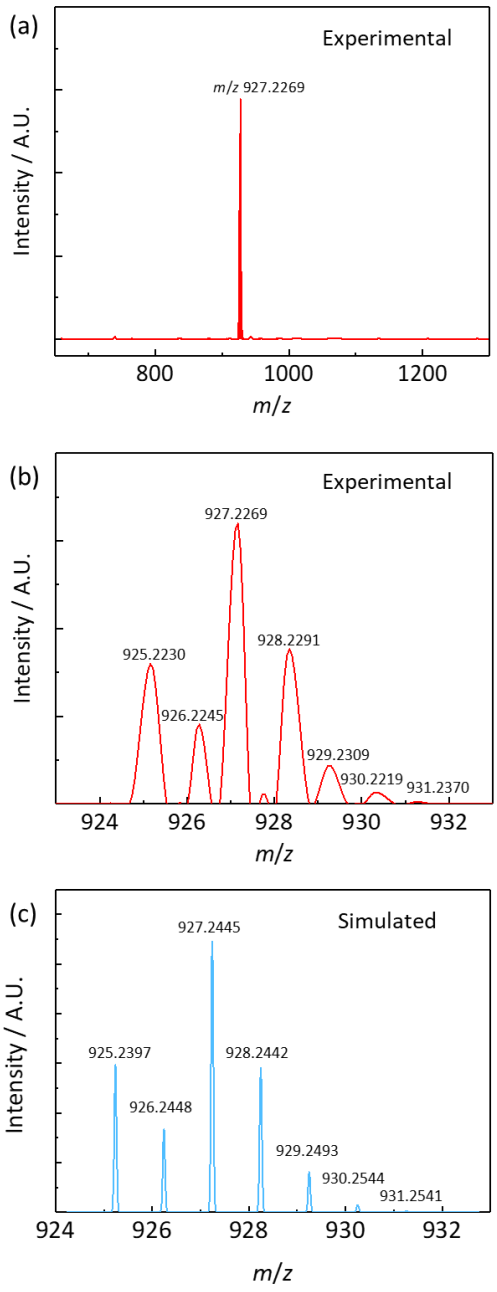

References

1. D. D. Perrin and W. L. F. Armarego, *Purification of Laboratory Chemicals*, Elsevier, Oxford, U.K., 2009.
2. B. D. Sherman, Y. Xie, M. V. Sheridan, D. Wang, D. W. Shaffer, T. J. Meyer and J. J. Concepcion, *ACS Energy Lett*., 2017, **2**, 124.
3. X. Chen, H. Wu, C.-M. Park, T. H. Poole, G. Keceli, N. O. Devarie-Baez, A. W. Tsang, W. T. Lowther, L. B. Poole, S. B. King, M. Xian and C. M. Furdui, *ACS Chem. Biol.*, 2017, **12**, 2201.
4. N. Toda, S. Asano and C. F. Barbas III, *Angew. Chem. Int. Ed.*, 2013, **52**, 12592.
5. M. Paul, M. Teubner, B. Grimm-Lebsanft, S. Buchenau, A. Hoffmann, M. Rübhausen and S. Herres-Pawlis, *J. Inorg. Biochem.*, 2021, **224**, 111541.
6. J. N. Demas and G. A. Crosby, *J. Phys. Chem.*, 1971, **75**, 991.
7. K. Suzuki, A. Kobayashi, S. Kaneko, K. Takehira, T. Yoshihara, H. Ishida, Y. Shiina, S. Oishi and S. Tobita, *Phys. Chem. Chem. Phys*., 2009, **11**, 9850.
8. V. A. Hackley and J. D. Clogston, *Characterization of Nanoparticles Intended for Drug Delivery*, ed. S. E. McNeil, Springer, New York, 2011, pp. 35 – 52.
9. M. Nonoyama, *Bull. Chem. Soc. Jpn.*, 1974, **47**, 767.
10. M. Martínez-Alonso, N. Busto, L. D. Aguirre, L. Berlanga, M. C. Carrión, J. V. Cuevas, A. M. Rodríguez, A. Carbayo, B. R. Manzano, E. Ortí, F. A. Jalón, B. García and G. Espino, *Chem. Eur. J.*, 2018, **24**, 17523.
11. D. Garcìa-Fresnadillo, Y. Georgiadou, G. Orellana, A. M. Braun and E. Oliveros, *Helv. Chim. Acta.*, 1996, **79**, 1222.

12. (a) S. Chakrabortty, B. K. Agrawalla, A. Stumper, N. M. Vegi, S. Fischer, C. Reichardt, M. Kögler, B. Dietzek, M. Feuring-Buske, C. Buske, S. Rau and T. Weil, *J. Am. Chem. Soc.*, 2017, **139**, 2512; (b) M. Azizi, H. Ghourchian, F. Yazdian, F. Dashtestani and H. A. Zeinabad, *PLoS ONE*, 2017, **12**, e0188639; (c) P. Zhang, H. Huang, S. Banerjee, G. J. Clarkson, C. Ge, C. Imberti and P. J. Sadler, *Angew. Chem. Int. Ed.*, 2019, **58**, 2350; (d) M. Jiang, S. Li, J. Wu, W. Li, X. Wen, H. Liang and F. Yang, *J. Inorg. Biochem*., 2021, **215**, 111318.

13. (a) J. F. Lovell, T. W. B. Liu, J. Chen and G. Zheng, *Chem. Rev.*, 2010, **110**, 2839; (b) T. C. Pham, V.-N. Nguyen, Y. Choi, S. Lee and J. Yoon, *Chem. Rev.*, 2021, **121**, 13454.

14. L. Abdel-Latif, B. K. Murray, R. L. Renberg, K. L. Neill, H. Porter, J. B. Jensen and F. B. Johnson, *J. Gen. Virol.*, 2006, **87**, 2539.

15. L. Wang, R. Guan, L. Xie, X. Liao, K. Xiong, T. W. Rees, Y. Chen, L. Ji and H. Chao, *Angew. Chem. Int. Ed.*, 2021, **60**, 4657.

16. S. P.-Y. Li, C. T.-S. Lau, M.-W. Louie, Y.-W. Lam, S. H. Cheng and K. K.-W. Lo, *Biomaterials*, 2013, **34**, 7519.